



International Symposium
on
Ligaments & Tendons - V

**Wyndham Washington, DC
Washington, DC**

February 19, 2005

*Edited by: Savio L-Y. Woo, PhD
Steven D. Abramowitch, PhD
Kazutomo Miura, MD, PhD*

**Musculoskeletal Research Center
Department of Bioengineering
University of Pittsburgh**

Volume 5

Symposium Sponsors



Aircast, Inc.



**Asian♦American Institute for
Research and Education**



**Department of Bioengineering
University of Pittsburgh**



FlexCell International Corporation



Musculoskeletal Research Center



**Orthopaedic Research Laboratory
Alumni Council**



**The Education and Special Projects
Committee of the
Orthopaedic Research Society**

**STEADMAN•HAWKINS
Research Foundation**



**Steadman Hawkins Sports
Medicine Foundation**

The
WHITAKER
Foundation

The Whitaker Foundation

International Symposium on Ligaments & Tendons - V

Saturday, February 19, 2005

Wyndham Washington, DC

Washington, DC

Welcome!

Welcome to the Fifth International Symposium on Ligaments and Tendons (ISL&T-V) in Washington, DC, U.S.A.! Again, we are having an exciting multidisciplinary program to cover the frontiers of ligament and tendon research.

ISL&T has been a focused meeting devoted to ligament and tendon biomechanics, biology, tissue engineering and clinical management of their injuries. Besides the podium and poster presentations of knee ligament, tendon biology and biomechanics, pathophysiology, tissue engineering and other hot topics, this year's meeting highlights three special symposia on Rotator Cuff Tendinopathy, Functional Tissue Engineering and Tendon Healing & ACL as well as a mini symposium on Gender-Related Differences and Knee Kinematics. We anticipate free exchange of current scientific information with lively discussion of cutting edge research at the highest scientific level.

We would especially like to thank the organizers of the symposia Drs. Lou Soslowsky, Evan Flatow, Al Banes, Steven Arnoczky, David Butler, Chih-Hwa Chen, Per Renström, Angela Smith, Ed Wojtys and Lars Engebretsen. In addition, we thank you for coming. Please take the opportunity to make new friends as well as to reunite with your colleagues and acquaintances.

With our very best wishes.

Sincerely,

Savio L-Y. Woo, PhD, DSc
Steven D. Abramowitch, PhD
Kazutomo Miura, MD, PhD

The ISL&T-V Planning Committee



Steven Abramowitch, Savio Woo, Kazutomo Miura

General Information

Aims of the Symposium

The *International Symposium on Ligaments & Tendons* provides a forum to discuss state-of-the-art ligament and tendon research. By bringing together some of the best minds in our field, we hope to address challenging problems in ligament and tendon biomechanics and biology, and set new research directions that hold great potential for the future.

Planning Committee

Savio L-Y. Woo, PhD, DSc (Hon.) – **Chair**
Steven D. Abramowitch, PhD
Kazutomo Miura, MD, PhD

Diann DeCenzo, MS— **Treasurer**
Serena Chan Saw, MS

International Program Committee

Paolo Aglietti, MD (Europe)
Steve Arnoczky, DVM (North America)
David Butler, PhD (North America)
Evan Flatow, MD (North America)
Joseph Iannotti, MD, PhD (North America)
Guoan Li, PhD (North America)
Jacques Menetrey, MD (Europe)
Scott Rodeo, MD (North America)
Louis Soslowsky, PhD (North America)
Rocky Tuan, PhD (North America)
Kazunori Yasuda, MD, PhD (Asia)

Peter Amadio, MD (North America)
Albert Banes, PhD (North America)
Lars Engebretsen, MD, PhD (Europe)
Cyril Frank, MD (North America)
Thay Lee, PhD (North America)
Helen Lu, PhD (North America)
Per Renström, MD, PhD (Europe)
Angela Smith, MD (North America)
Stavros Thomopoulos, PhD (North America)
Rene Verdonk, MD (Europe)

Instructions to Presenters

I. Podium Presenters

The time for presentations has been limited, in favor of discussion. Please see the presentation formats listed below. Your moderators have been asked to adhere to the time allotted for your presentation as well as the number of slides.

Important: All speakers are asked to check-in with the session moderators 15 minutes before the session in which they will present to meet the projectionist and the moderator.

Presentation Requirements

- *For 15 minute time slots*
 - 10 min. presentations each immediately followed by a 5 min. discussion.
 - Maximum **10 PowerPoint slides** for computer presentation.
- *For 5 minute time slots*
 - 5 min. presentations followed by a 5-10 min. group discussion of 2-3 papers.
 - Maximum **5 PowerPoint slides** for computer presentation.

An Important Note on Slides

Kindly note that all speakers must be prepared to present their paper using PowerPoint projection. We ask that you send your PowerPoint presentation file to us by **February 16, 2005** so that we can load all talks into a master computer prior to the symposium. Please make sure that you clearly label your file with the author's name and the title of your presentation.

Note: In view of time and the large number of talks, there will be no opportunity to use your personal computer or load your PowerPoint file during the symposium.

II. Poster Presenters

All posters should be no larger than 45 inches x 45 inches (114.3 cm x 114.3 cm). Poster boards will be available in the room adjacent to the presentations. Please set up your poster between 7:30 - 8:00 am and leave the posters up throughout the day. Posters are to be taken down at the end of the symposium.

Note: An opportunity has been provided for you to present your posters during different breaks. Please be sure to attend to your poster at the assigned time (see pages 6 and 9).

Symposium Awards

Similar to last year, the ISL&T-V is proud to continue to recognize our outstanding papers presented by students, fellows, and residents. To acknowledge their work, we will provide the following two awards:

Best Student Paper Award

Best Research Fellow Paper Award

These awards are designed to stimulate high quality scientific research by young investigators in the study of ligaments and tendons. The awardees will be selected by members of the program committee based on the quality of the abstract and presentation as well as the overall scientific merit of the study. To be eligible, the presenter must be the first author of the abstract.

Each award consists of a certificate and a check for US\$200 (donated by Flexcell International Corporation ).

Dinner

Dinner will begin at 6 pm with a cash bar. The award ceremony will follow dinner.

Tony Cheng Seafood Restaurant
619 H Street, NW
Washington, DC 20001
202-371-8669

Directions to the Restaurant (via the Metro)

- Turn LEFT after you exit the hotel onto M St. NW
- After about 4 blocks, turn LEFT onto Connecticut Ave
- Take the RED line at the FARRAGUT NORTH Metro Stop to the GALLERY PL - CHINATOWN stop (Fare \$1.35)
- Exit the Metro Stop and turn right onto H St. NW
- Walk towards 6th St., the restaurant will be on your right.

PROGRAM

7:30-8:00 am **Registration and Check-In**

8:00-8:15 am **Opening Ceremony, Welcome & Announcements**
Savio L-Y. Woo, PhD, DSc, Steven D. Abramowitch, PhD

Symposium: Rotator Cuff Tendinopathy
Moderators: Giuliano Cerulli, MD & Kai-Nan An, PhD

8:15 am	Keynote Lecture Rotator Cuff Biomechanics: An Overview <i>LJ Soslowsky</i>	p. 11
8:30 am	Keynote Lecture How Does Tendon Damage Initiate? <i>EL Flatow</i>	p. 12
8:45 am	In-Vivo Shoulder Biomechanics <i>PJ Boyer, R Papannagari, TJ Gill, SS Stewart, JP Warner, G Li</i>	p. 13
9:00 am	A Novel Reliable Classification of the Acromial Shape to Assess the Risk of Rotator Cuff Pathology <i>JH Stehle, DA Alaseirlis, RE Debski, PJ McMahon</i>	p. 14
9:15 am	Commercial ECMs for Rotator Cuff Tendon Repair or Reinforcement <i>AR Baker, MJ DeFranco, JP Iannotti, KA Derwin</i>	p. 15
9:20 am	A Technique for Measuring In-Vivo Tendon Strains with Biplane Radiography <i>MJ Bey, S Tashman, SK Brock, CM Les</i>	p. 16
9:25 am	Discussion	
9:30 am	Shoulder Internal Impingement: Effect of Horizontal Abduction and Anterior Capsular Laxity <i>T Mihata, L Duong, MH McGarry, TQ Lee</i>	p. 17
9:35 am	Biomechanics of Rotator Cuff Repair <i>N Zheng, H Harris</i>	p. 18
9:40 am	Discussion	

Break and Poster Session 1

- 9:45 - 10:15 am** Collagen Matrix Tension Regulates α -SMA Expression of Ligament Fibroblasts **p. 19**
C Agarwal, JH-C Wang
- Contributions of Aging and Genetic Background to Mouse Knee Laxity **p. 20**
T Banack, KJ Jepsen, EL Flatow, VM Wang
- Elastographic Determination of Strain Distribution at the ACL-Bone Insertions **p. 21**
JP Spalazzi, EE Konofagou, HH Lu

Symposium: Functional Tissue Engineering - Part 1

Moderators: Joanne Archambault, PhD & Toru Fukubayashi, MD

- 10:15 am** **Keynote Lecture** **p. 22**
The Tendon Transcriptome: Commonalities and Contrasts in Gene Expression Between Muscle and Tendon +/-IL-1B
AJ Banes
- 10:30 am** **Keynote Lecture** **p. 23**
Functional Tissue Engineering of Ligaments and Tendons
SL-Y Woo
- 10:45 am** Effects of Introducing Collagen Sponge on the Biomechanics and Histology of Stem Cell-Collagen Gel Constructs for Patellar Tendon Repair **p. 24**
N Juncosa-Melvin, DL Butler, GP Boivin, MT Galloway, C Gooch, JR West
- 11:00 am** Three-Dimensionality Regulates Scleraxis Expression During Tenogenesis of Mesenchymal Stem Cells **p. 25**
CK Kuo, RS Tuan
- 11:15 am** Recruitment of Bone Marrow Derived Cells During Achilles Tendon Healing in a Mouse Model **p. 26**
T Zantop, TW Gilbert, SF Badylak
- 11:30 am** Novel Multi-Phased Composite Scaffold for ACL-to-Bone Integration **p. 27**
JP Spalazzi, KL Moffat, SB Doty, HH Lu
- 11:35 am** Mechanical Stimulation of Tendon Tissue Engineered Constructs: Effects on Construct Stiffness, Repair Biomechanics and Their Correlation **p. 28**
JT Shearn, N Juncosa-Melvin, DL Butler, GP Boivin, MT Galloway, W Goodwin, C Gooch
- 11:40 am** Discussion

11:45 am	A Novel Ligament/Tendon Tissue Engineering Graft <i>HW Ouyang, JCH Goh, SL Toh, EH Lee</i>	p. 29
11:50 am	Human Fascia Lata as a Natural Scaffold for Soft Tissue Repair or Reinforcement <i>AR Baker, JP Iannotti, KA Derwin</i>	p. 30
11:55 am	Discussion	
12:00 pm - 1:00 pm	Lunch and Poster Viewing	

Symposium: Functional Tissue Engineering - Part 2

Moderators: Steven Arnoczky, DVM & Christos Papageorgiou, MD

1:00 pm	Keynote Lecture An Expanded Functional Tissue Engineering Paradigm: Application to Ligament and Tendon Tissue Engineering <i>DL Butler</i>	p. 31
1:15 pm	<i>In Vivo</i> Degradation of an ECM Bioscaffold for Achilles Tendon Repair: Importance for Constructive Remodeling <i>AM Stewart-Akers, A Simmons-Byrd, SF Badylak</i>	p. 32
1:20 pm	Novel Micro-Patterned Fluidic System for Osteoblast and Fibroblast Co-Culture <i>J Tsai, IE Wang, LC Kam, HH Lu</i>	p. 33
1:25 pm	Discussion	
1:30 pm	IL-1 β Increases the Transcription of Elastin in HTIF-Populated Bioartificial Tendons <i>J Qi, L Chi, D Bynum, AJ Banes</i>	p. 34
1:35 pm	Type I Collagen Expression in Mechanically Stimulated Mesenchymal Stem Cells <i>K Chokalingam, SA Hunter, CG Gooch, JL Florer, DL Butler, RJ Wenstrup</i>	p. 35
1:40 pm	Healing of an Intra-Articular Tissue Defect Using a Stabilized Provisional Scaffold <i>MM Murray, KP Spindler, C Devin, P Ballard, LB Nanney, KP Spindler</i>	p. 36
1:45 pm	Discussion	

Symposium: Tendon Healing and ACL

Moderators: **Chih-Hwa Chen, MD & Scott Rodeo, MD**

- 1:55 pm** **Keynote Lecture** **p. 37**
Physical Activity and Neuronal Plasticity After Tendon Rupture
P Renström
- 2:10 pm** Origin of Mesenchymal Cells in Tendon Healing: Using Tendon Chimeric Rat **p. 38**
Y Kajikawa, N Watanabe, H Sakamoto, M Kobayashi, Y Oshima, M Kawata, T Kubo
- 2:25 pm** Expression Profiling of Metalloproteinases and Tissue Inhibitors of **p. 39**
Metalloproteinases in Normal, Painful and Ruptured Achilles Tendon
GC Jones, AN Corps, CJ Pennington, IM Clark, DR Edwards, BL Hazelman, GP Riley
- 2:30 pm** TGF-Beta Isoforms Were Expressed in the Edges of the Wound in Healing **p. 40**
Patellar Tendons
SC Fu, YP Wong, CWC Hui, WMN Wong, LK Hung, P Wen, KM Chan
- 2:35 pm** Discussion
- 2:40 pm** A Novel In-Vivo Model of Tendon Fatigue Damage Accumulation **p. 41**
VM Wang, H Lee, L Rajan, DM Laudier, MB Schaffler, EL Flatow
- 2:45 pm** New Bioreactor System for Ligament and Tendon Tissue Engineering **p. 42**
T Majima, N Sawaguchi, N Iwasaki, T Funakoshi, K Shimode, T Onodera, A Minami
- 2:50 pm** Discussion
- 2:55 pm** Suture Plication, Thermal Shrinkage, and Sclerosing Agents: Effects on **p. 43**
Rat Patellar Tendon Length and Biomechanical Strength
A Aneja, S Karas, P Weinhold, H Afshari, L Dahners
- 3:00 pm** Characterization of the Mechanical Properties of the ACL Bone Insertion **p. 44**
KL Moffat, NO Chahine, CT Hung, GA Ateshian, HH Lu
- 3:05 pm** Aging Affects the Mechanical and Viscoelastic Properties of the Bundles of **p. 45**
Human ACL Differently: A Cadaveric Study
R Kilger, SD Abramowitch, DK Moon, SL-Y Woo
- 3:10 pm** Discussion

Break & Poster Session 2

3:20 pm- 3:50 pm	Bioscaffold Treatment Reduces the Cross-Sectional Area of the Healing Medial Collateral Ligament <i>DK Moon, Y Takakura, R Liang, SD Abramowitch, SL-Y Woo</i>	p. 46
	Semitendinosus Tendon Regeneration After ACL Reconstruction <i>S Li, A Nishino, T Manmoto, A Kanamori, T Fukubayashi</i>	p. 47
	Effects of Collagenase on the Material Properties of Small Intestinal Submucosa <i>JT Shearn, W Goodwin, DL Butler</i>	p. 48
	New Insights Into the Mesostructure of Connective Tissue <i>TC Doehring</i>	p. 49

Symposium: Gender-Related Differences and Knee Kinematics

Moderators: Angela Smith, MD & Thay Lee, PhD

3:50 pm	Keynote Lecture Biomechanics Associated with ACL Injury: Athlete Interview and Review of Injury Tapes <i>T Krosshaug, R Bahr, L Engebretsen</i>	p. 50
4:05 pm	Inferior Results Observed in Females Following Surgical Repair May Not Be Due to the Mechanical Properties of the Shoulder Capsule <i>SM Moore, PJ McMahon, RE Debski</i>	p. 52
4:10 pm	The Carpal Tunnel is Less Compliant in Female Than in Male <i>Z-M Li</i>	p. 53
4:15 pm	Gender Differences Associated with the Risk of Non-Contact ACL Injury: Kinematics During a Single Limb Drop Landing <i>Y Nagano, H Ida, M Akai, T Fukubayashi</i>	p. 54
4:20 pm	Discussion	

4:30 pm	The Role of Hamstrings Muscles to Protect the ACL <i>G Cerulli, M Lamontagne, A Caraffa, A Liti, F Vercillo, M Beaulieu</i>	p. 55
4:45 pm	Posterior Cruciate Ligament Function: Effect of Deficiency and Reconstruction on Joint Kinematics <i>JT Shearn, FR Noyes</i>	p. 56
4:50 pm	Determination of Angles of Knee Flexion for Graft Fixation in Double Bundle Anterior Cruciate Ligament Reconstruction <i>K Miura, M Thomas, R Brinkley, S Noorani, Y-C Fu, SL-Y Woo</i>	p. 57
4:55 pm	Discussion	
5:00-5:10 pm	Closing Remarks Savio L-Y. Woo, PhD, DSc	

Dinner and Award Ceremony
Tony Cheng Seafood Restaurant
619 H Street, NW
Washington, DC 20001
202-371-8669

6:00-6:30 pm	Cash Bar
6:30-	Dinner and award ceremony

ROTATOR CUFF BIOMECHANICS: AN OVERVIEW

L.J. Soslowsky
McKay Orthopaedic Research Laboratory
University of Pennsylvania
Philadelphia, PA 19104

Rotator cuff tears occur frequently and can cause significant pain and reduced function. The purpose of this presentation is to provide a general overview of biomechanical factors contributing to rotator cuff injury. Factors are often categorized as either intrinsic or extrinsic factors, though each and/or both clearly play a role in different circumstances.

Intrinsic factors are known to be important. Anatomic investigations have determined that a significant percentage of individuals have rotator cuff tears and that these numbers rise dramatically with age. Some of the controversy associated with the particular values comes from the methods of detection and the definitions of a cuff tear (small vs. large, partial vs. full, etc). Biomechanical testing studies have demonstrated a significant variation in supraspinatus tendon properties with the anterior and superficial regions being stronger than the posterior and deep regions, respectively. Vascular studies have historically demonstrated a “critical region” near the tendon to bone insertion site. More recent studies have demonstrated that there may be vascularity differences between the bursal and articular sides and that this may be important in initiation of cuff tears. Overuse and repetitive use syndromes are important intrinsic factors as these may result in microtrauma that may accumulate with time.

Extrinsic factors are also known to be important. Extrinsic factors have commonly focused on the shape and size of the coracoacromial arch with an increased incidence of Type III (hooked) acromia with rotator cuff tears compared with Type I (flat) acromia. Various measurements of the supraspinatus outlet dimensions, contact areas and pressures, and the role of the coracoacromial ligament have been performed and these have also been related to rotator cuff tears. Straightforward mechanical analyses demonstrate that a weakened or injured rotator cuff will further contribute to extrinsic contact, through superior migration of the humeral head, thus further exacerbating the condition. Internal impingement, recognized with increasing frequency over the past ten years is common in throwing athletes and results in articular side rotator cuff tears.

Certainly, most rotator cuff tears are multifactorial, including both intrinsic and extrinsic factors, as well as factors in combination. Further research is needed to determine the primary, initiating, causative factors for particular rotator cuff injuries.

HOW DOES TENDON DAMAGE INITIATE?

Evan L. Flatow, Vincent M. Wang, Lakshmi Rajan, Mitchell Schaffler
Department of Orthopaedics, Mount Sinai School of Medicine, New York, NY

Tendinopathy is a general term used to describe chronic tendon disorders of varying etiologies. Unlike acute tendon injuries which may result from direct laceration or sudden tensile overload, chronic injuries are widely believed to result from repetitive overuse, which leads to cumulative “microtrauma”, degeneration (tendinosis) and ultimately tendon failure. In humans, tendons particularly prone to tendinopathies include the rotator cuff (supraspinatus), Achilles, and patellar tendons. We hypothesized that damage accumulation induced during normal daily activities contributes to the material degradation and eventual failure of tendons, while eliciting a concurrent biological repair response. To test this hypothesis we developed an animal model of fatigue damage in rat tendons. Our initial studies in *ex vivo* rat tendons showed degradation of both tensile secant and tangent stiffness following fatigue loading. We furthermore separated the effects of transient (viscoelastic or recoverable) stiffness loss from permanent stiffness reduction, the latter of which is the manifestation of matrix failure.

Our next series of studies developed histological techniques to evaluate the physical consequences of this fatigue damage. Morphologic assessment of matrix damage is problematic as many of the tissue processing procedures used for standard histology do not work well for tendon. Since much of the early fatigue damage process in tendons is thought to occur by matrix microtearing and disruption, it is essential that histological approaches be developed to minimize tissue artifacts so that mechanisms of micro-failure can be understood. Based on normal (unloaded) and mechanically fatigued rat flexor digitorum longus (FDL) tendons, we developed a processing method that does not harden or distort dense collagenous tissues. Tendons processed in this manner were then embedded in normal paraffin, or in methylmethacrylate (MMA) for thin sectioning (light microscopy) or thick sectioning (confocal microscopy). In tendons subjected to low-level fatigue, we demonstrated subtle, localized fiber discontinuity in the presence of an intact synovium. This suggested that collagen bundles underwent microtearing and subsequently recoiled into the fiber matrix. We believe this is the ultrastructural correlate of material property degradation. In our confocal microscopy studies, tendons were bulk stained prior to embedding using Texas-Red labeled dextran to assess changes in permeability resulting from matrix disruption. We observed evidence of early tendon damage due to fatigue, including focal matrix disruptions as well as potential interface failures between tendon bundles.

We have also been investigating molecular mechanisms of tendon homeostasis, including MMP and TIMP levels and activity in different rodent tendons. Our studies, using Western blot analysis and gelatin zymography, show that constitutive levels of matrix metalloproteinases (MMP-2, MMP-3, MMP-13) are present in normal rat tendons suggesting that baseline remodeling occurs in tendons. Since MMPs and TIMPs work coordinately to regulate ECM remodeling, we used quantitative real-time PCR to assess TIMP gene expression in different tendon types. Our studies demonstrated that tendons from different anatomic locations (within an animal) exhibit distinct patterns of TIMP gene expression. These experiments suggest that the differences in TIMP gene expression among tendons may contribute to differences in their overall biology and therefore to differences in their susceptibility to damage.

We sought to identify and develop an animal model for *in vivo* fatigue tendon damage. We performed dissections of FDL, Achilles, patellar, supraspinatus and tail tendons in a variety of small animals (including mice, rats, cats, rabbits and dogs). Our criteria were: (1) An animal that was small and easily bred yet of a size allowing mechanical and histologic tendon analysis (2) A tendon to which a well-defined fatigue loading pattern could be applied with minimal tissue damage except from the loading (3) A tendon known to exhibit tendinopathy in humans, and (4) An animal for which biologic perturbation could be easily achieved. Only the patellar tendon, attached to bone at both ends, satisfied criterion #2, since the tendon itself would not have to be clamped or crushed to apply load. Furthermore, it is immediately subcutaneous allowing ease of surgical access. Finally, patellar tendinopathy is a common clinical problem in humans. While the mouse allowed biologic perturbation most easily, practical concerns with histology and tissue mechanical testing suggested that the rat was as small as was practical. Furthermore, the rat had been used as a model for tendon overuse and tendon healing and has been well characterized for acute injury. In this living animal model, subfailure loads may be repeatedly applied to the patellar tendon through its bone attachments. We have demonstrated histologic evidence of matrix damage and degradation of material properties after 2 weeks of cage activity. This is the first model of which we are aware that allows production of a precisely defined fatigue injury in a living tendon. This model will allow the elucidation of the fundamental microstructural and biologic mechanisms of chronic tendon failure.

IN-VIVO SHOULDER BIOMECHANICS

P.J. Boyer; R. Papannagari; T.J. Gill; S.S. Stewart; J.P. Warner; G. Li
 Bioengineering Laboratory, Department of Orthopaedic Surgery
 Massachusetts General Hospital/Harvard Medical School, Boston, MA, USA.
 Email: gli1@partners.org

INTRODUCTION:

The goal of shoulder surgery is to restore normal function. However, no data has been reported about glenohumeral (GH) joint contact and glenohumeral ligaments (GHL) function during in-vivo motion of the normal shoulder. This study investigated in-vivo kinematics of normal shoulders under active abduction using a dual-orthogonal fluoroscopic system [1]. The GH contact locations on the glenoid surface and GHLs elongation patterns were determined.

MATERIALS AND METHODS:

Five subjects with normal, healthy shoulders (2 left and 3 right, average age 26) were recruited under the IRB guidance. The shoulder was scanned with a 1.5T magnet (GE, Milwaukee, WI) using a FIESTA sequence. The MR images were used to construct 3D models of the humeral head, scapula and cartilage surfaces of the glenoid fossa and the humeral head using a 3D solid modeling software. The insertion areas of superior, middle and anterior band of inferior GHLs (SGHL, MGHL and AB-IGHL, respectively) were also outlined on the model (Fig. 1).

Then, the subject was positioned in a dual-orthogonal fluoroscopic system (Fig. 1A) and the active shoulder motion at 0° reference, 45°, and 90° of abduction in neutral rotation, and 90° abduction combined with maximal external rotation was imaged. The 3D shoulder model and the orthogonal images were then input into a virtual dual-fluoroscope system created in a solid modeling software. The 3D shoulder model positions were adjusted so that its projections on the orthogonal images matched those of the actual shoulder. The GH contact was determined by the overlapping of the glenoid and humeral cartilage surfaces. The centroid of the contact area was defined as the contact location of the GH joint. The centroids of insertion areas of each ligament were connected using a curve that wraps around the humeral head surface (Fig. 1C). The length of the curve was measured to represent in-vivo ligament length at that shoulder position. Ligament lengths at 0° reference was used as reference to quantify elongation of the ligaments.

RESULTS:

For all the abduction positions and the 90° abduction with maximal external rotation position, the GH contact locations were more than 5 mm away from the center of the glenoid surface and were located at the posterosuperior portion of the glenoid surface (Figs. 2A & B). Elongations of the SGHL and MGHL increased by 35±23% and 73±31%, respectively, from 0° to 45°, and reduced to -5±11% and -47±35%, respectively, at 90° of abduction (Fig. 2C). At 90° of abduction with maximal external rotation, both ligaments elongated to maximal of 24±40% and 102±66%, respectively. The AB-IGHL length increased continuously with abduction angle. The maximal elongation was 178±82% at 90° of abduction with maximal external rotation.

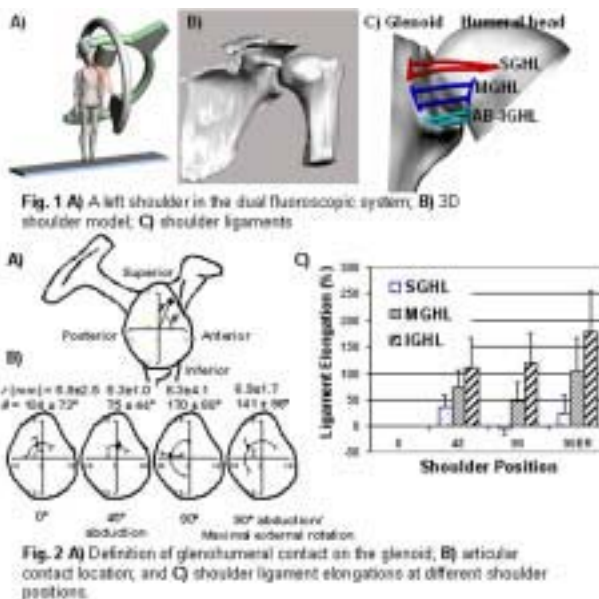
DISCUSSION:

The data has shown that in-vivo GH contact locations were not at the center area of the glenoid surface, instead, were at locations corresponding to thicker cartilage of the glenoid [2]. Further, GH contact was shown to be slightly different to that reported in cadaveric studies and this difference can be attributed to differences in muscular conditions. This information can be used as a base line for studies of abnormal shoulder function and restoration of articular mechanics after surgery.

While AB-IGHL was shown to elongate continuously with abduction, both SGHL and MGHL had maximal elongations at 45° of abduction. For all ligaments, abduction with maximal external rotation was shown to cause maximum elongation. These data can provide insight into the mechanism of shoulder instability as well as surgical repair, especially of the AB-IGHL.

REFERENCES:

- 1) Li G et al., *J Biomech Eng* 126:314-18, 2004.
- 2) Yeh L et al., *Skeletal Radiol* 27:500-504, 1998.



A NOVEL RELIABLE CLASSIFICATION OF THE ACROMIAL SHAPE TO ASSESS THE RISK OF ROTATOR CUFF PATHOLOGY

J.H. Stehle, D.A. Alaseirlis, R.E. Debski, P.J. McMahon

Musculoskeletal Research Center, Department of Bioengineering, University of Pittsburgh, Pittsburgh, PA,

INTRODUCTION:

Acromial morphology, specifically when the acromion encroaches on the supraspinatus tendon, correlates with rotator cuff pathology. The commonly used classification to describe the shape of the acromion qualitatively and assess the risk of rotator cuff pathology was introduced by Bigliani et al [2]. However, several studies showed poor to moderate interobserver repeatability of this classification [4]. Repeatable classifications are needed to reliably assess and compare the risk of rotator cuff pathology [4]. Quantitative methods have also been suggested that claimed a higher repeatability [1]. Therefore the objective of this study was to compare the interobserver repeatability of the common classification [2], the Acromial Angle classification (Figure 1) [1], and a novel classification (Figure 2) to assess the acromial shape.

METHODS:

Standardized lateral view radiographs of twenty-four human scapulas were made and hardcopies of the scanned pictures were produced. Three clinicians evaluated the hardcopies three times with intervals of at least 2 weeks for the intraobserver repeatability. Thirteen clinicians evaluated twelve of these hardcopies once for the interobserver repeatability. Each evaluation consisted of assessing the acromial shape with the common classification which distinguishes between Type 1 (flat), 2 (curved), 3 (hooked), and 4 (reversed curved) [2,5]. For the other classifications the anterior, posterior and highest point of the undersurface of the acromion were marked. The Acromial Angle and geometric dimensions for the novel classification were measured. The novel classification assigns acromions quantitatively to an acromial type according to specific criteria. The inter- and intraobserver repeatability was assessed with Kappa statistics (SAS®). A Kappa value ≤ 0 was defined as poor, >0 and ≤ 0.2 as slight, >0.2 and ≤ 0.4 as fair, >0.4 and ≤ 0.6 as moderate, >0.6 and ≤ 0.8 as good and a value >0.8 was defined as excellent repeatability [6].

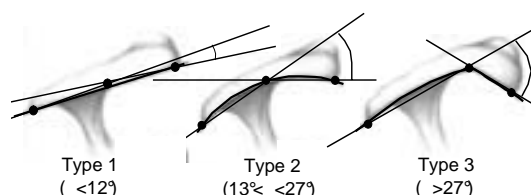


Figure 1: Acromial Angle classification [1], =Acromial Angle

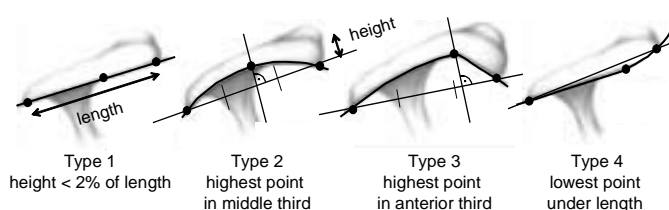


Figure 2: Novel Classification based on [3]

RESULTS:

The common classification showed moderate intra- (Kappa 0.41 to 0.58) and fair interobserver repeatability (Kappa 0.25). The Acromial Angle classification revealed good intra- (Kappa 0.60 to 0.89) and moderate interobserver repeatability (Kappa 0.44). The novel classification had good intra- (Kappa 0.53 to 0.79) and good interobserver repeatability (Kappa 0.62).

Table: Kappa values of the intra- and interobserver (bold) repeatability of the three classifications. Intraobserver values: median (range)

	Intra	Inter
Common class.	0.52 (0.40-0.58)	0.25
Acromial Angle class.	0.68 (0.60-0.89)	0.44
Novel classification	0.68 (0.53-0.79)	0.62

DISCUSSION:

This study compared the repeatability of different classifications of the acromial shape. The data suggest that the novel classification is most repeatable to assess the acromial shape. Therefore this novel classification should be used in future studies to more reliably assess acromial shape to compare risk of rotator cuff pathology. Future studies will determine the correlation between acromial shape assessed with this novel method and the contact area of the rotator cuff with the acromion while impingement tests are performed on a robot.

REFERENCES:

1. Toivonen et al 1995, 2. Bigliani et al 1986, 3. Epstein et al 1993, 4. Jacobson et al 1995, 5. Farley et al 1994, 6. Landis et al 1977.

COMMERCIAL ECMS FOR ROTATOR CUFF TENDON REPAIR OR REINFORCEMENT

A.R. Baker, *M.J. DeFranco, *J.P. Iannotti, †K.A. Derwin

Cleveland Clinic Foundation, Dept. of Biomedical Engineering and the Orthopaedic Research Center, Lerner Research Institute, *Dept. of Orthopaedic Surgery, Cleveland, OH (†corresponding author: derwink@ccf.org)

INTRODUCTION

Several natural extracellular matrices (ECMs) have been marketed as patches to reinforce soft tissue repair during rotator cuff surgery. These products include collagen-rich ECMs such as dermis (GraftJacket[®], Permacol[™], OrthoMend[™]) and small intestine submucosa (Restore[®]). To our knowledge there is no published study that describes the biomechanical and biochemical properties of these materials, specifically as they compare to tendon. Therefore, the aims of this study are to characterize the biomechanical, biochemical and cellular properties of several commercial ECMs that are available for rotator cuff tendon repair. We report our ongoing work here.

METHODS

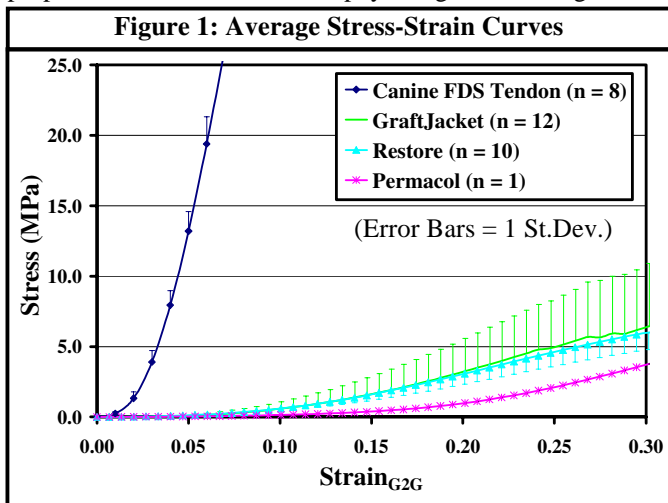
One 12 x 45 mm test strip was cut from each different lot to be tested: GraftJacket[®] (Wright Medical Technology, $n = 12$), Restore[®] (DePuy Orthopaedics, $n = 10$), and Permacol[™] (Tissue Science Laboratories plc, $n = 1$). Samples were rehydrated in physiologic saline (PBS) at 4°C overnight prior to testing. Samples were clamped in custom grips with a nominal gage length of 30 mm. Thickness was determined using a constant pressure LVDT probe. Uniaxial tension tests were performed in PBS at 37°C. Samples were preconditioned 5X to 2N then pulled immediately to failure at 10 mm/min. Modulus and stiffness were determined using grip-to-grip displacements from the slope of the stress-strain and load-displacement curves. Tendon samples were tested as part of another study (Baker AR *et al.*, *J Biomech* 37: 959-968, 2004). Kruskal-Wallis ANOVA and Dunn’s post-hoc test was used to compare ECM properties to tendon. A p -value <0.05 was considered significant.

RESULTS

To date we have completed a subset of our mechanical evaluations. Average stress-strain curves for the materials tested are shown in Fig. 1. The commercial ECMs are considerably more compliant than tendon at low strain (~5%), and stiffen at higher strains (20-30%). Stiffness and modulus were computed in two strain regions: (1) 4.5 to 5.5% (physiologic range for tendon) and (2) the “linear region” for each sample tested. Table 1 contains the median values of modulus for all groups. Also included is the range of strain that corresponded to the “linear region” for the samples tested for each material. The stiffness and modulus of Restore[®] and GraftJacket[®] were at least two orders of magnitude less than tendon in the 4.5 to 5.5% strain range and one order less if considering the “linear region” properties. Permacol appears to have similar material properties as those of Restore[®] and GraftJacket[®].

DISCUSSION

Our results demonstrate that commercial ECMs are significantly more compliant than tendon, especially at physiologic strains for tendon (~5%). Hence, if used as a load-sharing augmentation device for tendon repair, these materials likely carry negligible load. Alternately, if used as a primary graft to connect a stiff muscle-tendon to bone, these materials may stretch appreciably. Pre-stretching these materials at implantation may improve their functional contribution. However, for tendon repair commercial ECMs may offer more of a biologic advantage than a mechanical one. This study highlights the importance of reporting the mechanical properties of tissue engineering materials in the region of strain that corresponds to the particular in vivo application, rather than just the maximum properties obtained from a non-physiologic strain range. Further characterization of these ECMs is ongoing.



Group	n	4.5–5.5% Strain	Linear Region	
		Modulus (MPa)	Modulus (MPa)	Strain Range
Canine FDS	8	566.2 [514,629]	566.2 [514,629]	.045-.055
GraftJacket [®]	12	0.08‡ [0.02,1.2]	28.1† [16.9,43.6]	.20-.74
Restore [®]	10	4.7‡ [3.5,5.7]	32.7† [29.9,35.4]	.225-.25
Permacol [™]	1	1.5	32.0	.275-.30

‡, † Significantly different than tendon in respective strain region ($p < 0.05$)

A TECHNIQUE FOR MEASURING IN-VIVO TENDON STRAINS WITH BIPLANE RADIOGRAPHY

M.J. Bey, S. Tashman, S.K. Brock, C.M. Les
Bone and Joint Center, Henry Ford Hospital, Detroit, MI

INTRODUCTION

Measuring in-vivo tendon force or strain is important for understanding how tendons function under normal and pathologic conditions. In-vivo forces or strains have been measured with various techniques, including liquid metal strain gauges, buckle transducers, implantable force transducers, ultrasonography, and MRI [1,2]. The purpose of this project was to assess the feasibility of using a biplane radiographic system to measure in-vivo tendon strains.

METHODS

Surgical Procedures: Under IACUC approval, six 1.6 mm diameter tantalum beads were implanted into the shoulder of three 20-25 kg canines. To quantify precision, two beads were implanted in the humerus approximately 25 mm apart. To quantify tendon deformation and strain, two beads were sutured to the surface of the infraspinatus (INF) and deltoid (DLT) tendons (four beads total) by passing a 5-0 nylon suture through a 0.2 mm hole in the bead. Each pair of tendon beads was approximately 15 mm apart and parallel to the muscle's line of action.

Testing Procedures: In-vivo tendon function was assessed by measuring changes in tendon length (i.e., the distance between tendon bead pairs) during quiet standing, walking, and trotting using a high-speed (250 Hz), high-accuracy (± 0.1 mm), biplane x-ray system [3]. Biplane radiographic images were collected at 120 Hz from three trials of each activity at two weeks and three weeks post-surgery. Following the second day of testing, each tendon's zero-strain length was determined by euthanizing the dog, dissecting the tendons, securing the tendons within the imaging system, applying a static 1.0 N load, and then acquiring biplane radiographic images.

Data Analysis: After correcting the images for distortion and nonuniformity, custom software determined the 3D position of each bead and the 3D distance between the INF and DLT tendon bead pairs. One-dimensional tendon strain was computed as follows: $\text{Strain} = ((l_f - l_0) / l_0) * 100$, where l_f was the 3D distance between tendon bead pairs during walking and trotting, and l_0 was the 3D zero-strain distance. Precision was assessed by the variation in the measured distance between the implanted humerus beads (whose distance was not expected to change). For each tendon, the coefficient of variation (CV) of maximum tendon length was determined across trials and testing days.

RESULTS

The dogs tolerated the bead implant procedure very well and returned to treadmill walking with no lameness within one week of surgery. The data showed high precision, with the standard deviation of the distance between the implanted bone beads averaging 0.14 mm across all trials. The data were also highly repeatable (Fig. 1). Specifically, the day-to-day CV in maximum tendon length was less than 1.0% for both tendons. Similarly, the trial-to-trial CV in maximum tendon length was less than 1.8% and 0.7% for the INF and DLT tendons respectively.

DISCUSSION

The advantages of this approach for measuring tendon deformation and strain are that it is accurate and precise, it allows for longitudinal studies to determine changes in tendon function over time, and it is capable of simultaneously measuring strain from multiple tissues or from multiple regions within the same tissue. In addition, surgically implanting the tantalum beads does not appear to alter joint function or cause any morbidity. This approach can likely be applied to a wide variety of tissues. Limitations of this approach are that high-accuracy biplane radiographic systems are not readily available and the process of verifying that the tendon beads do not move independent of tendon motion is a challenging task. Future studies will use this approach to measure in-vivo strain of various tendons and ligaments.

REFERENCES

[1] Fleming and Beynon. *Annals Biomed Eng*, 32(3):318-28, 2004. [2] Ravary et al. *Clin Biomech*, 19:433-447, 2004. [3] Tashman and Anderst. *J Biomech Eng*, 125(2):238-45, 2003.

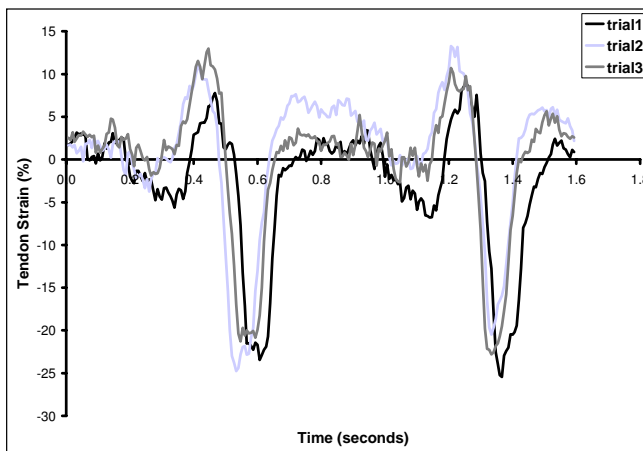


Fig. 1: Representative plot of INF tendon strain during three walking trials. Each trial consists of two complete gait cycles. Negative values indicate zero strain.

SHOULDER INTERNAL IMPINGEMENT: EFFECT OF HORIZONTAL ABDUCTION AND ANTERIOR CAPSULAR LAXITY

Teruhisa Mihata^{***}, Long Duong^{**}, Michelle H. McGarry^{**}, Thay Q Lee^{**}

^{*}Department of Orthopaedic Surgery, Takatsuki Red Cross Hospital, Osaka, Japan

^{**}Orthopaedic Biomechanics Laboratory, Long Beach VA Healthcare System and UC Irvine

INTRODUCTION

An impingement of the undersurface of the rotator cuff on the posterior superior labrum and glenoid during late cocking phase of throwing motion is called shoulder internal impingement. We hypothesized that hyper horizontal abduction in late cocking phase may result in pathologic shoulder internal impingement. The first objective was to assess the effect of shoulder horizontal abduction on shoulder internal impingement. Most of throwers have a stretched anterior shoulder capsule. The effect of stretched anterior shoulder capsule on shoulder internal impingement is still unclear. The second objective was to investigate the effect of the anterior capsular laxity on shoulder internal impingement.

METHODS

Eight cadaveric shoulders were tested using a custom shoulder testing system. Rotator cuff insertion points (supraspinatus anterior edge: SA, infraspinatus posterior edge: IP, middle point from SA to IP: MP) on humeral head were recorded using Microscribe (Immersion Corp, San Jose, CA) at maximum external rotation position. Glenohumeral pressure at maximum external rotation position was measured using Fuji-film. Rotational range of motion was measured by goniometer. Data were compared between scapular plane, 15° horizontal abduction from scapular plane, 30° horizontal abduction from scapular plane (simulated coronal plane), 45° horizontal abduction from scapular plane and between intact, after 20% stretching anterior capsule, and after anterior capsular plication. Data were analyzed using repeated measures analysis of variance followed by Tukey's post hoc test ($p < 0.05$).

RESULTS

SA and MP at 30° and 45° of horizontal abduction were significantly anteriorly located compared with SA and MP at scapular plane and 15° of horizontal abduction (Figure). IP at 45° of horizontal abduction was significantly anteriorly located compared with IP at scapular plane and 15° of horizontal abduction (Figure). SA at scapular plane after stretching was significantly posteriorly located compared with intact SA at scapular plane. Total pressure, peak pressure, and total area in posterior glenohumeral joint at 30° and 45° of horizontal abduction were significantly greater than those at scapular plane and 15° of horizontal abduction (Figure). External rotation at 30° and 45° of horizontal abduction was significantly less than that at scapular plane and 15° of horizontal abduction.

DISCUSSION

Cuff insertion points at maximum external rotation were moved to anteriorly with horizontal abduction. Cuff insertion points at more than 30° of horizontal abduction were anterior to the posterior edge of glenoid, suggesting that hyper horizontal abduction, which is greater than coronal plane, may result in pathologic shoulder internal impingement. Glenohumeral contact pressure increased with horizontal abduction. Anterior capsular condition may affect on shoulder internal impingement at low horizontal abduction..

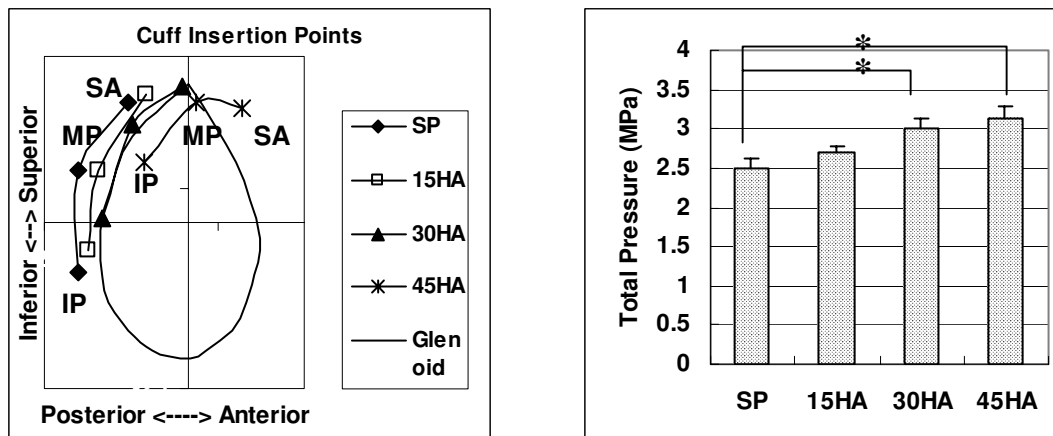


Figure: Left: Cuff insertion points at maximum external rotation. Right: Total pressure of posterior glenohumeral joint. SP: scapular plane, 15HA: 15° horizontal abduction, 30HA: 30° horizontal abduction, 45HA: 45° horizontal abduction, SA: supraspinatus anterior edge, IP: infraspinatus posterior edge, MP: middle point from SA to IP.

BIOMECHANICS OF ROTATOR CUFF REPAIR

N. Zheng, Ph.D. and H. Harris, M.D.

Biomechanics and Motion Analysis Lab, University of Florida, Gainesville, Florida
American Sports Medicine Institute

INTRODUCTION

The double-layer “anatomic” repair has been so successful for rotator cuff tears that it has become the standard for arthroscopic repair techniques. Understanding the biomechanics of the anatomic repair may provide some valuable information for functional tissue engineering. The *Permacol*[™] Surgical Implant (Tissue Science Laboratories plc, UK) is a chemically crosslinked, acellular sheet of collagen/elastin which is processed from porcine dermis. It has been clinically used for massive rotator cuff tear repair. The purpose of this study was to evaluate the anatomic repair during an ultimate strength test and a cyclic loading test. The ultimate strength and stiffness of a repair with the Permacol implant also were compared with repairs with rotator cuff tendons.

METHODS

Twenty-seven fresh frozen shoulder specimens were obtained for this study. Specimens were prepared to simulate a cuff defect and repaired using double layer miniopen procedure as previously described (Waltrip et al, 2003). Six shoulders and one Permacol implant were used for ultimate strength testing and 20 shoulders for cyclic loading testing. The ultimate strength tests were conducted at 25 mm/min, whereas the cyclic tests were conducted at 33 mm/sec and with peak force at 180 N and valley force at 10 N. Both tests were conducted using an 858 MiniBionix material testing system (MTS Systems Co., Eden Prairie, Minnesota). Data were collected at 100 Hz for strength testing and at peak and valley for cyclic testing.

RESULTS

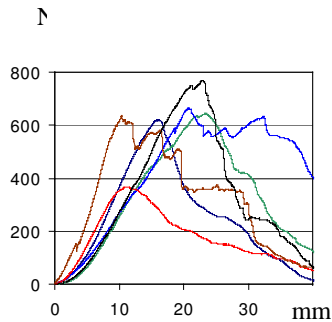


Fig. 1 Ultimate strength of anatomical repair

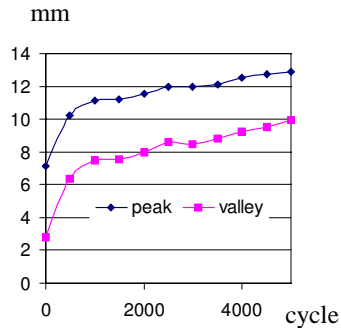


Fig. 2 Mean peak and valley displacement during cyclic test

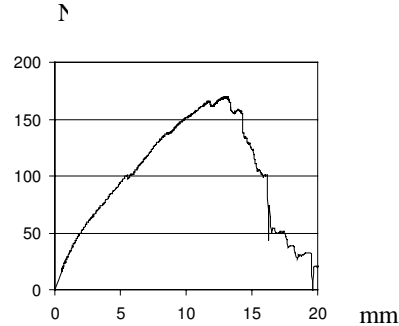


Fig. 3 Ultimate strength of anatomic repair with Permacol implant

Results are presented in Fig. 1, 2 and 3. The average ultimate strength of anatomical repair was over 600 N, whereas the ultimate strength of the repair with Permacol implant was less than 200 N. Seventeen of 20 specimens reached 5000 cycles. The tendon and repair complexes had about 7 mm displacement and 3 mm residual after the initial loading cycle. They reached 13 mm and 10 mm after 5000 cycles. The ultimate strength of the repair with Permacol implant was 165 N. The average stiffness of the repaired complexes was 37.5 N/mm with rotator cuff tendon and 12.6 N/mm with Permacol implant.

DISCUSSION

The double-layer anatomic repair was relatively strong, which may explain the good success of the repair. The repair with Permacol implant was not as strong and stiff as the repair with rotator cuff tendon. In the search for a graft of the rotator cuff tendon the ultimate strength and stiffness should be considered. An elastic graft may affect the force-length curve and function of the rotator cuff muscles. These insights may prove useful for functional tissue engineering.

REFERENCE

Waltrip et al: Rotator Cuff Repair – a biomechanical comparison of three techniques. *Am. J. Sports Med.* Vol. 31, No. 4, 493-7, 2003

COLLAGEN MATRIX TENSION REGULATES α -SMA EXPRESSION OF LIGAMENT FIBROBLASTS

Charu Agarwal, James H-C Wang[#]

MechanoBiology Laboratory, Departments of Orthopaedic Surgery and Bioengineering
University of Pittsburgh, Pittsburgh, PA, [#]412-648-9102, wanghc@pitt.edu

INTRODUCTION

Tension in wound healing sites was found to increase α -smooth muscle actin (α -SMA) expression in skin wounds (Hinz *et al.*, 2001). The expression of α -SMA signifies the presence of myofibroblasts, which produce excessive wound contraction and are responsible for tissue scarring (Nedelec *et al.*, 2000). Thus, this study was to determine the effect of matrix tension on α -SMA expression in ligament fibroblasts using a fibroblast-populated collagen gel (FPCG) model.

METHODS

Ligament fibroblasts were obtained from MCLs of three rats. To create FPCGs, 5×10^5 MCL fibroblasts/mL were incorporated into a collagen gel solution, made from the combination of collagen type I, 0.1 M NaOH, and 10x PBS. In free floating gel experiments, FPCGs were seeded in 6-well plates and either left attached to the bottom of the dish or completely released and left floating in medium (DMEM with 10% FBS and 1% P/S).

In addition, a dynamic culture force monitor system (DCFM) we have developed (Peperzak *et al.*, 2004) was used to quantitatively regulate collagen gel tension. Using the DCFM, gel tension was relaxed after 5 hrs.

To measure α -SMA protein expression, fibroblasts were removed from the collagen gels after 4 or 20 hrs for experiments in 6-well dishes and after 20 hrs for those connected to the DCFM and then lysed. Fibroblasts were assayed for α -SMA expression using Western blotting.

RESULTS

Expression of α -SMA was lower in free-floating FPCGs as compared to the anchored controls (**Fig. 1**). Free-floating FPCGs had about 75% and 60% α -SMA expression that of the anchored FPCGs at 4 and 20 hrs, respectively. In addition, relaxing the amount of tension in the matrix of FPCGs by 50 dynes, using the DCFM, decreased α -SMA expression to 69% of the tensioned controls (**Fig. 2**).

DISCUSSION

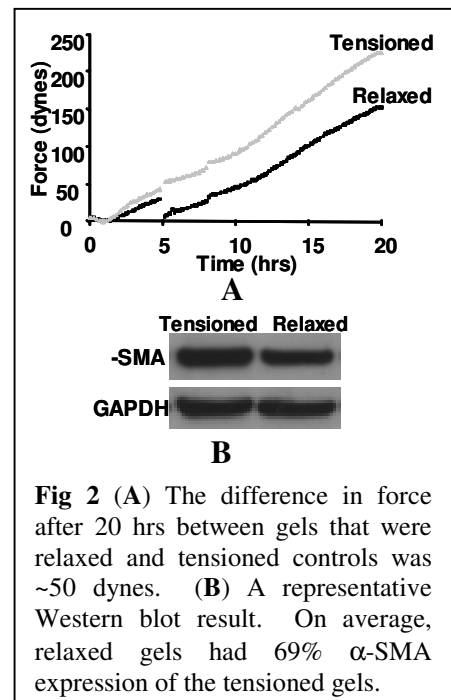
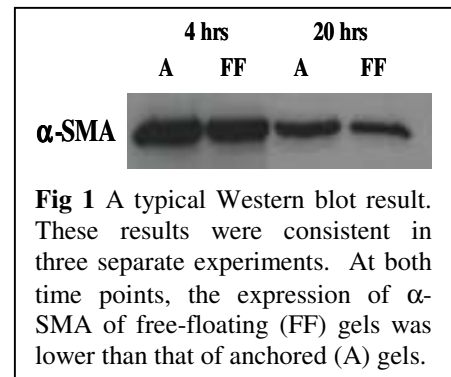
This study showed that decreasing tension in a collagen matrix decreases α -SMA expression. Since α -SMA is a specific marker of myofibroblasts, the result of this study indicates that matrix tension influences myofibroblast differentiation and hence tissue scarring. The result of this study is consistent with previous studies, which showed that α -SMA expression was lower in matrices no tension (i.e. free-floating collagen gels) compared to matrices with tension (i.e., anchored gels) (Grinnell 2000, Arora *et al.*, 1999). The unique feature of this study, however, was that it was able to use a novel system that can quantitatively alter the level of matrix tension over time. Future studies should look into the matrix tension-level dependent α -SMA expression and the relationship between matrix tension and collagen synthesis.

REFERENCES

Arora P *et al.*, *Am J Pathol*, 1999. Grinnell F, *Trends Cell Bio*, 2000. Hinz B *et al.*, *Am J Pathol*, 2001. Nedelec B *et al.*, *Hand Clin*, 2000. Peperzak, KA *et al.*, *Med Eng & Phys*, 2004.

ACKNOWLEDGEMENT

This work was supported in part by the Whitaker Foundation Grant and NIH AR049921 (JHW).



CONTRIBUTIONS OF AGING AND GENETIC BACKGROUND TO MOUSE KNEE LAXITY

Trevor Banack, Karl J. Jepsen, Evan L. Flatow, Vincent M. Wang
Department of Orthopaedics, Mount Sinai School of Medicine, New York, NY

INTRODUCTION

While ligament and tendon mechanical properties are known to decline with aging [7], the variation of normal joint laxity with age has not been well characterized. Recently, knee joint mechanics have been shown to demonstrate significant genotypic variability [1], consistent with clinical reports suggesting that joint laxity may be a heritable trait [3]. Therefore, the objectives of the present investigation were to quantify the effect of aging on knee joint laxity as well as to determine whether aging alters genotypic differences in joint mechanics.

METHODS

Female mice of two different age groups and three distinct genetic backgrounds were studied. The younger age group consisted of 16-week old A/J (n=7), C57BL/6J (B6, n=10), and C3H/HeJ (C3H, n=10) inbred mice. The older age group consisted of 37-week old A/J (n=8), 38-week old B6 (n=8), 62-week old B6 (n=8), and 43-week old C3H (n=7) mice. Following animal sacrifice, the right hind limb of each mouse was removed and dissected down to the knee joint while preserving the joint capsule. The proximal femur and distal tibia were potted in brass tubes using a quick-setting epoxy leaving the joint exposed.

Laxity tests were conducted at room temperature on a servohydraulic materials testing system (Instron 8872) as previously described [1,4]. Knees were positioned in 60° flexion [2] and preconditioned for 5 cycles using an antero-posterior displacement $d = \pm 0.25\text{mm}$. Due to the lower joint stiffness of the aged mice (of all inbred strains) and the 16-week A/J mice relative to those of the 16-week B6 and C3H groups, the laxity tests for the former group consisted of a displacement $d = \pm 0.75\text{mm}$ for 10 cycles, while the latter group was tested to $d = \pm 0.5\text{mm}$. This approach ensured loading into the lower linear region of the force-displacement curves for each of the different inbred strains and age groups.

For data analysis, a MATLAB program was used to fit three lines to both the upper ($\Delta d > 0$) and lower ($\Delta d < 0$) force-displacement curves, thereby partitioning each curve into a toe region and two linear regions [5]. Laxity was defined as the average displacement range of the toe region for the upper and lower curves. Toe and linear region stiffness data were calculated as the slopes of the respective linear regressions. Within each age group, joint laxity and stiffness data were compared among genotypes using a one-way ANOVA followed by Bonferroni post-hoc tests. For each inbred strain, a t-test was used to compare data between the younger and older age groups.

RESULTS

In comparison to the 16-week group, elderly A/J mice exhibited a significant ($p < 0.004$) increase in anterior and posterior stiffness but no differences ($p > 0.3$) in laxity and toe region stiffness were found. No significant differences ($p > 0.4$) in knee laxity and toe or linear stiffness were observed when comparing the 38-week and 62-week B6 mice, and therefore these data were pooled for statistical comparisons with the 16-week group.

	Laxity (mm)	Toe region stiffness (N/mm)	Anterior stiffness (N/mm)	Posterior stiffness (N/mm)
A/J*	0.8±0.1	1.0±0.6	2.0±0.9	2.4±0.7
A/J aged	0.8±0.1	0.8±0.5	3.9±1.1	3.9±0.7
B6*	0.5±0.1	1.4±0.7	4.5±1.3	4.9±1.2
B6 aged	0.8±0.1	1.4±0.8	4.1±1.8	4.8±1.9
C3H*	0.6±0.1	2.3±0.8	4.7±1.0	5.7±1.0
C3H aged	0.8±0.10	1.1±0.8	4.1±1.4	5.3±1.5

*: 16 weeks; for all strains, 16-week group not stat different from aged ($p > 0.08$)

Interestingly, elderly B6 and C3H mouse knees were significantly ($p < 0.0001$) more lax than those of their respective 16-week groups. In these inbred strains, no further differences ($p > 0.3$) could be attributable to aging with the exception of the C3H toe region stiffness ($p < 0.01$). For the elderly mice, no statistical differences ($p > 0.08$) were noted among inbred strains.

DISCUSSION

These results of the present study demonstrate that age-variations in knee joint function are strongly dependent on genotype. The knees of A/J mice, which were significantly more lax and less stiff than those of B6 and C3H mice at 16 weeks of age, showed increased stiffness in normal 37-week old mice. In contrast, B6 and C3H knees demonstrated increased laxity with aging. Among the aged animals studied, no significant differences in laxity and stiffness were observed. Furthermore, our findings are among the first to suggest that the development of spontaneous knee OA in elderly (>14 month) B6 mice [6] is not attributable to changes in joint laxity, as no significant differences were found in the laxity characteristics of 38-week and 62-week B6 knees.

REFERENCES [1] Banack T et al. *Trans ORS*. 2005; in press. [2] Blankevoort L et al., *J Biomech*. 1996; 29(6):799-806. [3] Bridges AJ et al., *Ann Rheum Dis*. 1992; 51(6):793-6. [4] Jepsen KJ et al. *J Biol Chem*. 2002; 277(38):35532-40. [5] Shrivastava N et al., *J Hand Surg [Am]*. 2003; 28(5):733-8. [6] Wilhelmi G and Faust R. *Pharmacology*. 1976;14(4):289-96. [7] Woo et al., in *Orthopaedic Basic Science*. 2nd Ed. 2000; AAOS, pp 581-616.

ELASTOGRAPHIC DETERMINATION OF STRAIN DISTRIBUTION AT THE ACL-BONE INSERTIONS

*J.P. Spalazzi, *E.E. Konofagou, and +*H.H. Lu

+*Department of Biomedical Engineering, Columbia University, New York, NY

INTRODUCTION

Over 250,000 Americans each year suffer anterior cruciate ligament (ACL) ruptures and tears, making the ACL the most commonly injured ligament of the knee[1]. The ACL inserts into bone through a transition zone consisting of ligament, fibrocartilage, mineralized fibrocartilage, and bone[2-4]. Autologous ACL grafts such as the hamstring tendon graft often fail at this junction, as the multi-tissue interface is never fully restored during the healing process[2]. Our long term goal is to regenerate the ACL-bone interface using a tissue engineering approach. To this end, an in-depth understanding of the structural and mechanical properties of the transition zone is needed in order to define relevant scaffold design parameters. To date, experimental determination of the mechanical properties and strain distribution at the interface have been difficult due to the small scale of the insertion area (<1mm). In this study, the localized strain distribution at the interface under tension will be imaged and identified using ultrasound elastography. Elastography allows the mapping of mechanical responses or properties *in vivo* or in the physiological setting of the tissue studied[5]. This novel method is ideal for examining the ACL-bone interface as it permits the characterization of a relatively small area of complex stress distributions. The ultrasound transducer scans the region of interest while an external load is applied to induce strain inside the tissue. Speckle tracking techniques are employed to analyze the collected radio-frequency (RF) ultrasonic data before and during incremental loading and to estimate the resulting strain[6].

MATERIALS AND METHODS

Ultrasound Scanning During Tensile Testing - Tibiofemoral joints of neonatal calves were isolated and mounted on an Instron MTS 858 Bionix Testing System (Fig. 1). The femur and tibia were aligned along the tensile axis and the sample was submerged in a saline bath during testing. The ACL was loaded at different strain rates and tested to failure while RF data were collected at 5 MHz. **Elastography and Image Analysis** - Axial strain elastograms between successive RF frames were generated using cross-correlation and lateral correction techniques using a 3 mm window size and 80% window overlap[6].

RESULTS

The interface between the ACL and the femoral (FI) or tibial (TI) bone was visible on the ultrasound images (Fig. 2A), and the largest displacement was observed in the ACL proper and femoral insertion (Fig. 2B). When the ACL-bone complex was tested in the tibial alignment on the MTS system, compressive strain was found at the tibial insertion, indicated by yellow-red regions on the elastogram (Fig. 2C, arrows). Regions of tensile strain are also observed at the interface as indicated by the blue regions (Fig. 2C).

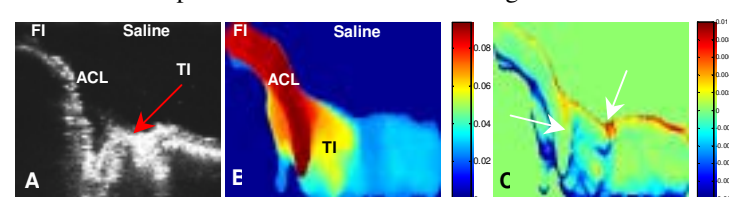


Figure 2: A) Ultrasound image of tibial insertion (posterior view), B) Corresponding displacement map (displacement in mm), C) Corresponding elastogram with arrows indicating compressive strain (yellow-red regions) at the insertion.

DISCUSSION

The results of this study demonstrate that the strain distribution throughout the insertions is highly complex, with both tensile and compressive strain localized at the insertion site. When tested under tension, the strain profile found at the interface was predominantly compressive in nature, while tensile strains were found at the ligament proper as expected. These preliminary results agree with those of FEM model predictions reported by Matyas *et al.* which predicted that when the medial collateral ligament (MCL) is under tension, the principle stress component found at the femoral insertion is compressive[5]. While the angle of insertion differs between MCL and ACL, fibrocartilage tissue, which is generally found in regions of compression, is the dominant tissue type seen at the insertions of both ACL and MCL. Ongoing studies focus on in-depth evaluation of the mechanical properties and the structure-function relationship existing at the ACL to bone insertion.

REFERENCES: 1) AAOS Publications,1998; 2) Weiler et al., *Arthroscopy*, 18(2):124-135,2002; 3) Gao et al., *J Anat* 188:367-373,1996; 4) Visconti et al., *Arch Biochem Biophys* 328(1):135-142,1996; 5) Konofagou, *Ultrasonics*, 42:331-336, 2004; 6) Konofagou and Ophir, *Ultrasound Med Biol*,24(8),1183-1199,1998; 7) Matyas et al., *J Biomech*, 28(2):147-157, 1995. **ACKNOWLEDGEMENTS:** Whitaker BME (Lu and Konofagou)

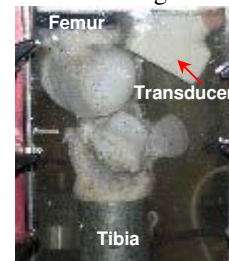


Figure 1. Tibiofemoral joint mounted in MTS

THE TENDON TRANSCRIPTOME: COMMONALITIES AND CONTRASTS IN GENE EXPRESSION BETWEEN MUSCLE AND TENDON +/- IL-1B

A.J. Banes^{1,2,3,4}, X. Yang¹, A.M.² Fox, A. Nation², J. Qi⁴.

Orthopaedics¹, Joint Biomedical Engineering Department², Curriculum in Applied and Materials Sciences³, University of North Carolina, Chapel Hill, NC, Flexcell Intl Corp⁴, Hillsborough, NC

INTRODUCTION: Tendon and muscle are physically connected at a musculotendinous junction. It was hypothesized that tenocytes and myocytes might share common characteristics despite their disparate roles as contractile organs and tensioning cables respectively. Moreover, results from a differential display experiment revealed that muscle genes such as titin were expressed in tenocytes both in vitro and in vivo. However, not surprisingly, tissues sampled from the midpoint of the murine gastrocnemius muscle or Achilles tendon, quite distant from the intersection of the two organs, expressed more genes in common than were different. We hypothesized that some subset of the tendon transcriptome might characterize tendon from muscle and vice versa. In addition, a separate gene array study was performed wherein human tenocytes were treated with IL-1b to drive a catabolic phenotype to simulate a pathologic condition in tendon. The hypothesis was that genes induced during matrix degradation would be stimulated and that other genes in catabolic pathways would be expressed as well.

Methods: Gastrocnemius muscle and Achilles tendon tissues were collected at their anatomic midpoints with separate sterile instruments and pooled from 6 wild type (*w/t*) mice (E129 genetic background) weighing 26 g and immediately frozen in liquid N₂. Tissues were thawed and homogenized with a TissueLyser in Trizol. Human tendon epitenon cells from the FDP were collected from surgical specimens, cultured in M199 in vitro and treated with 100 pM IL-1b for 6 h. Cells were used at passage three for gene array experiments. Nucleic acids were extracted, precipitated, and the samples subjected to DNase treatment. RNA was purified using Qiagen columns. RNA was eluted with water and stored in ethanol at -80C. Samples were reconstituted in water and the quality of the RNA checked by separation in an acrylamide gel with a ratio comparison of 18 to 28 S rRNA bands equal to 2. RNA was then prepared for a reverse transcriptase reaction using random hexamers to prepare cDNAs. Mouse Achilles tendon RNAs were reverse transcribed into cDNAs labeled with Cyanine 3- (green dye fluorophore, Cy3) as the control dye while gastrocnemius muscle RNAs were labeled with cyanine 5 (red dye fluorophore). cDNAs from each sample were mixed in equal proportions then hybridized with arrayed DNA sequences on either a UNC microarray chip with 20k genes or an Agilent DNA microarray chip with 40k genes. Hybridized arrays were then imaged and fluorescence quantitation was made for each dye and each spot. The ratio of fluorescence intensities for red and green for each spot is proportional to the relative abundance of each cDNA in the target specimens.

Results: Approximately 40,000 genes were assessed with the Agilent mouse microarray chip comparing tendon and muscle expression levels that were graded as positive. Data show the numbers of genes expressed most highly at 2,4,8 and 16 fold and higher in tendon or muscle. For instance, given a minimum of a 2 fold difference in gene expression as a baseline to determine differences, about 7% of the genes were expressed more in tendon than muscle, 1.27% at 4 fold, 0.41% at 8 fold, 0.178% at 16 fold. We used ArrayAssistTM by Ariadne (Stratagene) Sixty-eight genes had an expression level that was changed greater than 16 fold, however, only 49 of these had names attributed to them. Data show a cluster or connectivity diagram for the 49 most highly expressed genes with multiple associations with other proteins. Surprisingly, genes that were most highly expressed in tendon compared to muscle were loricrin and other keratins. Other highly expressed genes included a serine proteinase inhibitor, filaggrin, calmodulin, plakophilin and cartilage oligomeric protein, among others. For the +/- IL-1b-treated human tenocytes, about 2000 genes of 20k were 2 fold or more changed. Predictably, expressions of some of the MMPs were among the genes with the most dramatic change in expression. However, surprises in gene expression included mucin gene expression altered by IL-1b.

Discussion: These are the first results of gene array experiments revealing comparisons of tendon to a nearest neighbor tissue, muscle or to a treatment with a cytokine, IL-1b, thought to be involved in tendon pathology. Clearly, more similarities exist in expression types and amounts than do differences. Inspection of the entire gene list for lower fold changes in expression show other candidate genes such as tenomodulin, thought to be a marker for tendon, or titin, thought to be a marker for muscle that was expressed to an even greater degree in tendon. Further analysis of the data with data mining programs such as ArrayAssist, or other custom programs, will allow more insight into specific pathways, particularly those that result in a tenocyte marker list and a list of genes altered by pathology or mechanical load.

FUNCTIONAL TISSUE ENGINEERING OF LIGAMENTS AND TENDONS

Savio L-Y. Woo, Ph.D., D.Sc.

Musculoskeletal Research Center, Department of Bioengineering, University of Pittsburgh, Pittsburgh, PA, U.S.A.

Functional tissue engineering aims to develop biological substitutes to restore, maintain or improve tissue function based on principles and methods of engineering and life sciences toward structure-function relationships of normal tissues. The restoration of “function” as well as identification of critical structural and mechanical requirements are the most important consideration in designing, manufacturing and optimizing tissue engineered constructs.

These approaches have been recently been utilized to enhance the quality of healing ligaments. Known strategies include the use of growth factors, viral gene transfer technology, antisense gene therapy, biological scaffolds and so on. Specifically, the restoration of the morphological appearance and biochemical constituents, e.g. levels and types of collagen to improve the mechanical properties (or the quality) of the healing ligament have been explored.

Promising results with the use of antisense oligonucleotides to lower excessive decorin and collagen production (Types III & V) have been found in the healing MCL [1]. As a result, there was an increased larger collagen fibrils and a significant 85% increase in load to failure at 6 weeks under uniaxial tension. Most notably, when the collagen fibril diameters are regulated, the mechanical properties of healing tissue is improved.

Biological scaffolds, such as the porcine small intestinal submucosa (SIS), an organized natural scaffold composed mainly of aligned Type I collagen, has been used to promote cell migration and encourage revascularization [4,5]. In an *in vivo* animal study, the tangent modulus of a gap injured MCL followed by SIS treatment was found to be doubled compared to that of untreated controls at 12 weeks post-injury. Furthermore, this effect persisted up to 26 weeks post-injury. At which time the SIS-treated group continued to show a 33% higher tangent modulus than the non-treated group. Correspondingly, the ratio of collagen type VI was 28.4% lower and collagen fibril diameters were 22.2% larger than those for the non-treated group at 12 weeks.

With a greater understanding of the mechanisms behind these approaches, there is a possibility of developing new strategies to further improve the ligament healing process. Promising examples include functional tissue engineered scaffold with seeded cells, plus incorporating growth factors, antisense oligonucleotides and so on are being investigated. Should these treatment strategies be successful, there may be potential application to other tendons and ligaments that have little or no healing capability. To accomplish these, it is our belief that there must be an emphasis on bringing molecular biologists, biochemists, bioengineers, engineers, physical therapists, and clinicians to work together in a seamless manner for solving these extremely difficult problems. Only then will improved functional tissue engineering strategies be developed to restore normal ligament and tendon properties.

1. Shimomura T., Jia F., Niyibizi C., Woo S L-Y.: *Connective Tissue Research*. 2003;44(3-4):167-72.
2. Musahl V, Abramowitch SD, Gilbert TW, Tsuda E, Wang JH, Badylak SF, Woo S L-Y. *J Orthop Res* 2004;22(1):214-20.
3. Liang R, Moon, DK, Takakura Y, Jia FY, Abramowitch, SD., Woo, SL-Y. Functional tissue engineering can enhance the healing of the medial collateral ligament: a multidisciplinary study. Annual Meeting of Orthopedic Research Society. Washington DC. Feb.,16th-19th, 2005
4. Badylak S, Arnoczky S, Plouhar P, Haut R, Mendenhall V, Clarke R, et al. Naturally occurring extracellular matrix as a scaffold for musculoskeletal repair. *Clin Orthop* 1999(367 Suppl):S333-43.
5. DeJardin LM, Arnoczky SP, Clarke RB. Use of small intestinal submucosal implants for regeneration of large fascial defects: an experimental study in dogs. *J Biomed Mater Res* 1999;46(2):203-11.

EFFECTS OF INTRODUCING COLLAGEN SPONGE ON THE BIOMECHANICS AND HISTOLOGY OF STEM CELL – COLLAGEN GEL CONSTRUCTS FOR PATELLAR TENDON REPAIR

N. Juncosa-Melvin¹, D.L. Butler¹, G.P. Boivin¹, M.T. Galloway², C. Gooch¹, J.R. West³

¹ Departments of Biomedical Engineering and Pathology and Lab Medicine, University of Cincinnati, Cincinnati, OH; ²Cincinnati Sports Medicine and Orthopaedic Center, Cincinnati, OH. ³Wright State University, Dayton, OH.

INTRODUCTION

Tendon tissue engineering using mesenchymal stem cells (MSCs) and collagen gel is attractive [1-3] but repair stiffness and strength do not yet meet in vivo loading demands [4]. This study investigates the effects of introducing a collagen sponge scaffold on the biomechanics and histology of mesenchymal stem cell – collagen gel constructs for rabbit patellar tendon repair.

METHODS

Thirty-one 1yr-old NZW rabbits were assigned to two study groups. **Group 1 (n=16):** A cell-gel (CG) construct was formed by mixing MSCs (0.1M cells/ml) in 2.6 mg/ml of collagen gel before pipetting it into silicone dishes [3]. The construct was then implanted at surgery into a full-length central rabbit patellar tendon (PT) defect. **Group 2 (n=15):** A cell-gel-sponge (CGS) construct (same MSC and collagen gel concentrations as Gr. 1 but seeded onto a collagen sponge) was implanted in one knee and an acellular gel-sponge (GS) control construct was implanted in the other. The effects of adding the sponge to a cell-gel construct were determined by between subject comparisons of the biomechanics of the CG and CGS repairs. The effects of adding cells into gel-sponge constructs were determined by paired intra-animal comparisons of CGS and GS repairs. Repair specimens for biomechanical testing (n=12 for CGS and GS; n=13 for CG) were isolated and failed in tension from which force-elongation and stress-strain curves were plotted to determine structural and material properties. Results were also compared to peak in vivo force (IVF) and displacement (IVD) thresholds for normal tendon (N) [4]. Samples for histology (n=3 for each group) were stained with H&E for studying cellular alignment.

RESULTS

Adding the sponge significantly increased the structural and material properties of the cell-gel repairs ($p = 0.001$). Average maximum force and linear stiffness of the CGS repairs were approximately 60% and 75% of normal PT values compared to only 30% of normal for the CG repairs (Fig. 1). Maximum stress and modulus of the CGS repairs averaged 50% and 30% of normal PT values, compared to 30% and 20% of normal for the CG repairs [3]. The CGS repairs also matched normal tangent stiffness up to peak in vivo forces and displacements (IVF, IVD; Fig 1) and showed cellular alignment comparable to that of normal tendon. Adding cells to the gel-sponge constructs (CGS) also significantly increased repair properties compared to the acellular (GS) group ($p = 0.001$) although the increases were less than for adding the sponge to the cell-gel constructs (Fig. 1).

DISCUSSION

Cell-gel-sponge (CGS) repairs achieved higher maximum force, maximum stress, linear stiffness and modulus than cell-gel repairs (CG) without sponge [3] and gel-sponge repairs (GS) without cells. Ectopic bone was not seen in either treatment [2]. The combined improvements found when using cells and sponge are encouraging but each must be optimized. Further improvements in tangent stiffness are still likely required if these repairs are to exceed the current in vivo force and displacement thresholds associated with even higher activities of daily living [4]. We are currently examining other biomaterials as well as the effects of mechanically stimulating these constructs in culture before surgery with strain signals that mimic in vivo mechanical patterns [4].

ACKNOWLEDGMENTS. Partial support from NIH (AR46574).

REFERENCES. 1. Young et al, JOR, 1998. 2. Awad et al, JOR, 2003. 3. Juncosa-Melvin et al, Tissue Eng, in press. 4. Juncosa et al, J Biomech, 2003. 5. Butler et al, CORR, 2004.

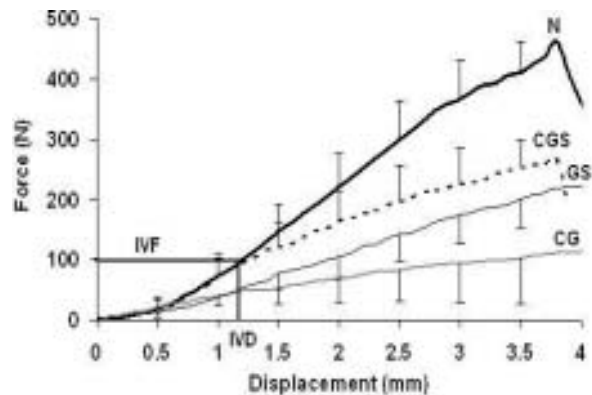


Fig. 1 Average (mean \pm SD) force vs. displacement curves for the normal PT (N; $n = 8$) [2], cellular (CGS; $n = 12$) and acellular (GS; $n = 12$) gel-sponge PT repairs, and cell-gel repairs without collagen sponge (CG; $n = 13$) [3]. IVF: in vivo force. IVD: in vivo displacement [5].

THREE-DIMENSIONALITY REGULATES SCLERAXIS EXPRESSION DURING TENOGENESIS OF MESENCHYMAL STEM CELLS

C.K. Kuo and R.S. Tuan

Cartilage Biology and Orthopaedics Branch, National Institute of Arthritis, and Musculoskeletal and Skin Diseases, National Institutes of Health, Department of Health and Human Services, Bethesda, MD

INTRODUCTION

Much work has investigated tissue engineering tendon and ligament with mesenchymal stem cells (MSCs) seeded in collagen type I gels maintained under static or dynamic tension [1-2]. Differentiation of the MSCs has been characterized by extracellular matrix molecule expression, collagen type I production, and morphological characterization of the tissue constructs. Scleraxis, a basic helix-loop-helix transcription factor, has recently been shown to be a specific marker for tendon and ligament during embryogenesis [3]. While the function of scleraxis has yet to be elucidated, it is expressed in the presumptive tendon progenitor cells during embryogenesis, and expression is continuous through tendon development. We have developed a system to investigate tendon and ligament engineering under the effects of tractional forces exerted by human, adult bone marrow-derived MSCs in three-dimensional (3D) constructs. We hypothesize that forced scleraxis expression will drive MSCs toward tenogenesis, and that differentiation will be further enhanced by cell and matrix alignment due to tractional forces exerted in a 3D construct. The current study focuses on the latter hypothesis by examining endogenous scleraxis expression as a function of three-dimensionality and static tension.

METHODS

Human MSCs were isolated from the bone marrow of femoral heads obtained from total hip arthroplasty, and expanded in monolayer cultures in vitro. MSCs were grown in both two-dimensional (2D) and 3D cultures. For 2D cultures (monolayer), cells were plated near confluency on tissue culture polystyrene. For 3D cultures, cells were suspended at 2×10^6 cells/mL in collagen type I solution with polymer concentration of either 1.5 or 3 mg/mL, poured into siliconized wells with and without 2 fixed point mounted dissecting pins 1 cm apart, and allowed to gel for 1-2 h at 37°C. The 2D and 3D cultures were maintained in basal medium at 37°C. Medium was changed every two days. Constructs were fixed, cryosectioned and stained with Hematoxylin-eosin (H&E), or picrosirius red for visualization of matrix alignment under polarized microscopy. Gene expression was analyzed by real-time RT-PCR for triplicate samples; reported values were normalized to GAPDH.

RESULTS

Three-dimensional cultures in both 1.5 mg/mL (3D 50%) and 3 mg/mL (3D 100%) gels with fixed points (anchored) contracted into long, thin constructs (Figure 1), whereas constructs cultured in the absence of fixed points (free) contracted into pellets. In anchored constructs, H&E staining showed cell alignment along the axis of tension (not shown), while polarized microscopy revealed birefringent fiber alignment in constructs cultured under tension (Figure 2).



Figure 1



Figure 2

At 11 days, scleraxis expression was significantly upregulated in MSCs of both 3D 50% and 3D 100% anchored constructs with respect to 2D cultures (Figure 3). In contrast, scleraxis expression of MSCs cultured in anchored constructs (3 mg/mL) was not significantly different than that of MSCs cultured in free constructs at 11 days (Figure 4).

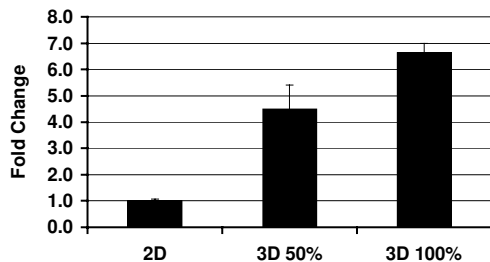


Figure 3

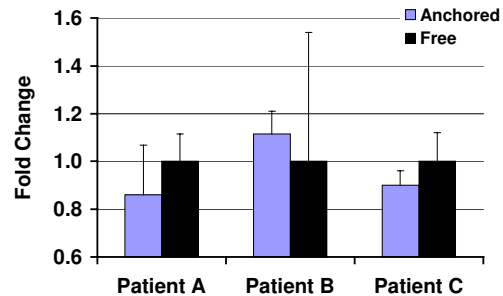


Figure 4

DISCUSSION

Scleraxis expression of MSCs in 3D constructs appeared to be regulated by the collagen concentration of the gel scaffold, as indicated by the significant increase in scleraxis expression when the collagen concentration of the gel was doubled. Static traction of the collagen gels did not significantly alter scleraxis expression in short term cultures (11 days).

REFERENCES: [1] Awad et al., *J Biomed Mater Res* 51: 233-240, 2000; [2] Altman et al., *FASEB J* 10.1096/fj.01-0656fje, 2001; [3] Schweitzer et al., *Development* 128:3855-3866, 2001

RECRUITMENT OF BONE MARROW DERIVED CELLS DURING ACHILLES TENDON HEALING IN A MOUSE MODEL

T. Zantop, T.W. Gilbert, S.F. Badylak

McGowan Institute for Regenerative Medicine, University of Pittsburgh, Pittsburgh, PA

INTRODUCTION

Acellular porcine small intestinal submucosa (SIS) has been shown to promote constructive remodeling of musculotendinous tissues in both preclinical studies (2, 3, 6) and clinical use(5). One of the contributing factors to this change in the normal healing process is thought to be the degradation product resulting from the ECM. It has been shown that an SIS bioscaffold is completely degraded within 3 months of implantation, and the degradation product has antibacterial activity(7), serves as a chemoattractant to endothelial cells(4), and recruits bone marrow derived cells to the site of healing(1). The purpose of this study was to determine the fate of bone marrow derived progenitor cells recruited to an injury site within the Achilles tendon of a mouse when treated with SIS compared to autologous tendon repair.

MATERIALS AND METHODS

Forty C57BL/6J mice with their bone marrow replaced with bone marrow from C57BL/6J mice that expressed green fluorescent protein (GFP) in all of their cells were anesthetized with isoflurane and a 1.5-2 mm gap was produced in each tendon. Half of the tendons were repaired by replacing the resected section and the other half were repaired with a single layer sheet of lyophilized SIS using 7-0 proline. Four animals from each treatment group were survived for 1, 2, 4, 8, and 16 weeks. At necropsy, the repaired tendon and the contralateral control were harvested and fixed in 4% paraformaldehyde. Histological sections were obtained for staining with H&E and Masson's trichrome, and for fluorescence microscopy.

RESULTS

At one and two weeks after surgery, both treatment groups showed a robust accumulation of GFP-expressing marrow-derived cells at the site of tendon remodeling in the SIS group, generally associated with areas of angiogenesis and inflammation. By four weeks after implantation, the SIS treated group showed an increased presence of GFP-expressing cells. By 16 weeks, the SIS treated group still showed GFP expressing cells in the body of the remodeled tendon, while the autologous repair group only had GFP expressing cells the fatty tissue surrounding the tendon as shown in Figure 1. In the SIS treated group, the GFP expressing cells also showed a variety of morphologies, although additional work is required to determine the phenotype of these cells.

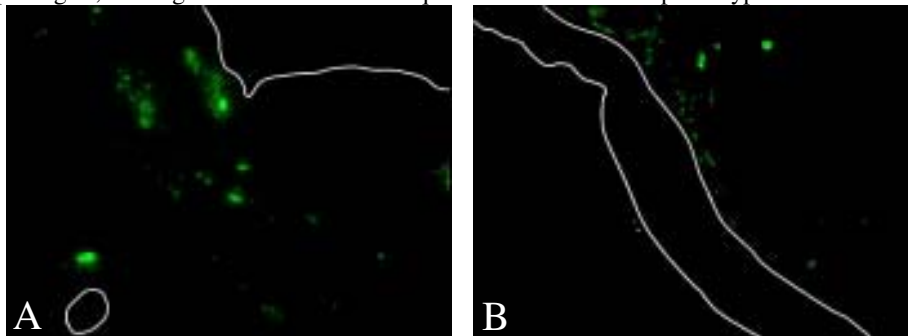


FIGURE 1. A) SIS Treated tendon and B) Autologous Repair after 16 weeks of healing. Green indicates GFP expressing cells and white outline indicates the outline of the tendon.

DISCUSSION

Previous studies have shown that degradation byproducts of ECM bioscaffolds are chemoattractant for numerous cell types including marrow-derived progenitor cells. We conclude that ECM bioscaffolds used for tendon repair support constructive remodeling of site specific tissue. We speculate that the constructive remodeling process is due at least in part to the presence of autogenous circulating marrow-derived progenitor cells that are attracted to the site of ECM remodeling, differentiate in response to local environmental cues, and contribute to tissue organization and differentiation.

REFERENCES

- 1) Badylak SF, et al. *Exp Hematol* 29:1310-8, 2001
- 2) Badylak SF, et al. *J Biomed Mater Res* 29:977-85, 1995
- 3) DeJardin LM, et al. *Am J Sports Med* 29:175-84, 2001
- 4) Li F, et al. *Endothelium* 11:199-206, 2004
- 5) Metcalf MH, et al. *Oper Tech Orthop* 12:204-8, 2002
- 6) Musahl V, et al. *J Orthop Res* 22:214-220, 2004
- 7) Sarikaya A, et al. *Tissue Eng* 8:63-71, 2002.

NOVEL MULTI-PHASED COMPOSITE SCAFFOLD FOR ACL-TO-BONE INTEGRATION

*J.P. Spalazzi, *K.L. Moffat, **S.B. Doty, and +*H.H. Lu

*Department of Biomedical Engineering, Columbia University, New York, NY

**Hospital for Special Surgery, New York, NY

INTRODUCTION

The anterior cruciate ligament (ACL) is the most often injured ligament of the knee, and reconstruction grafts are limited by donor site morbidity and/or the lack of a continuous interface with bone tissue[1]. The natural ACL-bone interface consists of three regions: ligament, fibrocartilage (non-mineralized and mineralized) and bone[2-4]. The degree of graft integration is a critical factor governing its clinical success and we believe interface regeneration will significantly improve the long term outcome. Our approach is to regenerate the interface through biomimetic scaffold design and the co-culture of osteoblasts and fibroblasts. The interface exhibits varying cellular, chemical, and mechanical properties across the tissue zones, which can be explored as scaffold design parameters. This study describes the design and testing of a multi-phased scaffold with controlled heterogeneity for the formation of multiple tissues. This continuous scaffold (Fig. 1) consists of three phases: Phase A for soft tissue, Phase C for bone, and Phase B for interface development. Each phase was designed with optimal composition and geometry suitable for the tissue type to be regenerated. Fibroblasts were seeded on Phase A and osteoblasts were seeded on Phase C, and the interactions of osteoblasts and fibroblasts (ACL and hamstring tendon) during co-cultures on the scaffolds were examined *in vitro*.

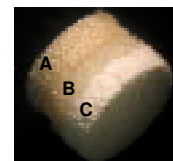


Fig. 1: Multi-Phased Scaffold

MATERIALS AND METHODS

Scaffold Fabrication and Characterization- Phases A, B, and C consist of poly(lactide-co-glycolide) (PLAGA,10:90) woven mesh, PLAGA (85:15) microspheres, and PLAGA(85:15)/Bioactive Glass (45S5,BG) composite microspheres, respectively (Fig. 1). The microspheres were formed via a double emulsion method[5], and the continuous multi-phased scaffolds were formed by sintering above the polymer T_g . Scaffold porosity and pore diameter were determined by porosimetry (Micromeritics, n=3) and the samples were tested under uniaxial compression (MTS 810, n=5) at 1.3 mm/min up to 5% strain with 10 N preload.

Co-Culture on Multi-Phased Scaffolds- Bovine and human osteoblasts (bOB and hOB), and bovine ACL fibroblasts (bFB) and human hamstring tendon fibroblasts (hFB) were obtained through explant culture. In experiment I, bOB and bFB (5×10^5 cells each/scaffold) were co-cultured on the scaffold, and cell viability, attachment, migration and growth were evaluated by electron and fluorescence microscopy. The bOB were pre-labeled with CM-DiI, and both cell types were labeled with calcein AM (Molecular Probes) prior to imaging. Matrix production and mineralization were determined by histology. After ascertaining cell viability on the scaffolds, a more extensive experiment using hOB and hFB was conducted in which cell proliferation and differentiation and above analyses were investigated. The mechanical properties of the seeded scaffolds were also measured as a function of culture time.

RESULTS

Mechanical and Structural Properties- Compression testing of scaffolds indicated an average modulus of 120 ± 20 MPa and yield strength of 2.3 MPa. The intrusion volume, porosity and pore diameter data are summarized in Table 1.

Table 1	Intrusion Volume (μL)	Porosity (%)	Mode Pore Diam. (μm)
Phase A	41 ± 8	58 ± 5	73 ± 11
Phase B	28 ± 7	34 ± 4	75 ± 7
Phase C	12.5	25.7	83

Cell Tracking and Morphology- The fibroblasts and osteoblasts were localized primarily at the two ends of the scaffolds after initial seeding, with few cells found in Phase B. After 28 days, both cell types migrated into Phase B (Fig.2-II), and extensive cell growth was observed in Phases A and C (Fig. 2-I, III).

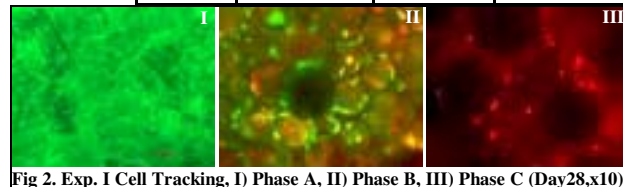


Fig 2. Exp. I Cell Tracking, I) Phase A, II) Phase B, III) Phase C (Day28,x10)

Extracellular Matrix Production- Extensive collagen-rich matrix production was found throughout the three phases at day 28 (Fig.3-I, III).

DISCUSSION

The biomimetic, multi-phased scaffolds supported the growth and ECM production of both osteoblasts and fibroblasts. After 28 days of culture, collagen production was evident in all three phases and mineralized matrix was found in the bone and interface regions. Osteoblast and fibroblast interaction at the interface (Phase B) suggests that these cells may play an important role in the development of a functional insertion site. These findings demonstrate that this novel scaffold is capable of simultaneously supporting the growth of multiple cell types and can be used as a model system to regenerate the soft tissue to bone interface. Future studies will focus on scaffold optimization and the development of the interface on the novel scaffold.

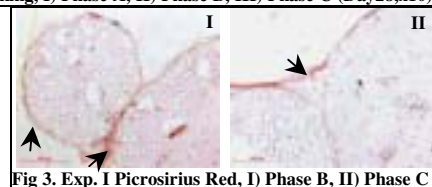


Fig 3. Exp. I Picrosirius Red, I) Phase B, II) Phase C

REFERENCES: 1) AAOS Publications, 1998; 2) Weiler, *Arthroscopy*, 18(2):124-135,2002; 3) Gao, *J Anat*,188:367-373,1996; 4) Visconti CS, *Arch Biochem Biophys* 328(1):135-142, 1996; 5) Lu, *J Biomed.Mater Res.*,1:64A(3):465-74,2003. **ACKNOWLEDGMENT:** Funding from the Whitaker Foundation – (HHL)

MECHANICAL STIMULATION OF TENDON TISSUE ENGINEERED CONSTRUCTS: EFFECTS ON CONSTRUCT STIFFNESS, REPAIR BIOMECHANICS AND THEIR CORRELATION

JT Shearn¹, N Juncosa-Melvin¹, DL Butler¹, GP Boivin¹, MT Galloway², W Goodwin¹, C Gooch¹

¹Departments of Biomedical Engineering and Pathology and Lab Medicine, University of Cincinnati, Cincinnati, OH; ²Cincinnati Sports Medicine and Orthopaedic Center, Cincinnati, OH

INTRODUCTION. Improving tendon repair using tissue engineering is attractive if repair properties can be improved. This study was designed to determine: 1) whether a mechanical stimulus delivered in culture would affect the in vitro construct stiffness as well as PT repair material and mechanical properties after surgery, and 2) if in vivo and in vitro linear stiffnesses are correlated.

METHODS. Nine 1 yr-old female NZW rabbits were used. Constructs were formed with 0.1×10^6 MSCs/ml in 2.6 mg/ml of collagen gel and incorporated into a type I collagen sponge. Stimulated (S) constructs received one cycle with a 4% peak strain (based on in vivo data [2]) every 5 minutes for 8 hours per day for 2 weeks. Non-stimulated (NS) constructs were also placed in culture for 2 weeks with no external strain. The in vitro constructs

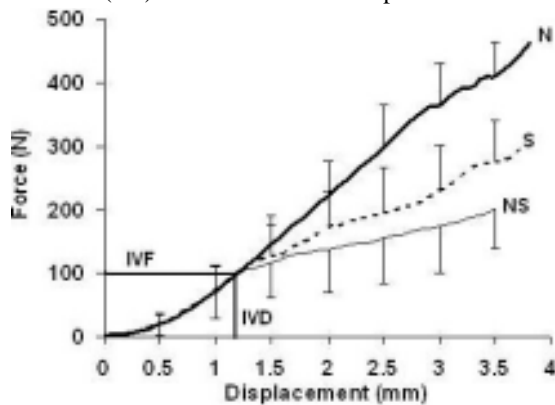


Fig. 2 Force-displacement curves (mean \pm SD) for normal PT (N; n = 8), non-stimulated (NS; n = 6), and stimulated repairs (S; n = 6). IVF: in vivo force. IVD: in vivo displacement [2,3].

after surgery were positively correlated ($R=0.6$; Fig. 3).

DISCUSSION. The stimulated constructs produced repairs that were equivalent to normal tissue 25% beyond recorded IVF and IVD thresholds. The moderate correlation between the in vitro and in vivo results represents, to our knowledge, the first time that in vivo outcome has been predicted from an in vitro parameter using matching cells and stimuli. Future studies will focus on optimizing the stimulus signal to produce the stiffest construct in vitro and the stiffest and strongest repairs in vivo. In particular, we will determine if in vivo strain profiles optimize construct and repair outcomes.

ACKNOWLEDGMENTS. Partial support from NIH (AR46574). John West for his assistance with mechanical testing.

REFERENCES. 1 Awad et al, JOR, 2003. 2 Juncosa et al, J Biomech, 2003. 3. Butler et al, CORR, 2004.

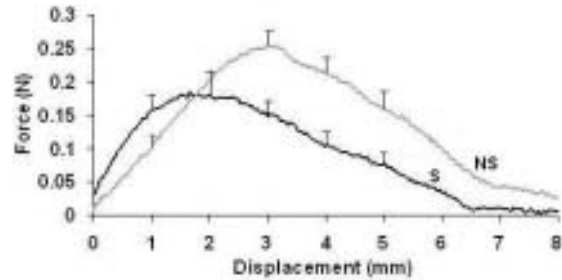


Fig. 1 Force-displacement curves (mean \pm SD) for the non-stimulated (NS; n = 9), and stimulated constructs (S; n = 9).

were failed in tension to determine linear stiffness. Identical, autogenous S and NS constructs were sutured into bilateral full-length central third PT defects at surgery. After 12 weeks, repair tissues were isolated and failed to determine mechanical and material properties. Repair tissues were also compared to normal tendon [1, 2] up to peak in vivo force (IVF) and displacement (IVD) thresholds [2, 3].

RESULTS. S constructs were 50% stiffer than NS constructs ($p = 0.054$, Fig. 1). S-based repairs also showed significantly greater load-related properties than NS controls ($p < 0.01$). Maximum forces for the S and NS groups averaged 307.5 ± 5.2 N and 269.9 ± 6.6 N (mean \pm SEM) and linear stiffnesses averaged 124.7 ± 4.2 N/mm and 83.2 ± 4.1 N/mm, respectively (Fig. 2). Tangent stiffnesses for the S-based repairs and normal tendon were similar up to 125N (Fig. 2). Construct linear stiffness at 14 days in culture and repair linear stiffness at 12 weeks

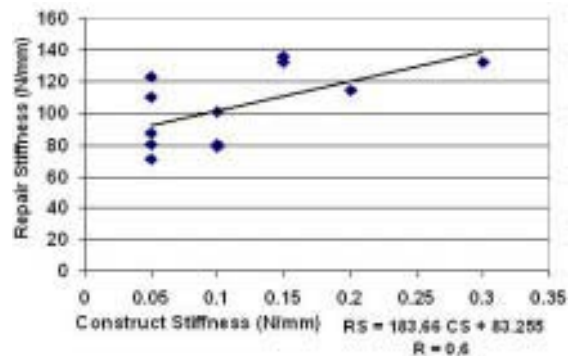


Fig. 3 Positive correlation between construct stiffness (at 14 days in culture) and repair stiffness 12 weeks after surgery.

A NOVEL LIGAMENT/TENDON TISSUE ENGINEERING GRAFT

HW Ouyang¹, JCH Goh^{1,2}, SL Toh², EH Lee¹

¹ Department of Orthopaedic surgery, National University of Singapore, Singapore

² Division of Bioengineering, National University of Singapore, Singapore

Introduction: Disadvantages of current therapies on tendon/ligament injuries have boosted research on tissue engineering strategy. In this strategy, the basic principle is to construct cell-scaffold composite. However, current cell seeding techniques are accompanied with some disadvantages, such as the low efficiency of cell attachment to fibre scaffolds and the limited nutrient transmission in gel system. Our previous studies [1,2] have shown that mesenchymal stem cells from bone marrow seeded on knitted PLGA scaffold with fibrin gel can improve Achilles tendon repair. However, when applied to anterior cruciate ligament reconstruction in the knee joint, it was found that cell-gel composite will separate from the scaffold during the joint movement. We recently found that mesenchymal stem cell from bone marrow can form cell sheets in vitro [3]. This study aims to fabricate the mesenchymal stem cell sheet for engineering ligament/tendon.

Method: After mesenchymal stem cells were isolated from bone marrow by adherence to plastic, they were cultured in the presence of ascorbic acid. Once a sheet of mesenchymal stem cells was obtained, it can be detached and assembled with the knitted scaffolds by wrapping technique. Then the assembled structure was held in place in cell culture condition for 4 weeks. The macro morphology, histology and biomechanics of the graft were evaluated.

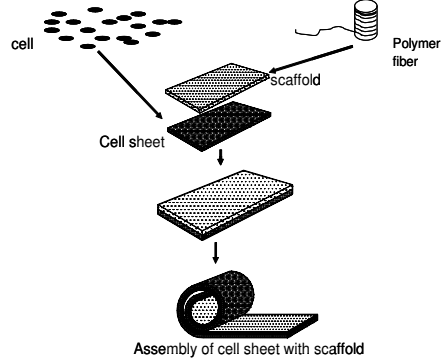


Fig.1. Procedure of fabricating and assembling bMSC sheet with knitted PLLA

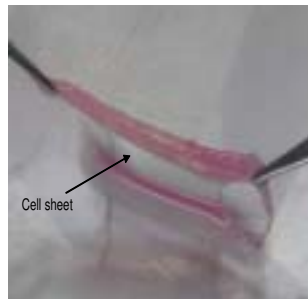


Fig.2 The Assembly of cell sheet with scaffold

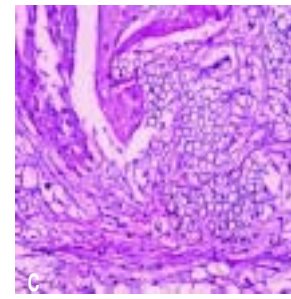


Fig.3. Cross-section of the ligament analogs after 4 weeks of culture (H&E, 100X)

Results: Bone marrow derived mesenchymal stem cells proliferated fast and could grow as multilayer. They formed cell sheet within 2 to 3 weeks under ascorbic acid. Once assembling cell sheet with macro-porous knitted PLGA scaffold, cell sheets adhered to scaffold firmly after short term culture. After 4 weeks of culture, the composite of cell sheet/PLGA scaffold looks like tendon/ligament analogs. Histology showed a large number of cells present in rich eosinophilically stained (H&E stain) connective tissue that filled and wrapped the scaffold. The mean tensile stiffness of cellsheet/scaffold group (n=6) and scaffold only group (n=6) were 20.6 ± 1.417 N/mm and 27.6 ± 1.449 N/mm respectively. The mean tensile stiffness of cellsheet/scaffold group was significantly lower than that of scaffold group ($p < 0.05$). The failure force of cellsheet/scaffold group and scaffold group were 46.68 ± 2.29 N and 43.58 ± 2.41 N respectively. The failure force of cell sheet/scaffold group was higher than that of scaffold group ($p < 0.05$).

Conclusion and Discussion: This study presented a novel technique of engineering ligament/tendon by assembling of mesenchymal stem cell sheet with macroporous fiber scaffold. It increases the cell-seeding efficiency and lessens the usage of biomaterials, then lessens the biomaterial related inflammatory reaction.

Reference:

1. Ouyang HW, Goh JCH, Mo XM, Teoh SH, Lee EH. The efficacy of bone marrow stromal cell-seeded knitted PLGA fiber scaffold for Achilles tendon repair. *Ann N Y Acad Sci.* Jun; 961:126-9. 2002.
2. Ouyang HW, Goh JCH, Thambyah A, Teoh SH, Lee EH. The use of knitted PLGA and MSCs for Achilles tendon repair in rabbit model. *Tissue Engineering.* Vol 9, No.3, 431-439, 2003

HUMAN FASCIA LATA AS A NATURAL SCAFFOLD FOR SOFT TISSUE REPAIR OR REINFORCEMENT

A.R. Baker, *J.P Iannotti, †K.A. Derwin

Cleveland Clinic Foundation, Dept. of Biomedical Engineering and the Orthopaedic Research Center, Lerner Research Institute, *Dept. of Orthopaedic Surgery, Cleveland, OH (†corresponding author: derwink@ccf.org)

INTRODUCTION

In recent years natural extracellular matrices (ECMs) have been marketed for clinical use as patches to reinforce soft tissue repair, several with specific indication for rotator cuff. These products include collagen-rich ECMs such as dermis (GraftJacket[®], Permacol[™], OrthoMend[™]) and small intestine submucosa (Restore[®]). Auto- and allograft fascia lata has been used clinically for tendon repair for several decades, and the biomechanical properties were shown to be on the same order as tendon (Butler, 1984). However, the concept of delivering fascia lata as an off-the-shelf product for soft tissue repair has not been explored or developed. Toward that objective, the aims of this study were twofold: 1) To assess the regional variability in mechanical properties of fresh human fascia lata; 2) To assess the effects of a proprietary allograft tissue processing method (ATP-ST), which utilizes antibiotic soak treatment and subsequent lyophilization, on the mechanical properties of human fascia lata.

METHODS

Ten pairs of human fascia were obtained from the Musculoskeletal Transplant Foundation (Edison, NJ). One from each pair was used to assess the biomechanical variability of fresh fascia, and the other to assess the effects of processing (antibiotic treatment and lyophilization). Each fascia was trimmed to ~6x12 cm, in alignment with the iliotibial tract. Four, 12x45 mm test strips were punched from the fresh fascia, one from each quadrant. Two, 12x45 mm test strips were punched from the processed fascia, one from each of two quadrants. Processed samples were rehydrated in physiologic saline (PBS) at 4°C overnight prior to testing. Sample thickness was determined using a constant pressure LVDT probe. Nominal gage length was 30mm. Samples were tested in PBS at 37°C. Samples were preconditioned 5X to 2N and then pulled immediately to failure at 10 mm/min. Modulus_{G2G} and stiffness were determined using grip-to-grip displacements from the slope of the stress-strain and load-displacement curves between 4.5–5.5% strain. To evaluate the within donor variability in fresh fascia, a random effects linear model was fit to the variables of interest (Cross-Sectional Area, Modulus_{G2G}, and Stiffness). To assess whether a systematic difference in locations existed in any of the measures, the quadrant was included in the random effect model. A paired t-test was used to assess differences between the two treatment groups. A *p*-value of 0.05 was considered significant.

RESULTS

For fresh fascia, the effect of quadrant was not significant for any parameters measured. Therefore, the four strips from each 6x12 cm fascia sample were considered equivalent and, thus, repeated measures for that sample. The average properties of fresh and processed fascia are given in Table 1. There was a significant difference in the measured cross-sectional area between groups; however there was no difference in stiffness or modulus.

DISCUSSION

Our findings suggest that there is minimal variability in mechanical properties within a defined 6x12 cm region of the iliotibial tract of human fascia lata. However, it should be noted that estimates of variability both between and within donors were generally imprecise because of the relatively small number of donors assessed. Secondly, the initial processing steps in the development of human fascia as a market-ready biological scaffold did not alter the biomechanical properties. The measured biomechanical properties for both fresh and processed groups were similar to what has been reported previously for human fascia, and at physiologic strain (~5%) the modulus of human fascia is on the same order as tendon (Butler, 1984). Together, these results demonstrate that antibiotic treated / lyophilized human fascia lata has favorable biomechanical properties for tendon repair or reinforcement. Further development of this product is ongoing.

ACKNOWLEDGEMENTS: Musculoskeletal Transplant Foundation (Edison, NJ) for funding and support.

REFERENCES: Butler DL, *et al.*, *J Biomech* 17: 579-596, 1984.

	Fresh (<i>n</i> = 10, 4 repeated measures each)	ATP-ST/Lyophilized (<i>n</i> = 10, 2 repeated measures each)	<i>p</i> -value
Cross-Sectional Area (mm ²)	6.7 ± 1.4	8.4 ± 1.6	.02*
Stiffness (N/mm)	85.1 ± 15.4	98.2 ± 16.2	.08
Modulus _{G2G} (MPa)	385.9 ± 57.0	360.7 ± 90.9	.47

* *p*-value < 0.05 considered significant

AN EXPANDED FUNCTIONAL TISSUE ENGINEERING PARADIGM: APPLICATION TO LIGAMENT AND TENDON TISSUE ENGINEERING

David L. Butler

Department of Biomedical Engineering, University of Cincinnati, Cincinnati, OH

Since first introduced in 2000 [3], functional tissue engineering has sought to create more effective repair constructs by 1) measuring activity-related in vivo forces and deformations acting on normal tissues that later require repair [7,8,10,11,13], and 2) delivering these mechanical signals to tissue engineered constructs while still in culture to precondition them to their future environment [3-5,12]. This approach is particularly important for cell-scaffold constructs [1,2,6,9,14] that have the capacity to heal tendon and ligament injuries but are often too compliant and weak to withstand in vivo forces post surgery. Biomaterials selection is critical to protecting the constructs while avoiding stress shielding of the cells. Mechanical stimulation is just now being shown to stiffen both the constructs in culture and the repairs after surgery [12] but the pattern of these signals (e.g. amplitude, frequency, duration, duty cycle, time of first exposure) has yet to be optimized. Developing in vitro predictors of in vivo repair outcome is also appealing to speed development while reducing repeated in vivo studies [12]. The same applies for chemical stimulation which could benefit construct and repair properties if only the timing, concentrations, patterns, and types of growth factors delivered to the cells could be optimized. Ultimately, improving repair stiffness to rapidly match the biomechanics, structure, chemistry, and biology of normal tissue in the expected range of in vivo utility will likely require that functional tissue engineering parameters (FTEPs) be identified and that mechanical, chemical and possibly other stimuli be applied in a coordinated and timely manner [5]. This presents a substantial experimental design challenge given the extremely large number of treatment combinations and permutations that can be imposed. Simple yet effective statistical design strategies will be required that rapidly identify the primary treatment factors and repeatedly sample potential interactions. Decisions to limit the number of animal and tissue models may also be needed to establish well-understood systems to assess these treatment factors. The large number of resulting datasets must also be managed as a type of “bioinformatics” problem to better correlate relevant biomechanical, structural, biological, and clinical response measures.

Other challenges must also be addressed to create truly functional tissue engineered constructs. 1) Tissue engineers will need to consider growth and development questions as they attempt to create cell-based constructs in a time frame of weeks when normal development and maturation of a tissue occurs over a matter of years. 2) This “mapping” process may need to consider not only donor age but the age, type, and gender of the cell source to be implanted at surgery. 3) Finally, the tissue engineer will need to account for the “chronicity” of the injury site into which the construct will be placed, given that early inflammation can be expected in acute injuries and that increased laxity of secondary structures will likely occur in the neighborhood of the injury in chronic cases.

Ligament and tendon tissue engineering could and should lead the way in these efforts, given the highly-organized and more linear nature of the structures and our extensive cell, matrix, and in vivo signaling databases. However, cooperative efforts will be required among engineers, biologists, and clinicians if we are to succeed in creating, assessing and utilizing these tissue engineered structures in the near future.

ACKNOWLEDGMENTS. Partial support from NIH (AR46574 and EB002361) and Cincinnati Sports-medicine and Orthopaedic Center. Special thanks for discussions and research contributions from Drs. Jason Shearn, Shawn Hunter, Greg Boivin, Marc Galloway, and Matthew Dressler, Ms. Natalia Juncosa-Melvin, Mr. Victor Nirmalanandhan, Mr. Kumar Chokalingam, Ms. Cindi Gooch and Ms. Wendy Goodwin.

REFERENCES. 1. Awad HA et al, Tissue Engr. 5:267, 1999. 2. Awad HA, et al, J. Orthop Res. 21:420, 2003. 3. Butler, DL et al, J. Biomech. Engr. 122:570-575, 2000. 4. Butler DL.,et al, Annu Rev Biomed Eng 6: 303, 2004. 5. Butler, DL et al, Clin Orthop Relat Res, 427-S, S190, 2004. 6. Chokalingam K et al, ISLT, 2005. 7. Holden, JP, et al, J. Biomech 27:517, 1994. 8. Juncosa, N, et al, J Biomech 36: 483, 2003. 9. Juncosa-Melvin N, et al, ISLT, 2005. 10. Korvick, DL, et al, J. Biomech 29: 557, 1996. 11. Malaviya, P, et al, J Biomech 31: 1043, 1998. 12. Shearn, JT, et al, ISLT, 2005. 13. West, JR; et al, J. Biomech 37: 1647, 2004. 14. Young R, et al, JOR 16:406, 1998.

IN VIVO DEGRADATION OF AN ECM BIOSCAFFOLD FOR ACHILLES TENDON REPAIR: IMPORTANCE FOR CONSTRUCTIVE REMODELING

A.M. Stewart-Akers¹, A. Simmons-Byrd², S.F. Badylak¹

¹ McGowan Institute for Regenerative Medicine, University of Pittsburgh, Pittsburgh, PA USA

² ACell, Inc., West Lafayette, IN USA

INTRODUCTION

Bioscaffolds derived from porcine (xenogenic) extracellular matrix (ECM) have been used successfully as templates for tendon and ligament repair in both preclinical animal studies and in human clinical applications¹⁻⁴. Naturally occurring bioscaffolds that are not chemically crosslinked show rapid *in vivo* degradation⁵ with replacement by host tissues that in turn modulate their structure and function in response to local environmental stressors such as mechanical loading. The objective of the present study was to quantify the rate of degradation of an ECM bioscaffold derived from the small intestinal submucosa (SIS) that is currently used for Achilles tendon repair in humans. In addition, we sought to identify the biologic fate of the ECM degradation products.

MATERIALS AND METHODS

Twelve adult female dogs were divided into six groups of 2 dogs each. All dogs were subjected to segmental resection of 1.5 cm of the Achilles tendon and replacement of the missing segment by an ECM bioscaffold composed of ¹⁴C labeled SIS. The animals were placed in a tube splint to allow immediate partial weight bearing. The splint was removed after 28 days and the dogs allowed free ambulation without external support. One group of animals was sacrificed at each of the following timepoints: 3, 7, 14, 28, 60, and 90 days post-surgery. Quantitative measurements of ¹⁴C were made and histopathologic examination of excised tissue was performed. The ¹⁴C concentration of excretion products, blood, and tissues was monitored for all animals during the recovery period and at the time of sacrifice.

RESULTS

Immediate degradation of the ECM bioscaffold began following surgical implantation. Twenty percent of the ¹⁴C labeled SIS bioscaffold was degraded by 14 days post-surgery, and 60% was degraded by 28 days post-surgery. Virtually all of the ECM bioscaffold was degraded and replaced by host tissue at 60 days post-surgery. Histopathology showed constructive remodeling of the replaced SIS-ECM scaffold with organized dense and vascular collagenous tissue within the first 28 days. There was increased organization of the connective tissue into a tendon-like structure following removal of the tube splint. Greater than 95% of the ¹⁴C labeled degradation products were eliminated via urinary excretion.

DISCUSSION

Degradation of naturally occurring bioscaffolds composed of ECM occurs rapidly and completely. Well differentiated tendon-like tissue forms at the site of scaffold degradation. Bioscaffold degradation products are eliminated via urinary excretion. Complementary studies have shown that ECM degradation products play an active role in the remodeling process. Local tissue stressors such as mechanical loading are important in the remodeling process.

1. M Metcalf, FH Savoie, B Kellum. Surgical technique for xenograft (SIS) augmentation of rotator-cuff repairs. *Oper Tech Orthop.* 12:204. 2002.
2. LM DeJardin, SP Arnoczky, BJ Ewers, RC Haut, R Clarke. Tissue-engineered rotator cuff tendon using porcine small intestinal submucosa. Histologic and mechanical evaluation in dogs. *Am J Sports Med.* 29:175. 2001.
3. LM DeJardin, SP Arnoczky, RB Clarke. Use of small intestinal submucosal implants for regeneration of large fascial defects: an experimental study in dogs. *J Biomed Mater Res.* 46:203. 1999.
4. SF Badylak, R Tullius, K Kokini, KD Shelbourne, T Klootwyk, SL Voytik, MR Kraine, C Simmons. The use of xenogenic small intestinal submucosa as a biomaterial for Achilles tendon repair in a dog model. *J Biomed Mater Res.* 29:977. 1995.
5. SF Badylak, B Kropp, T McPherson, H Liang, PW Snyder. Small intestinal submucosa: a rapidly resorbed bioscaffold for augmentation cystoplasty in a dog model. *Tissue Eng.* 4:379. 1998.

NOVEL MICRO-PATTERNED FLUIDIC SYSTEM FOR OSTEOBLAST AND FIBROBLAST CO-CULTURE

J. Tsai, I.E. Wang, L.C. Kam and H.H. Lu

Department of Biomedical Engineering, Columbia University, New York, NY

INTRODUCTION

The anterior cruciate ligament (ACL) is the major intrarticular ligament of the knee and injuries to the ACL are largely repaired using semitendinous grafts. However, a significant limitation of this type of reconstruction grafts is its inability to integrate and re-establishing a continuous interface with bone tissue[1]. The native ligament to bone interface spans less than 400 μ m[2], arranged linearly from ligament to fibrocartilage and to bone[3], and it acts to minimize stress concentrations across soft and hard tissue. We believe that interface regeneration will improve the integration of semitendinous grafts. Currently, the mechanisms behind interface formation and regeneration are not known. It has been reported that over time *in vivo*, a fibrocartilage layer interfacing tendon and bone is formed within the bone tunnel[4]. Thus, we hypothesize that fibroblasts (fb) and osteoblasts (ob) interactions play an important role in interface formation. In order to evaluate the interactions between osteoblasts and fibroblasts, we have developed novel *in vitro* microscale co-culture models of these cells. This micro-co-culture system mimics the microscale of the native interface, and utilizes microfluidics to exert spatial control in cell distribution (Fig. 1b). This model can be used to examine how cell-cell interactions may regulate interface formation locally at the micro-scale. The objective of this study is to optimize the fabrication parameters of this model and begin initial evaluation of osteoblastic and fibroblastic responses using this system.

MATERIALS AND METHODS

Channel Design: Channels were designed having a bimodal non-intersecting serpentine geometry with 200 μ m features. The design was implemented using SU-8 25 (Microchem) photoresist[5] and a mold was patterned using Polydimethylsiloxane (PDMS, Dupont). In this design, osteoblast and fibroblast channels were first separated by PDMS, which was later removed to allow cell to cell interactions.

Osteoblast-Fibroblast Co-Culture: Bovine primary osteoblasts and fibroblasts were obtained from explant cultures, and grown in supplemented DMEM at 37°C and 5% CO₂. Osteoblast or fibroblast suspension (20x10⁶ cells/ml) was perfused into its respective microchannels. Cells were allowed to attach for 1hr prior to PDMS removal. Cell migration was tracked by labeling fibroblasts with CM-DiI and osteoblasts with CFDA-SE (Molecular Probes) prior to seeding. **Cellular Response:** Analyses were performed at 1, 2, 6 days. Alkaline Phosphatase (ALP) activity was ascertained with Fast-blue stain (Sigma), and type-I collagen deposition was examined by immunohistochemistry (Chemicon).

RESULTS

Cell Proliferation: Both cell types migrated and proliferated beyond their initial seeding zone (Fig.2) and grew into physical contact by day 1. Local confluency and cross-migration were seen at day 2.

ALP Activity and Type-I Collagen Deposition: ALP activity was observed in the osteoblast region (Fig. 3a), while type-I collagen was found in all regions (Fig. 3b).

DISCUSSION

We have reported here on the development of a novel osteoblast-fibroblast co-culture model. The interactions between these cells in a micro-co-culturing environment were examined. Both cell types proliferated beyond the initial seeding region and maintained their phenotypes as indicated by ALP activity of osteoblasts and type-I collagen deposition by these cells. The cell-to-cell cross-migration at day 2 resulted in a host of homotypic and heterotypic cell interactions which we will evaluate in depth in future studies. In summary, micropatterning of multiple cell types offers a unique opportunity to control the local micro-environment and permit the in-depth examination of cell-cell interactions. This understanding will aid in the identification of mechanisms driving interface formation.

REFERENCE

1) Jackson et al., Am. Acad. Orthop. Surg. Bull. 40, 10-11, 1992. 2) Cooper et al., J. Bone Joint Surg. 52A:1-20. 3) Wang et al., ORS transaction paper 138, 2004. 4) Rodeo et al., J. Bone Joint Surg. 75A:1795-1803, 1993. 5) Wu H. et al., J. Am. Chem. Soc. 2003 Jan 15; 125(2):554-9.

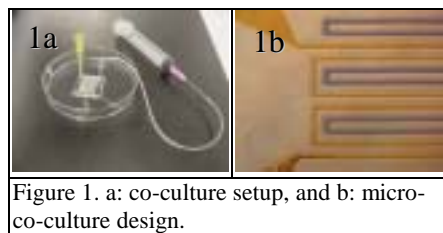


Figure 1. a: co-culture setup, and b: micro-co-culture design.



Figure 2. fb and ob in co-culture, 5x. (from left to right): day 0, day 1, day 2. yellow: fb, green: ob. (scale bar = 200 μ m)



Figure 3. a: ALP stain on fb (yellow) and ob, day 2, 20x. b: type I collagen stain, day 6, 20x.

IL-1 β INCREASES THE TRANSCRIPTION OF ELASTIN IN HTIF-POPULATED BIOARTIFICIAL TENDONS

Jie Qi¹, Liquan Chi¹, Donald Bynum², Albert J. Banes^{1,2,3,4}

Flexcell International Corporation¹, Hillsborough, NC, Orthopaedics Department², Biomedical Engineering³, Applied and Materials Sciences⁴, University of North Carolina, Chapel Hill, NC.

INTRODUCTION Elastin is responsible for the elastic properties of vertebrate tissues. It is especially important in tissues that undergo repetitive physical deformation or strain, such as lung, blood vessels and tendon. The elastic properties are also a major aspect for engineered tissues. Therefore, the regulation of elastin expression is important for both in vivo and in vitro applications. However, elastin mRNA has a short half-life. The steady state mRNA level may be increased either by stabilizing mRNA or increasing transcription rate. Human recombinant interleukin-1 β (rIL-1 β) can regulate elastin expression, either increasing or decreasing it depending on the cell type and culture conditions (1, 2). In this study, results indicated that IL-1 β increased the steady state level of elastin mRNA by stimulating its transcription in human tendon internal fibroblast-populated bioartificial tendons.

METHODS Primary human tendon internal fibroblasts (HTIFs) were isolated from discarded human tendon tissue as described previously (3). HTIFs from passages 2-4 were used in this study. Bioartificial tendons (BATs) were fabricated at a cell density of 2×10^5 cells/200 μ L collagen gel suspension/BAT (Vitrogen) (4). BATs were incubated at 37 $^{\circ}$ C for 24 h before addition of 100 pM rIL-1 β , 10 μ g/mL cycloheximide or 7 μ g/mL actinomycin D. BATs were collected 24-hour post-addition of rIL-1 β and/or cycloheximide or actinomycin D. Total RNA was isolated and quantitative RT-PCR was carried out to check the expression level of elastin. Results were confirmed with HTIFs from two patients.

RESULTS The expression of elastin is regulated mainly at the mRNA and splicing levels. rIL-1 β increased elastin level without changing its splicing (Fig. 1). Cycloheximide (inhibitor of protein synthesis) increased the elastin steady state mRNA level both in the presence and absence of rIL-1 β (Fig. 2). This result may be due to the inhibition of the on-going synthesis of proteins which stabilize elastin mRNA. Actinomycin D, a transcriptional inhibitor, blocked the effect of rIL-1 β on elastin expression (Fig. 2).

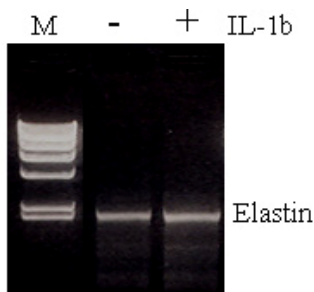


Figure 1. RT-PCR of full length elastin. M, λ /HindIII DNA marker. -/+ , without and with rIL-1 β . cDNA of IL-1 β treated sample was diluted 10 fold. IL-1 β did not change the splicing of elastin mRNA

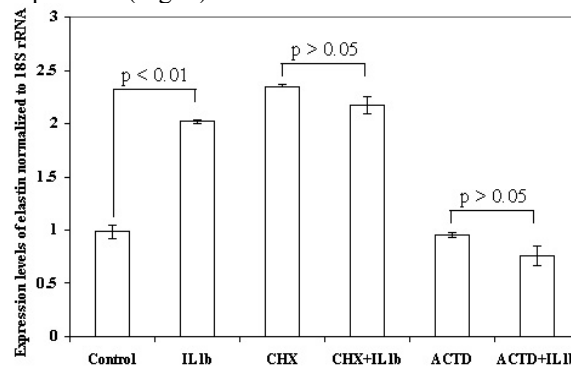


Figure 2. Regulation of elastin by rIL-1 β in the absence or presence of cycloheximide or actinomycin D. CHX, cycloheximide; ACTD, actinomycin.

DISCUSSION

Elastin provides elasticity to the matrix of soft connective tissues. These results indicate that rIL-1 β increased elastin expression at least partially, if not totally, through stimulating its transcription.

REFERENCES

1. Mauviel et al., 1993: JBC, 268: 6520-6524. 2. Berk et al., 1991: JBC, 266: 3192-3197. 3. Banes et al., 1988: Tendon Synovial Cells Secrete Fibronectin In Vivo and In Vitro. J Ortho Res. 6: 73-82. 4. Garvin et al., 2003: A Novel System for Engineering Bioartificial Tendons and Application of Mechanical Load. Tissue Engineering: 967-979.

ACKNOWLEDGEMENTS: Flexcell International Corporation. Albert J. Banes is president of Flexcell International Corporation and is compensated as such.

TYPE I COLLAGEN EXPRESSION IN MECHANICALLY STIMULATED MENSENCYHMAL STEM CELLS

K. Chokalingam¹, S.A. Hunter¹, C.G. Gooch¹, J.L. Florer², D.L. Butler¹, R.J. Wenstrup²

¹Noyes Tissue Engineering Laboratory, Dept. of Biomedical Engineering, University of Cincinnati, Cincinnati, Ohio

²Dept. of Pediatrics, Division of Human Genetics, Cincinnati Children’s Hospital Medical Center, Cincinnati, Ohio

INTRODUCTION

Functional tissue engineering is an attractive alternative for treating tendon and ligament injuries. However, tissue engineered products are hampered by long development cycles which are expensive and time consuming. Hence, a real time assessment technology to shorten product development cycles would be of great value towards clinical application. Of particular interest is a rapid method for evaluating the influence of mechanical stimulation on cell phenotype, cell differentiation, and extracellular matrix production, especially that of collagen. Our objectives were to 1) create a transgenic mouse having a type I collagen promoter enhanced yellow fluorescent protein (EYFP) that is activated when type I collagen is produced and 2) analyze the effects of dynamic tensile strain on EYFP expression in transgenic mesenchymal stem cells (MSCs) placed in cell-carrier constructs.

METHODS

MSCs were harvested from the femoral and tibial bone marrow of six-week old transgenic mice (three mice from two transgenic lines) containing human type I collagen promoter EYFP. Cells were grown in monolayer for 7 days and then placed into 3-D constructs in culture. Gelatin-based sponges (Surgifoam 1975; Johnson & Johnson) alone and in combination with agarose (2% w/v) were chosen as biomaterials. Sponges were cut to fit within wells in a custom silicone dish having two posts to provide a means for loading. Two conditions (free swelling and dynamic tensile loading) were examined. The experimental design is shown in Table 1. A total of four constructs, one in each group, was made per animal. Each construct was seeded with 250,000 cells. Groups B and D were subjected to a 4% tensile strain in a custom pneumatic system at 1 Hz for 6 mins followed by a rest period of 18 mins. This was repeated 60 times a day for 12 days. Feeding media (BGJb supplemented with 10% fetal calf serum) was replaced every other day. After day 12, slices of the constructs (1-2 mm thick) randomly selected from the area between the posts were examined using a Zeiss Axiovert fluorescent microscope (Groups A & B) or a Zeiss LSM 510 confocal microscope (Groups C & D).

Table 1: Experiment Design

	Biomaterial	Culture Conditions
Group A	Surgifoam	Free swelling
Group B	Surgifoam	Loaded in tension
Group C	Surgifoam + agarose	Free swelling
Group D	Surgifoam + agarose	Loaded in tension

RESULTS

Cell fluorescence was observed in all 3-D constructs (Figs. 1 & 2), although not all cells were fluorescing. There were no apparent differences in the number or morphology of fluorescent cells between the non-loaded and loaded constructs placed in Surgifoam (Groups A & B, respectively; Fig. 1). However, in the Surgifoam + agarose constructs, cells experiencing tensile strains in Group D appeared elongated compared to more rounded cells in the non-loaded Group C (Fig. 2).



Fig. 1: Fluorescent cells in Surgifoam without (Group A) and with (Group B) loading (superimposed bright field image on left)

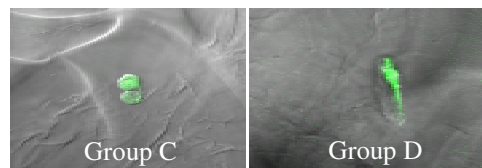


Fig. 2: Morphologic differences between cells in Groups C & D

DISCUSSION

This preliminary study showed qualitative evidence that 3-D culture and tensile loading stimulate type I collagen production in mouse MSCs within 12 days. The morphologic differences observed may be indicative of cell differentiation to a fibroblast phenotype. Further studies are currently underway to quantify the effects of cell concentration and tensile stimulation in a simplified biomaterial (Vitrogen collagen gel), as the sponge hindered visualization of the cells. The use of these transgenic cells will prove useful in selecting those mechanical and even chemical stimuli that best promote collagen gene expression and production in tissue engineered replacements.

ACKNOWLEDGMENTS

This study was supported by NIH Grants 1R21EB002361-01 & 1R01AR46574.

HEALING OF AN INTRA-ARTICULAR TISSUE DEFECT USING A STABILIZED PROVISIONAL SCAFFOLD

M.M. Murray, K.P. Spindler, C. Devin, P. Ballard, L.B. Nanney, K.P. Spindler
Department of Orthopaedic Surgery, Children's Hospital of Boston, 300 Longwood Ave, Boston, MA
Vanderbilt Sports Medicine, Department of Orthopaedic Surgery and Rehabilitation Vanderbilt University,
Nashville, TN

BACKGROUND

Failure of an injured musculoskeletal tissue to heal is referred to as a "non-union". Tissues within joints have non-union rates as high as 90%, while tissues found outside of joints have nonunion rates closer to 2%. Extra-articular tissues heal by forming a provisional fibrin scaffold at the wound site which is gradually invaded by surrounding cells and remodeled into healing scar. This provisional scaffold is not seen within intra-articular tissue defects. We hypothesize that this early loss of the provisional scaffold leads to gap formation and tissue non-union for intra-articular tissues.

METHODS.

The canine anterior cruciate ligament central defect model was used to study the intra-articular healing response with and without placement of a stabilized provisional scaffold. Histology and MRI were used to assess the response to injury for treated and control groups. A total of 19 canines were used in this study.

RESULTS

The untreated ACL defects remained open, even at the six week time point. In contrast, the ACL defects treated with a stabilized provisional scaffold had a histologic and biochemical response similar to the extra-articular control groups (MCL and PT). However, the treated ACL had only partial defect filling whereas the PT and MCL defects had almost complete filling of the injury site with repair tissue.

CONCLUSIONS

Use of a stabilized provisional scaffold can stimulate healing of an intra-articular defect histologically. Improving the success rates of healing of intra-articular tissues using a stabilized scaffold may lead to higher success rates for primary repair of these tissues and may change the focus of treatment for these injuries from resection and reconstruction toward repair and regeneration.

PHYSICAL ACTIVITY AND NEURONAL PLASTICITY AFTER TENDON RUPTURE

+*PW Ackermann, *DK-I Bring, *PAFH Renström

+*Section of Sports Medicine, Department of Surgical Sciences, Karolinska Institutet, Stockholm, Sweden

INTRODUCTION Clinically, it is well known that physical activity promotes tissue regeneration after injury. The exact mechanisms for this mechano-biological transduction, i.e. mechanical stimuli into tissue regeneration, are still largely unknown. Accumulating data, however, suggest that a variety of neuronal mediators, so called neuropeptides, besides cytokines and growth factors play an important role of tissue repair [1]. Recently we demonstrated that ruptured tendons exhibit extensive new nerve fibre ingrowth during the early regenerative phase of healing (week 1-4) [2]. This new nerve fibre ingrowth is followed by a specific temporal expression of sensory neuropeptides during healing, which may reflect a role in angiogenesis and/or proliferation/differentiation of different cell types in tissue repair. This brings about means of delivering neuropeptides directly into the healing area. Given that neuropeptides mediate trophic effects, it may prove that physical activity, i.e. early mobilisation after injury, can regulate the nerve regenerative capability and/or the neuropeptide occurrence during healing. In the present study of healing Achilles tendon 4 weeks after rupture, we analyzed the occurrence of nerve fibres and a specific sensory transmitter at three different activity levels post injury, i.e. running, free mobility and immobilisation.

METHODS Twenty-five male Spontaneously hypertensive rats (265g) were housed individually, and divided into three groups according to the degree of physical activity after tendon rupture. 1.) Eight rats had access to a running wheel, permitting unlimited voluntary activity (Run-group). 2.) Eight rats were housed without a running wheel but allowed free mobility (Mob-group). 3.) Nine rats were cast immobilized on their operated leg with a padded Plaster of Paris (Immob-group). **Surgery:** The rats were anaesthetized by an injection of ¼ Midazolam® and ¼ Hypnorm® in sterile water. Subsequently all rats were subjected to a blunt rupture of their right Achilles tendon. The skin was closed with 5/0 non resorbable Ethilon®. All rats were killed after four weeks by an injection of sodium pentobarbitone. The experiments were approved by the local animal ethics committee. **Microscopy:** The right Achilles tendons were dissected, and the tissues fixed in 4% paraformaldehyde solution containing 0.2% picric acid, sectioned (15µm) and stained according to the avidin / biotin and the Hematoxylin-Eosin method. The sections were incubated with primary antisera for protein gene product 9.5 (PGP), a general nerve marker, and calcitonin gene-related peptide (CGRP), a sensory neuropeptide. A Nikon® epifluorescence microscope was used to examine the sections. Subjective assessments of the histologic maturation and the occurrence of the PGP and CGRP were done. Pictures were taken with a Nikon® digital camera for computerized analysis. **Computerized analysis:** For each rat, three sections from different longitudinal levels of the tendon were stained. The tendon diameter, was determined in the microscope according to the width of the organized tendon tissue at the ruptured area. Semi-quantitative image analysis was used to assess the fractional area occupied by nerve fibres immunoreactive to PGP and CGRP in relation to the total area [2]. Statistical analysis was performed by the Mann-Whitney U test.

RESULTS The histologic examination of the healing tendons at week 4 demonstrated that increased physical activity was associated with a higher degree of maturation and regeneration of the connective tissue. The highest amount of organized collagen fibres was found in the running group, while the immobilized group exhibited the lowest amount. Moreover, the occurrence of inflammatory cells decreased with increased physical activity. The tendon diameters in the immobilized (1.62 ± 0.64) and freely mobilized groups (2.1 ± 0.79), respectively were 47.3% ($p=0.001$) and 32.0% ($p=0.02$) smaller than in the running group (3.1 ± 0.48) (Fig. 2B). Immunohistochemistry at week 4 after rupture showed, in agreement with earlier published findings [2], an extensive neuronal ingrowth into the healing tendon area, which occurred in all studied groups (Fig. 1A-B). The occurrence of PGP and CGRP was most pronounced in the immobilized group, while the occurrence in the running group was more sparse than in the other groups. Semi-quantitative image analysis confirmed the subjective evaluation and indicated that the level of physical activity was inversely related to the occurrence of PGP and CGRP. The occurrence of PGP in the immobilized and freely mobilized groups was 125% ($p=0.02$) and 39% ($p=0.17$), respectively, higher than in the running group. The difference in PGP occurrence between the immobilized and freely mobilized groups was not significant ($p=0.08$). The CGRP occurrence in the immobilized group was 134% ($p=0.02$) and in the freely mobilized group 113% ($p=0.02$) higher than in the running group (Fig. 2A).

DISCUSSION The present study of healing Achilles tendon at 4 weeks after rupture demonstrates increased tendon regeneration and decreased nerve and CGRP occurrence, associated with intensive physical activity. Immunohistochemistry at week 4 demonstrates an extensive neuronal ingrowth into the healing tendon, of all studied groups. This is in agreement with earlier published studies on freely mobilized rats showing nerve ingrowth, in the tendon tissue normally devoid of nerves, already at week 1, reaching a peak at week 4, followed by successive withdrawal from the healed tendon [2]. An early ingrowth of nerves in traumatized tissue is suggested to provide a delivery system of neuronal mediators, essential for healing. In fact CGRP has been shown not only to induce vasodilation, but also to stimulate cell differentiation, angiogenesis and tissue regeneration [1]. It may prove that high levels of physical activity induces enhanced earlier neuronal ingrowth resulting in a more rapid healing process as seen by highly regenerated tendons, followed by an early nerve withdrawal, i.e. before week 4.

ACKNOWLEDGMENTS This study was supported by grants from the Swedish National Center for Research in Sports.

REFERENCES

1. Schäffer et al., Arch. Surg., Vol. 133, 1998 2. Ackermann et al., J. Ortho Res., Vol. 20, 2002 3. Clemow et al., J. Cell Physiol., Vol. 183, 2000

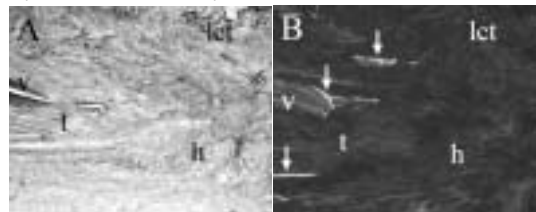


Figure 1A-B. Micrographs of two serial sections of the Achilles tendon, immobilized post rupture. Morphology of the healing area (h) (A). Nerve fibres (arrows) positive to PGP-9.5 surrounding the healing area (B). t = tendon tissue; v = blood vessel; lct = loose connective tissue

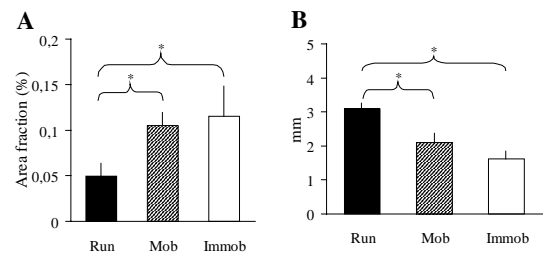


Figure 2A-B Area fraction occupied by nerve fibres immunoreactive to CGRP in relation to total tendon area (A). Diameter of organized collagen in the healing area (B). (mean \pm s.e.m.) (* = $p < 0.05$).

ORIGIN OF MESENCHYMAL CELLS IN TENDON HEALING -USING TENDON CHIMERIC RAT-

*Y. Kajikawa; * +N. Watanabe; **H. Sakamoto; * M. Kobayashi; *Y. Oshima; **M. Kawata; *T. Kubo

+*Department of Orthopaedics, Graduate School of Medical Science,
Kyoto Prefectural University of Medicine, Kyoto, Japan

**Department of Anatomy and Neurobiology, Graduate School of Medical Science,
Kyoto Prefectural University of Medicine, Kyoto, Japan

INTRODUCTION

The healing process after the tendon injury involves the formation of fibrous tissue, in which an influx of mesenchymal cells occurs¹. Although these cells play a critically important role for healing, it is under debate whether they arise from adjacent to injured sites or circulating cells². Understanding the cellular origin of mesenchymal cells in the injured tendon should be the pilot data to engineer the healing process for regenerating the normal tendon properties. The proliferating cells adjacent to the injured sites have been demonstrated in several soft tissues. It was thus hypothesized that mesenchymal cells arise from adjacent to the injured tendon and migrate into the injured site. For following tendon cells adjacent to the injured sites, establishment of the model that no markers exist, except for the tendon, should be optimal. Marker positive adjacent tendon cells can be followed in the healing tendon by using this model. As a marker, green fluorescent protein (GFP) has no immunological rejection in rat *in vivo*. The objective of this study was to develop a tendon chimeric rat model, using GFP transgenic rats and wild-type rats and to follow GFP signal positive cells adjacent to tendon injured sites.

METHODS

Genetically identical female green fluorescent protein (GFP) transgenic rats (Seven-week-old n=20) and SpraguDawley (SD) wild-type rats (Twelve-week-old n=20) were used. Patella tendons of GFP rats were harvested and transplanted into the extensive full-thickness defects of wild type rats' patella tendons to create tendon chimeras. At 2 weeks after the transplantation, the patella tendons were harvested and serial frozen sections were made. The sections were stained with hematoxylin and eosin (HE) and GFP signals were examined with confocal laser scanning microscopy (LSM 510, Zeiss) to confirm the establishment of chimeric tendon at 2weeks (2weeks chimeric rats). Lateral partial perpendicular lacerations were made in the middle of the patella tendons of 2weeks chimeric rats. At 3 and 7 days after laceration, patella tendons were harvested and the GFP signals of injured part were detected. The bone marrow cells and blood cells were observed by a confocal laser scanning microscopy to confirm that GFP signals were not present in these cells of 2weeks chimeric rats and experimental periods after laceration.

RESULTS

In 2 weeks chimeric rats, the fibrous union was observed between the graft and host, and the interface had become indistinct. GFP signal positive tendon cells were found in the transplanted tendons but the number increased up to 1.5 times in comparison with that of normal. There were no signals neither in the bone marrow nor peripheral blood cells. At 3 days after laceration of 2 weeks chimeric rat tendons, the injured parts were repaired by fibrous tissue. GFP signal positive ovoid to spindle shaped mesenchymal cells were found in the injured sites (Fig.1). At 7 days, the fibrous tissue became dense and the alignment of collagen bundles became partially regular. The number of GFP positive mesenchymal cells increased in the circumference of the defects (Fig.2).

DISCUSSION

In this study, GFP signal positive cells were extensively found in the whole tendon 2 weeks after the transplantation. The histology was not different from that of normal tendon at 2 weeks however there were no GFP positive signals except for tendons. Further, GFP positive cells were clearly followed in the injury site using this model at 3 and 7 days after laceration. Thus, it was conceivable that the tendon chimeric rat model using GFP rats were beneficial to follow tendon cells during tendon healing. Regarding cellular behavior, spindle shaped GFP positive cells, resembling fibroblasts in shape, infiltrated in the injury site at 3 days and the number increased over time. It was found that adjacent tendon cells migrated in the injury site and would aid in healing of the injured tendon.



Fig.1. 3days. T: grafted tendon D: defect



Fig. 2. 7days.

REFERENCES

- 1.Woo SL-Y, Clin Orthop 1999 ,2.Prockop D.J.,Science 1997

EXPRESSION PROFILING OF METALLOPROTEINASES AND TISSUE INHIBITORS OF METALLOPROTEINASES IN NORMAL, PAINFUL AND RUPTURED ACHILLES TENDON

Gavin C Jones¹, Anthony N Corps¹, Caroline J Pennington², Ian M Clark²,
Dylan R Edwards², Brian L Hazleman¹ and Graham P Riley¹.

¹ Rheumatology Research Unit, Addenbrooke's Hospital, Cambridge, United Kingdom.

² School of Biological Sciences, University of East Anglia, Norwich, United Kingdom.

INTRODUCTION

Tendon tissue is of low cellularity and its biomechanical properties are primarily a feature of the extracellular matrix (ECM). The ECM is in a state of dynamic equilibrium between synthesis and degradation. Metalloproteinases are a clan of enzymes implicated in extracellular proteolysis that include the MMP (matrix metalloproteinase), ADAM (a disintegrin and metalloproteinase) and ADAMTS (a disintegrin and metalloproteinase with thrombospondin motifs) groups. The most important endogenous inhibitors of these enzymes are believed to be members of the TIMP (tissue inhibitors of metalloproteinases) family. The aim of this study was to profile the expression of the 23 known MMP, 19 known ADAMTS, 4 known TIMP and ADAM-8, -10, -12 and -17 (TACE) genes in normal, painful and ruptured human Achilles tendon.

METHODS

Tendon specimens were obtained from tissue discarded during surgery, from 14 patients suffering chronic painful tendinopathy for more than 6 months, and from 14 patients undergoing repair of ruptured tendon within 48 hours of the rupture occurring. Macroscopically normal specimens were obtained from cadaver material (14 individuals) within 48 hours of death. Total RNA was isolated from frozen tissue samples by a modified Tri-Spin protocol as described previously {Ireland et al, 2001}. mRNA expression of all gene targets was analysed by quantitative real-time RT-PCR, normalised to 18S RNA. Statistical analysis was performed on the relative gene expression levels. Significant differences between the normal, painful and ruptured tendon groups were determined using a Kruskal-Wallis H test and pair-wise comparisons made using a 2-sided Mann-Whitney U Test with Bonferroni correction for multiple comparisons between groups. Linear regression modelling was used to test for confounding effects of age and sex. $P < 0.05$ was chosen as the cut-off for significance.

RESULTS

Comparing across all genes, the normal, painful and ruptured groups each had distinct expression profiles. Of the 50 genes investigated, only 3 (MMP-20, MMP-26 and ADAM-10) were not detected. Overall, the most highly expressed genes were MMP-2, MMP-3 and TIMP-1, -2 and -3. Genes with the lowest detectable expression were MMP-8 and ADAMTS-7, -8, -18 and -20. 16 genes showed no significant difference in mRNA expression between the 3 groups; these were MMP-2, -8, -21, -24, ADAMTS-1, -3, -7, -8, -9, 13, -15, -16, -18, -19, -20 and ADAM-17. The greatest differences in expression in painful tendinopathy compared to normal tendons were lower MMP-3 (75-fold) and MMP-10 (140-fold) and higher ADAM-12 (19-fold). The greatest differences in ruptured compared to normal tendons were higher MMP-1 (630-fold), MMP-7 (25-fold), MMP-9 (44-fold), MMP-19 (32-fold), MMP-25 (34-fold), ADAM-8 (32-fold) and ADAM-12 (94-fold) and lower MMP-7 (25-fold). The greatest differences in ruptured compared to painful tendons were higher MMP-1 (170-fold), MMP-10 (29-fold), MMP-19 (18-fold), MMP-25 (23-fold) and lower MMP-7 (21-fold). For each pathological group a number of genes could be identified which showed significant differences between that particular group and each of the other groups. Of these, only ADAM-12 was significantly different in every pair-wise comparison between groups.

DISCUSSION

This is the first comprehensive mRNA expression profile of all the known MMP, ADAMTS and TIMP genes in tendon. The distinct gene profile of each tendon group suggests differences in extracellular proteolytic activity, affecting the production and remodelling of the tendon ECM. For example, MMP-1 is implicated in the degradation of fibrillar collagen after tendon rupture, whereas MMP-13 may be involved in collagen turnover in chronic tendinopathy. MMP-3, which was highest in normal tendon, has been proposed as a central regulator of MMP activation, and its down-regulation in tendinopathy may serve to limit MMP activation within the tissue. Chronic painful tendons are shown to be a distinct group from ruptured tendons and some proteolytic activities are potentially implicated in the maintenance of normal tendon. However, the role and activity of many of these enzymes has yet to be determined. This data provides a foundation for further study of the processes underlying the pathology of tendon.

REFERENCES

Ireland D, Curry V, Holloway G, Hackney R, Hazleman BL and Riley GP. Multiple changes in gene expression in chronic human Achilles tendinopathy. *Matrix Biology* 2001;20:159-69.

TGF-BETA ISOFORMS WERE EXPRESSED IN THE EDGES OF THE WOUND IN HEALING PATELLAR TENDONS

S.C. Fu, Y.P. Wong, C.W.C. Hui, W.M.N. Wong, L.K. Hung, P. Wen, K.M. Chan

Department of Orthopaedics and Traumatology, The Chinese University of Hong Kong, Shatin, Hong Kong

INTRODUCTION

TGF-beta is a multifunctional growth factor which plays an important role in tendon healing. Elevated levels of TGF-beta are observed in tendon adhesion and tendinosis, this indicates that TGF-betas may play a pivotal role in switching the healing process from normal to pathologic. There are three TGF-beta isoforms in mammals and they are highly conserved in amino acid sequence, but their biological activities are not all the same. Previous studies demonstrated the effects of TGF-beta isoforms on collagen production in cultured tenocytes but the expression of TGF-beta isoforms in healing tendons has not been explored systematically. In this study, the expression of the three TGF-beta isoforms in healing patellar tendon will be measured.

METHODS

A window injury was created on patellar tendon of SD rats as previously reported¹. Samples were harvested on day 4, 7, 14 and 28 for fixation, tissue processing and sectioning. Tissue sections were stained using in situ hybridization with RNA probes against TGF-beta1, beta2 and beta3, and the protein expression of the TGF-beta isoforms was examined by immunohistochemistry.

RESULTS

We found that the expression of all 3 TGF-beta isoforms was increased at day 4 and day 7 post injury and decreased from day 14 to day 28 post injury. TGF-beta 1 was detected in the wound site as well as the edge of the wound at day 4 post injury, but TGF-beta 2 and 3 were detected only in the edges of the wound. In situ hybridization showed that the cells surrounding the wound were positive for the mRNA of TGF-beta 1, 2, and 3. This zone of TGF-beta became more confined to the edges at day 28 post injury.

DISCUSSIONS:

TGF-beta expression is chiefly located at the edges of the wound, and the zone of TGF-beta positive cells were narrowing during the course of healing. It indicates that the edges of the wound are active regions to modulate matrix reconstitution, while the cells in the wound site are respondent cells since TGF-b receptors are chiefly concentrated in repair sites². Different TGF-beta isoforms exhibited minor differences in the regulation of matrix genes; it is thus possible that the combination of TGF-beta isoforms would contribute to the transition of a provisional matrix to a mature collagen matrix.

REFERENCES:

1. Chan BP et al (1998) JOR 16: 597-603.
2. Ngo M et al (2001) Journal of Anatomy. 199(Pt 3):231-40, 2001

A NOVEL IN VIVO MODEL OF TENDON FATIGUE DAMAGE ACCUMULATION

Vincent M. Wang, Henry Lee, Lakshmi Rajan, Damien M. Laudier, Mitchell B. Schaffler, Evan L. Flatow
Department of Orthopaedics, Mount Sinai School of Medicine, New York, NY

INTRODUCTION

Despite its prevalence and debilitating clinical manifestations, the etiopathogenesis of tendinopathy is poorly understood. While tendon rupture is widely attributed to degeneration due to cumulative microtrauma, little is known as to the extent to which fatigue-damaged tendons are able to undergo matrix-level repair. This paucity in our understanding stems in part from the scarcity of early stage disease tissue from humans, and from the lack of reliable animal models in which tendon response to sub-rupture matrix damage can be studied. The objective of this study was to develop an in vivo model of tendon injury enabling controlled doses of fatigue loading to gain insights into fundamental structural, mechanical, and molecular mechanisms underlying tendon damage and intrinsic repair.

METHODS

Our primary criteria for selecting the rat as our animal model were animal size, cost, ethics, suitability for biologic investigation, and relevance to human tendinopathy. Furthermore, the rat has been used as a model for tendon overuse [3] and healing [2] and has been well characterized for acute injury. The patellar tendon was selected as it has two prominent bony attachments that are easily gripped, through small surgical incisions, to load the intervening tendon. Using this approach, we can load the tendon to a wide range of sub-rupture damage levels, and titrate the amount of fatigue damage from degradation in tendon secant stiffness [1], which is an engineering proxy for matrix damage. *Experiments:* Under anesthesia and aseptic conditions, rats were positioned on a servo-hydraulic mini-testing system (Instron 8841). Hindlimbs (with knees flexed 90°) were placed in the actuator and custom clamps secured the tibia and patella in order to apply loads to the patellar tendon. Following preconditioning, tendons were fatigue loaded until a prescribed loss of secant stiffness (20% stiffness decrease from baseline). Following loading, skin incisions were suture-closed and rats were returned to their cages and received post-treatment analgesia. Contralateral limbs were examined as intact controls. Additional sham animals received only patellar and tibial skin incisions, gripping and skin closure. Rats were sacrificed at one or two weeks post-loading and the patellar tendons were harvested for biomechanical and histologic analyses. All procedures have been approved by our IACUC.

RESULTS

At one week post-loading, histological analyses (Figure 1) demonstrated ruptured fibers localized near the tibial insertion of fatigued patellar tendons while non-loaded control tendons showed intact fibers integrating cleanly into the proximal tibia; sham tendons were similar to intact controls. At two weeks post-loading, the cross-sectional area of fatigued tendons were 24% greater than those of controls. However, tendon modulus and maximum stress were less than half of control values (Figure 2). Sham and intact control tendons had equivalent properties.

DISCUSSION

We have developed a novel rat patellar tendon model to induce cumulative (fatigue) damage in vivo and investigate tendon response to sub-rupture matrix damage. In contrast to existing animal models of laceration and repair of healthy tendons, ours is the first model that allows the investigation, in a living animal, of the microstructural, mechanical, and biologic mechanisms of fatigue damage in tendons in a controlled mechanical environment.

In our studies to date, this loading approach produced a pronounced loss of mechanical properties and extensive collagen fiber disruption at the tibial insertion of the patellar tendon, demonstrating that our in vivo fatigue model is an effective means of inducing matrix damage in patellar tendons. Using this new model, our future in vivo studies will induce subfailure matrix damage over a variety of “dose levels” to systematically characterize the temporal sequence of structural and cellular repair responses to different levels of in vivo tendon fatigue damage.

REFERENCES

[1] Flatow EL et al. *Trans Orthop Res Soc.* 2002;27:621. [2] Lin et al., *J Biomech.* 2004;37:865-77. [3] Soslowsky et al., *J Shoulder Elbow Surg.* 2000; 9:79-84.

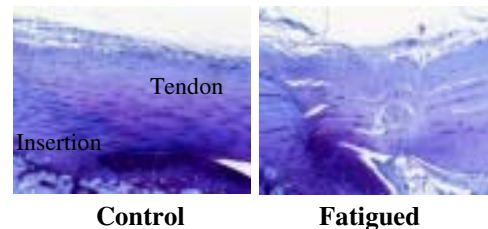


Figure 1: Patella tendon histology

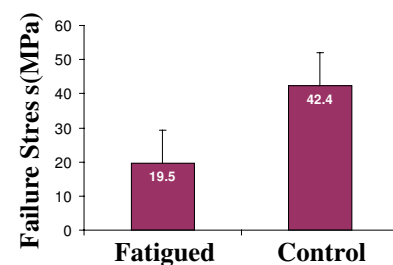


Figure 2: Biomechanical results

NEW BIOREACTOR SYSTEM FOR LIGAMENT AND TENDON TISSUE ENGINEERING

T. Majima, N. Sawaguchi, N. Iwasaki, T. Funakoshi, K. Shimode, T. Onodera, A. Minami
Department of Orthopedic Surgery, and Frontier Research Center for Post-genomic Science and Technology,
Hokkaido University school of Medicine, Sapporo, Japan.

INTRODUCTION

Tissue engineering is an emerging scientific approach that attempts to develop biological substitutes made from isolated cells and three-dimensional (3D) scaffolds. Mechanical stress is one of a key component of tissue engineering, providing a controlled environment to modulate cell function and tissue development in vitro. We developed new bioreactor system to apply complex concurrent mechanical strains to 3D scaffold for ligament and tendon tissue engineering. Purpose of the present study is to assess the effect of mechanical stress on cell proliferation and extra cellular matrix production in 3D scaffold made from chitosan and hyaluronan.

MEETHODS

The bioreactor provides independent but concurrent control over translational and rotational strains imparted to the growing tissue housed in CORNING 50ml tubes. Custom designed parts are machined from SUS 304. Off of the shelf items are made from SUS 18-8 set screws, silicon O-rings. All parts can be steam and gas sterilized. Two high torque stepper motors with accompanying micro-step drivers are controlled by motion programmable controller. Several different cycles with varying strain regimes can be programmed and run for duration of an experiment. A load cell was attached to loading apparatus in order to measure real time load applied to the scaffold. Chitosan-Hyaluronan hybrid 3D scaffold seeded with rabbit patella tendon fibroblasts was attached to this system under 90° rotational and 2 mm translational deformity that applied 5% strain at 0.5Hz for 18 hours, and 6 hours rest. DNA content was determined to quantify cell proliferation compared to static culture (Hoechst #33258). To assess the mRNA levels of the ECM products, Real-Time-RT-PCR analysis was performed. Threshold cycle (Ct) of each mRNA (collagen I, collagen III, decolin, fibromodulin, and biglycan) was normalized using GAPDH.

RESULTS

DNA content of the bioreactor group was significantly higher than that of the static group at 21 day after cultivation ($p < 0.05$). The mRNA level of type I, III collagen and fibromodulin in the bioreactor group was significantly higher than in the static group ($p < 0.001$) [Fig.1].

DISCUSSION

The present study showed that bioreactor culture had significantly higher fibroblast proliferation, and ECM production compared with static culture. These results indicate that mechanical stress imparts superior biological effects on the fibroblasts in a 3D culture system.

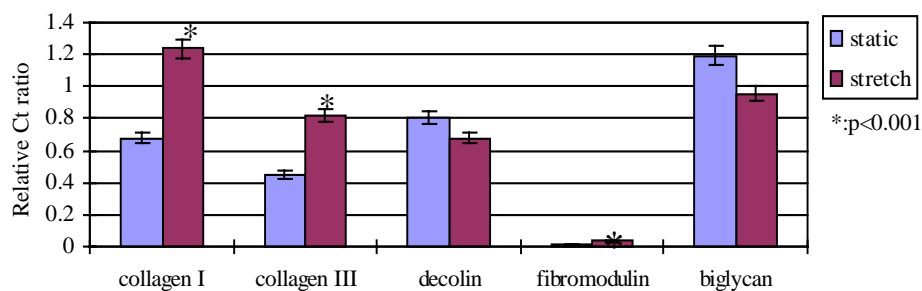


Figure 1. Relative Ct ratio of mRNA

Acknowledgement

Grant-in-Aid for Science Research from Japanese Ministry of Education, Culture, Sports, Science & Technology (B-1539044) and Grant-in-Aid for New Energy and Industrial Technology Development Organization (03A04002a).

SUTURE PLICATION, THERMAL SHRINKAGE, AND SCLEROSING AGENTS: EFFECTS ON RAT PATELLAR TENDON LENGTH AND BIOMECHANICAL STRENGTH

*A. Aneja, *S. Karas, *+P. Weinhold, *H. Afshari, *L. Dahners

*Department of Orthopaedics, + Department of Biomedical Engineering, University of North Carolina, Chapel Hill, NC USA

INTRODUCTION

There are several clinical situations, most notably shoulder instability, where a method for tightening and strengthening collagenous capsulo-ligamentous structures would be helpful. The purpose of this study was to compare the effect of surgical suture plication, radiofrequency thermal shrinkage combined with suture plication, and a 5% sodium morrhuate sclerosing injection on the length and biomechanical strength of the rat patellar tendon as a model of dense collagenous tissue. Suture plication, the current gold standard to tighten lax ligaments works by folding the tissue upon itself to take stress off the structure, and permit the body's natural healing process to contract the tissue. Thermal shrinkage is a relatively new procedure for ligament laxity which uses radiofrequency energy to heat and thus shorten elongated soft-tissue. Sclerosing agents, reported to be very successful by osteopathic physicians for some time, have been documented to induce fibroplasia and collagen deposition at the site of inflammation, resulting in an increase in the structure's thickness, mass, and strength.

METHODS

Forty-six female retired breeder rats were split into four groups each receiving one of the three aforementioned treatments plus a control group that received a saline injection. After four weeks survival, the length and biomechanical properties of the patellar tendons were measured and compared to the contra-lateral untreated tendon. Statistical analysis was performed to evaluate for differences in length and biomechanical strength within and between treated groups.

RESULTS

Rats treated with suture plication had tendons that were 11% shorter and no stronger than the intact contralateral tendons. Radiofrequency thermal shrinkage combined with suture plication yielded tendons that were both 7% shorter and 40% stronger than the untreated contralateral tendons. The sodium morrhuate injected tendons were not significantly different in length but were significantly stronger (36%) than the contralateral untreated tendons. The saline treated tendons were also not different in length but were significantly weaker (17%) than the untreated contralateral tendons. Suture plication resulted in the shortest tendons among the four groups. There was no significant difference in strength between groups.

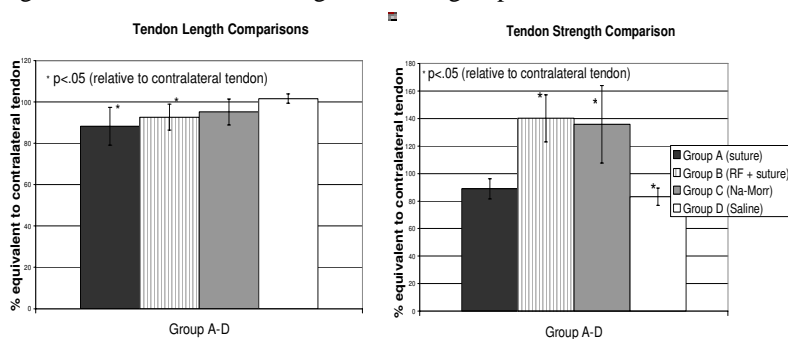


Fig 1 (left). Rat Patellar Tendon length as a percent of contralateral untreated tendon. Fig 2 (right). Rat patellar tendon max load normalized for body weight and expressed as a percentage of the contralateral untreated tendon. Data for both figures presented as mean \pm standard error.

DISCUSSION

Overall, the results suggest that surgical suture plication without radiofrequency shrinkage is most effective at shortening the length of the rat patellar tendon while radiofrequency thermal shrinkage combined with suture plication, and 5% sodium morrhuate injection are effective at increasing the strength of rat patellar tendons one month post-operatively. Therefore, judicious use of thermal shrinkage in combination with suture plication may improve ligament strength and decrease laxity in cases of shoulder instability. In concordance with past literature, our results demonstrate that the efficacy of thermal shrinkage treatment may vary depending on the site of tissue to be treated, and its effective ability to be immobilized. Though a single 100 L injection of 5% sodium morrhuate strengthened the tendons, it did not produce statistically shorter tendons. Therefore, more studies are required to determine whether higher concentrations of a single sodium morrhuate injection might be effective in treating joint laxity.

CHARACTERIZATION OF THE MECHANICAL PROPERTIES OF THE ACL BONE INSERTION

*K.L. Moffat, *N.O. Chahine, *C.T. Hung, *G.A. Ateshian, and +*H.H. Lu
 +*Department of Biomedical Engineering, Columbia University, New York, NY

INTRODUCTION

The anterior cruciate ligament (ACL) functions as the primary restraint to anterior tibial translation and limits varus-valgus rotation[1]. It interfaces with bone tissue through the femoral and tibial insertion sites via a fibrocartilage (FC) layer which can be further divided into non-mineralized and mineralized FC. ACL tears and ruptures often occur at the insertion site[2], and the interface is not fully regenerated after reconstruction. While the mechanical properties of the ACL have been investigated extensively, those of the ACL insertion sites are not yet well understood. We believe this understanding will be critical in interface regeneration and eventual graft integration. The purpose of this study is to characterize the mechanical properties of the FC region of the ACL insertion sites. We have elected to test the insertion under uniaxial, unconfined compression since FC is often found in regions subjected to compressive forces. It has been suggested that ligament insertion sites may experience tension, shear and compression[2,3], and principle compressive stresses have been reported along the inner curvature of the femoral insertion of the MCL when loaded in tension[3].

MATERIALS AND METHODS

Sample Preparation: Intact ACL and insertion sites of three neonatal (<1 week) bovine tibiofemoral joints were excised (Fig. 1A).

Rectangular samples (Table 1, n=3) containing regions of bone (B), fibrocartilage (FC) and ligament (L) were isolated (Fig. 1B).

Unconfined Compression Testing: Samples were tested in a custom unconfined compression microscopy device as previously described[4]. Briefly, samples were stained with Hoechst 33258 (Sigma) nuclear dye (Fig. 2B) and loaded between two impermeable glass platens while the device was mounted on the stage of an epifluorescence microscope (Olympus). A tare strain of 10% was first applied and a sample image was acquired at equilibrium. Next, compression was applied at ~1 m/s in 5% increments (up to 30% strain). At equilibrium, sample images were acquired and load was recorded for each increment. Strain analysis was performed using optimized digital image correlation[4]. Axial strains (ϵ_{xx}) were calculated using linear regression of the displacement versus tissue width; yielding distinct strain behaviors in the FC and the bone regions (Fig. 2A). The incremental Young's modulus (E_Y) of the FC was calculated from the slope of axial stress (σ_{xx}) vs. strain (ϵ_{xx}) in that region.

Table 1	Sample Width (m)	FC Width (m)	B Width (m)	Cross Section (mm ²)
Femoral	1832 ± 170	692 ± 98	785 ± 191	4.96 ± 2.03
Tibial	1871 ± 167	1171 ± 204	570 ± 224	2.83 ± 0.25

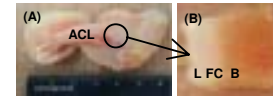


Fig.1: A. ACL and insertion sites
 B. Sample image

RESULTS/DISCUSSION

The resulting displacement (Fig. 2A) and strain (as indicated by the slope of the displacement curves) in the FC region was significantly greater than in the bony region for both femoral and tibial insertions. A depth dependent variation in displacement was observed across the FC region, likely due to the presence of non-mineralized and mineralized FC. The stress in FC increased nonlinearly with increasing strain, indicative of strain-stiffening behavior reported for FC tissue[5]. The resulting stress in the tibial FC was significantly greater than in the femoral FC ($p < 0.05$) at all compressive strains. E_Y increased linearly with increasing strain for both tibial and femoral FC (Fig. 3, $R^2 > 0.97$), and was significantly greater for the tibial FC ($p < 0.05$). In comparison to bovine shoulder articular cartilage (AC) tested under similar conditions[6], at 5-15% strain, only the E_Y of the femoral FC is similar to AC. At >15% strain, the magnitude of E_Y for both insertion FCs are greater than that of AC. Differences between the mechanical properties of the femoral and tibial insertion sites may be related to morphological differences, in particular the angle of insertion and degree of collagen fiber alignment. Future studies will determine structure-function relationships at the interface and their relevance in graft integration.

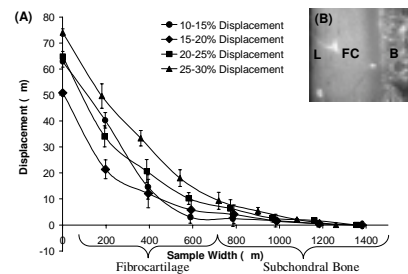


Fig. 2: A. Displacement v. sample width, B. Sample image

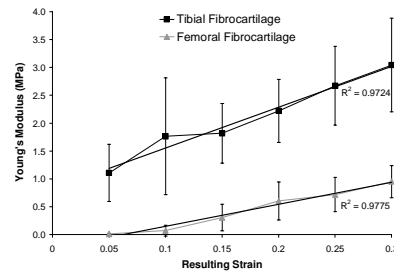


Fig.3: E_Y vs. resulting compressive strain

REFERENCES [1]The Anterior Cruciate Ligament: Current and Future Concepts, 1993; [2]Injury and Repair of the Musculoskeletal Soft Tissues, 1987; [3]Matyas et al., *J. Biomech.*, 28(3):147-157, 1995; [4]Wang et al., *J. Biomech. Eng.*, 124:557-567, 2002; [5]Leslie et al., *Proc. Instn. Mech. Engrs.*, 214(6):631-635, 2000; [6]Chahine et al., *J. Biomech.*, 37:1251-1261, 2004.

AGING AFFECTS THE MECHANICAL AND VISCOELASTIC PROPERTIES OF THE BUNDLES OF THE HUMAN ACL DIFFERENTLY: A CADAVERIC STUDY

R. Kilger, S. Abramowitch, D. Moon, S.L-Y. Woo

Musculoskeletal Research Center, Department of Bioengineering, University of Pittsburgh, Pittsburgh, PA

Introduction: An increasing number of surgeons are currently performing double bundle ACL reconstruction using hamstring tendons [1] to be as close as possible to the intact ACL. Previous studies have shown that these bundles have different functional roles [2]. Moreover, these properties might change with increasing age which might lead to a higher risk of injury. Therefore, the objective of this study was to determine the mechanical and viscoelastic properties of the antero-medial (AM) and postero-lateral (PL) bundles of the human ACL and evaluate their age related differences. Based on the knowledge that the structural properties of the whole ACL decrease with age [3], we hypothesized that the mechanical and viscoelastic properties of the PL and AM bundle decrease with age.

Methods: The AM and PL bundle of the ACL were removed from eight human cadaver knees (age: 42 ± 10 y; 4 male/4 female) with bone blocks from the femur and tibia. The cross-sectional area of each bundle was determined using a laser micrometer system [4-5]. Two reflective markers were used to determine the strain by means of a video analysis system. The Bone-Bundle-Bone-Complex (BBBC) was then mounted in a materials testing machine. During testing each BBBC was kept in a saline bath (33°C). Custom made adjustable clamps provided alignment of the bundles, which were oriented along the longitudinal axis to uniformly load each specimen. After a 2 N preload, the BBBC was preconditioned 10 cycles between 5% strain. With one hour of recovery before and between tests, the static (1 hour) and cyclic stress-relaxation (30 cycles) behaviors of the bundles up to 5% strain were determined. Subsequently, the stress-strain relationships were determined from a load to failure test. The crosshead speed was set at 10mm/min. A paired t-test was utilized to show differences between the bundles and a linear regression analysis revealed their trends in the data versus age. Significance was set at $p < 0.05$.

Results: It was found that the percentage of stress relaxation for the PL bundle was slightly larger than that for the AM bundle ($21.1 \pm 5.0\%$ vs. $17.3 \pm 8.7\%$, respectively; $p > 0.05$). From the load to failure test, the stiffness was 124 ± 27 N for the AM-BBBC and 71 ± 37 N for the PL-BBBC ($p < 0.05$). The ultimate load was found to be 497 ± 212 N for the AM-BBBC and 226 ± 138 N for the PL-BBBC ($p < 0.05$). The poor bone quality of cadaver specimen resulted in inconsistent failure modes. Thus, only the modulus could be reported. The modulus showed significantly higher values for the AM bundle (190.7 ± 60.5 vs. 128.1 ± 75.1 ; $p < 0.05$). Both BBBC showed decreasing stiffness and ultimate loads with age (Fig. 1 and 2). The results showed a decreasing trend of the stress relaxation of the AM bundle ($p < 0.05$), whereas the modulus did not show a trend ($p > 0.05$). On the other hand, the PL bundle showed an opposite trend. The stress relaxation of the PL bundle did not show a trend, whereas the modulus decreased significantly with age ($p < 0.05$).

Discussion: Previous studies showed comparable age dependent structural properties for the whole ACL [6] and the mechanical properties are comparable to historical data [7]. Our hypothesis only was partially confirmed. There were statistically significant differences in the mechanical properties for AM and PL Bundle (i.e. modulus) indicating that the AM and PL Bundle are exposed to different loads during daily activities. Further, the different trends of modulus and stress relaxation behavior with age seem to also support this conclusion. In the future, more in vivo research is suggested to evaluate the different loads on the ACL during daily activities and trauma.

References:

1. Survey, ACL Study Group, Sardinia, Italy 2. Woo S. L-Y. AJSM, 1999; 3. Woo S. L_Y., AJSM, 1991, 4. Lee TQ, JBME, 1988, 5. Woo S. L-Y. JBME, 1990, 6. Woo S. L-Y, JOR, 1999, 7. Butler D.L. J Biomech, 1992

Acknowledgements:

NIH Grant AR39683 and the technical support of Jesse Fisk and Scott Hanford are gratefully acknowledged.

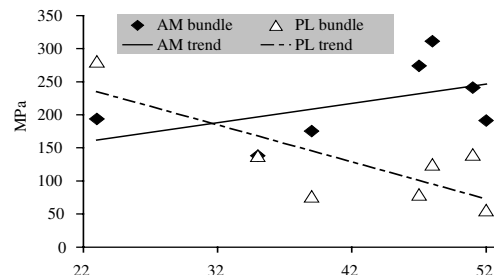


Fig.1: Modulus vs. age for AM/PL bundle

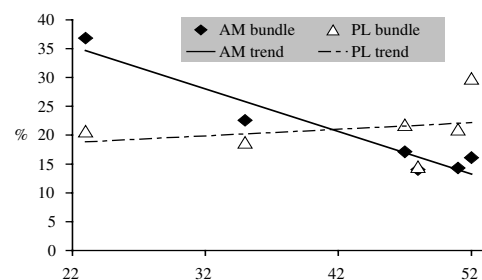


Fig.2: Stress relaxation vs. age for AM/PL bundle

BIOSCAFFOLD TREATMENT REDUCES THE CROSS-SECTIONAL AREA OF THE HEALING MEDIAL COLLATERAL LIGAMENT

D.K. Moon, Y. Takakura, R. Liang, S.D. Abramowitch, S.L-Y. Woo

Musculoskeletal Research Center, Department of Bioengineering, University of Pittsburgh, Pittsburgh, Pennsylvania

INTRODUCTION: The medial collateral ligament (MCL) of the knee is frequently injured in sports and work related activities [1]. Recent basic science and clinical studies have shown that the biochemical, histomorphological and mechanical properties of the healing MCL remain abnormal compared to the intact, normal MCL [2, 3]. However the healing ligament's inferior mechanical properties are compensated by an increased cross-sectional area. Cross-sectional shape is also an important, especially for documenting morphological changes in the tissue during healing. A bioscaffold, porcine small intestinal submucosa (SIS), offers the possibility of improving the quality of the newly forming tissue while simultaneously restricting growth of the healing tissue [4]. Therefore, the objective of this study was to assess the effects of SIS treatment on the cross-sectional shape and area of the healing MCL. Due to guidance provided by the bioscaffold, we hypothesize that SIS-treated MCLs will be more similar in shape to the intact MCL and have a reduced cross-sectional area than non-treated healing MCLs.

METHODS: Twenty-two skeletally mature female rabbits were used for this study. Under general anesthesia, a 6 mm gap injury centered at the joint line was made in the MCL of the right knee. A single layer of SIS (Cook® Biotech Inc., Bloomington, IN), was secured on top of the gap injury (luminal side of SIS facing down) in 11 rabbits. The injuries in the 11 remaining rabbits were left untreated. The left MCLs served as sham-operated controls in all rabbits. All animals were sacrificed at 26 weeks post-surgery and their hind limbs were harvested. The cross-sectional shape and area was measured at three locations along the midsubstance using a laser micrometer system [5]. The ligament's shape was then quantified by finding the major and minor axis. Paired t-tests were used to compare each treatment group to their respective sham controls. Unpaired t-tests were used to compare SIS-treated and non-treated groups. Significance was set at $p < 0.05$.

RESULTS: The cross-sections of the sham-operated controls appeared more flattened in shape than the SIS-treated and non-treated groups and their cross-sectional areas were significantly smaller than both treatment groups ($p < 0.05$; Figure 1). No significant differences were found in the cross-sectional shape between SIS-treated and non-treated MCLs. However, the cross-sectional area of the SIS-treated group was 28 % less than that of the non-treated group ($p < 0.05$; Figure 1).

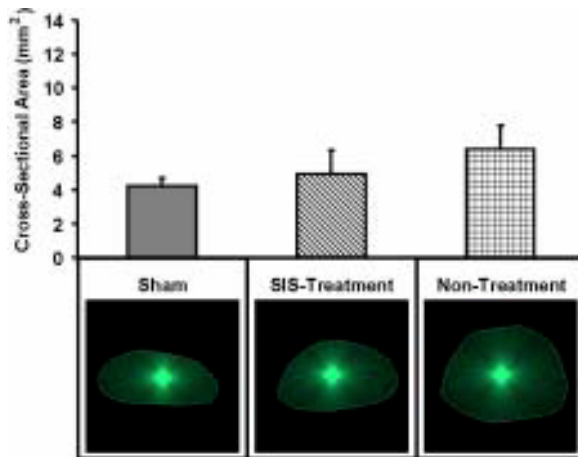


FIGURE 1. The comparison of the cross-sectional shape (under each bar graph) and area of sham-operated, SIS-treated and non-treated groups at 26 weeks post-surgery as detected with the laser micrometer system.

DISCUSSION: SIS-treatment significantly reduced the cross-sectional area of the healing ligament in comparison to non-treated healing ligaments. These results suggest that SIS may aid ligament healing by guiding the growth and remodeling of the healing tissue, thus helping it to more closely resemble intact tissue in terms of cross-sectional area and improved mechanical properties. This finding is exciting because previous attempts to enhance MCL healing at our research center have resulted in increased cross-sectional areas [6].

REFERENCES: [1] Miyasaka K et al. *Am J Knee Surg*, 1991; [2] Frank C et al. *Am J Sports Med*, 1983; [3] Weiss J et al., *J Orthop Res*, 1991; [4] Musahl V et al. *J Orthop Res*, 2002; [5] Lee T et al. *J Biomech Eng*, 1988; Hildebrand K et al., *Am J Sports Med*, 1998

ACKNOWLEDGEMENTS: The support of NIH Grant AR 41820 is appreciated.

SEMITENDINOSUS TENDON REGENERATION AFTER ACL RECONSTRUCTION

S. Li¹, A. Nishino², T. Manmoto³, A. Kanamori⁴, T. Fukubayashi⁵

¹ Kanto Central Hospital, Tokyo, ² University of Tokyo, Tokyo, ³ Kitaibaraki City General Hospital, Ibaraki, ⁴ Ibaraki Prefectural University of Health Science, Ibaraki, ⁵ University of Waseda, Tokyo, Japan

INTRODUCTION

The potential for tendon regeneration after ACL reconstruction using hamstrings tendon has been reported. The purpose of this study is to assess the features of the regenerated tendon using MRI, gross observation and histological findings.

METHODS

MRI to assess the position of the regenerated tendon and the musuclotendinous junction was performed in 20 patients who had undergone ACL reconstruction with a semitendinosus tendon (ST).

A gross observational and histological study was performed in 8 patients that had previously undergone ACL reconstruction with a ST. During a follow-up surgery to remove the tibial screw, the harvested site of the ST was opened and a tendon biopsy was performed in 6 patients. During ACL revision using the regenerated ST tendon, tendon and musuclotendinous junction biopsy was performed in 2 patients.

RESULT

Regenerated tendon was confirmed in 70% of the patients on MRI. The position of the regenerated tendon was almost the same as a normal tendon, except at the insertion; however the position of the musuclotendinous junction shifted proximally.

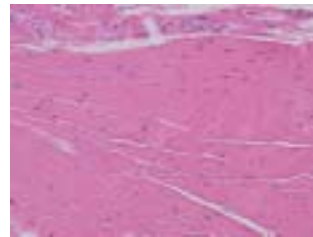
In the gross observational findings, the regenerated tendon had a smooth appearance similar to a normal tendon; however the thickness varied in each patient. The musuclotendinous junction had no scar similar to a normal musuclotendinous junction. (Figure 1)

In the histological findings, the collagen bundles were oriented along the longitudinal axis, and the nuclei of the fibroblast were oval in appearance. The regenerated tendon was more mature in subjects with a longer postoperative period. At the musuclotendinous junction, the muscle tissue was connected directly to the tendon tissue. (Figure 2)

Figure 1: regenerated ST tendon



Figure 2: tendon (HE stain, x100)



CONCLUSION

The regenerated tendon looked normal in MRI, gross observational and histological findings. The mechanism of tendon regeneration is still unknown; however in vivo tendon regeneration was confirmed in this study.

REFERENCES

Eriksson K, et al. The semitendinosus tendon regenerates after resection: a morphologic and MRI analysis in 6 patients after resection for anterior cruciate ligament reconstruction. *Acta Orthop Scand.* 2001 Aug;72(4):379-84.

Ferretti A, et al. Regeneration of the semitendinosus tendon after its use in anterior cruciate ligament reconstruction: a histologic study of three cases. *Am J Sports Med.* 2002 Mar-Apr;30(2):204-7.

EFFECTS OF COLLAGENASE ON THE MATERIAL PROPERTIES OF SMALL INTESTINAL SUBMUCOSA

JT Shearn¹, W Goodwin¹, DL Butler¹

¹Department of Biomedical Engineering, University of Cincinnati, Cincinnati, OH

INTRODUCTION

Small intestinal submucosa (SIS) has recently been used to repair a wide variety of tissues including the rotator cuff tendons [1,2]. Concerns persist, however, about the degradation of these tendon repairs after surgery, particularly if they should become unloaded. Our laboratory has shown that in the absence of loading, normal tendon loses 67% of its stiffness and 90% of its maximum force when exposed for 20 hours to 60U/ml of collagenase [3]. These changes were significantly reduced (no loss in stiffness and a 27% loss in maximum force) in the presence of immediate or delayed static loading equivalent to 4% peak strain. In this study involving SIS, we sought to first examine how a much longer but lower concentration exposure to collagenase (0.3U/ml for 2 weeks) would affect SIS properties in the absence of loading. We hypothesized that even this lower collagenase concentration would significantly degrade the SIS, resulting in a lower linear modulus.

METHODS

Single-layer SIS specimens (S. Badylak, U. Pittsburgh) were cut in the longitudinal direction into 19 dogbone-shaped specimens. The first group (dry; n = 4) was designed to determine SIS properties prior to hydration. The second group (hydrated [H]; n = 5) was used to determine the effects of hydration on linear modulus. A third group (hydrated and antibiotic/ antimicrobial solution [HAA]; n = 6) was designed to determine the effect of an antibiotic/antimicrobial solution. The last group (hydrated, antibiotic/ antimicrobial solution, and collagenase exposure [Degraded]; n = 4) was designed to determine the effect of collagenase on SIS linear modulus. The HAA and Degraded groups remained in an incubator (37°C, 5% CO₂, 95% RH) for 2 and 14 days, respectively. The Degraded specimens were fed advanced DMEM with ascorbic acid, 5% FBS and 0.3 U/ml bacterial type I collagenase twice weekly and then washed with PBS containing 10% EDTA at 2 weeks to halt the collagenase activity. The H, HAA and Degraded samples were stored in PBS at 4°C until testing. Each sample was failed in tension at a strain rate of 10%/s. All specimens but the dry [D] group were tested in a bath at room temperature.

RESULTS

Modulus, Fig. 1: Hydrating the SIS samples (Dry vs. H) and incubating them with collagenase (HAA vs. Degraded) significantly reduced linear modulus. The modulus for the degraded samples was a third of the modulus for the H and HAA groups ($p < 0.014$) and only 11% of the modulus for the dry group ($p < 0.001$). The moduli for the H and HAA groups were not significantly different from each other, but still only a third of the modulus for the dry group ($p < 0.001$).

DISCUSSION

Previous studies [3, 4, 5] have shown that unloading significantly weakens tendons and tendon subunits cultured subcutaneously or in vitro, possibly by exposing cleavage sites for collagenase [3]. Collagenase appeared to have a similar effect on unloaded SIS in vitro although the mechanism must still be identified. Future studies will need to examine whether, like tendon, the degradation of SIS is diminished in the presence of different mechanical stimulation regimes, particularly those based on physiologic parameters. For biologically derived scaffolds, this information will help to establish critical design parameters for determining how long a scaffold can remain mechanically viable as a replacement or repair after tendon injury.

ACKNOWLEDGMENTS

Support provided by the NIH Grant AR46574 and Cincinnati Sportsmedicine and Orthopaedic Research Foundation. SIS was supplied by S. Badylak and T. Gilbert at the University of Pittsburgh.

REFERENCES

1. DeJardin LM et al, *AJSM*, 2001.
2. Badylak SF, *J Biomed Mater Res*, 1995.
3. Nabeshima Y et al, *JOR*, 1996.
4. Yamamoto E et al, *J Biomech Eng*, 2003.
5. Muneta T et al, *JOR*, 1994.

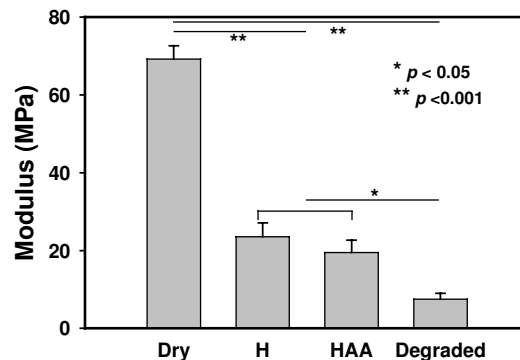


Figure 1. Linear modulus (mean \pm SEM) for the dry group is significantly greater than for the other groups.

NEW INSIGHTS INTO THE MESOSTRUCTURE OF CONNECTIVE TISSUES

Todd C. Doehring

Department of Biomedical Engineering, Lerner Research Institute, Cleveland Clinic Foundation
Cleveland, OH, USA, email: doehrint@ccf.org

INTRODUCTION

Understanding the differences in structure of tissues such as tendons and knee menisci is fundamental to understanding injury mechanisms, the progression of disease, and the effects of surgical or pharmaceutical interventions. An example is the famous diagram of Kastelic et al. (1), which describes the hierarchical nature of tendon microstructure. This diagram is often referenced as the standard structural model for connective tissues, however, it ends at the fascicle scale. Delineating larger mesostructures (i.e. fascicle groups) is difficult because histological methods tend to affect all of the collagen, regardless of local fiber orientations or interfaces. Hence, our goal was to develop a new sectioning and imaging technique to reveal collagen mesostructure at larger scales. Results from two tissues are presented; the human Achilles tendon, and canine knee meniscus.

METHODS

Specimens were freshly dissected and divided into sequential cross-sections using a specially designed cutting tool, consisting of up to 11 histological sectioning blades connected in parallel with 0.5 or 1 mm spacing. The tool was placed over the specimen and struck with a hammer, producing up to 10 uniform sequential sections. Sections were placed into a microscope equipped with elliptical polarizing filters previously described (2), with the specimen placed between crossed-polars. Because collagen is birefringent, the resulting color patterns depend on thickness, orientation, and strength of alignment. Contrast between mesostructures is therefore achieved without the need for fixing, embedding, or staining the tissue.

RESULTS

Achilles tendon: (Fig. 1) Images revealed distinct fascicles and fascicle bundles ranging in size from small (0.2 mm diameter) to large (2-3 mm diameter). Extending from the periphery and surrounding the fascicles was a thin collagen fiber network (endotenon) that appeared to maintain transverse structural integrity. In close-up images (10x), wavy patterns, cells, and concentric structures within the fascicles were found (Fig. 1A, inset).

Meniscus: Fascicles and fascicle bundles again were found, but these fascicles were smaller (~0.1 of Achilles tendon, see Fig. 1B inset) and grouped into larger fascicle bundles. Fibers also extended inward from the periphery, however these fibers (likely the so-called “tie fibers”) were often much larger than in the Achilles tendon.

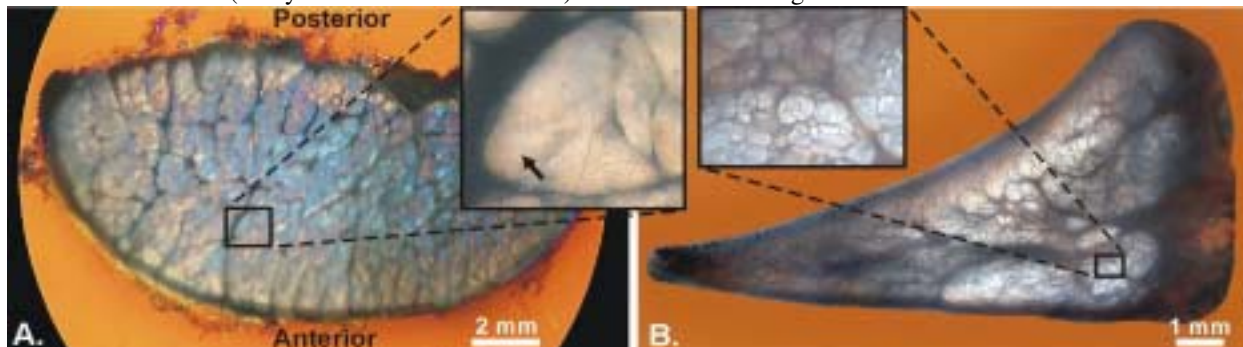


Figure 1. Cross-sections of (A) human Achilles tendon and (B) canine meniscus. In (A), the endotenon can be seen as the dark web-like structures. The arrow denotes cells (black dots) embedded within a concentric structure.

DISCUSSION

Distinctly different mesostructures were found for the two specimens. It is likely that a human meniscus would have larger mesostructures. To our knowledge, the concentric structures we found have not been previously reported. Current work is focused on reconstructing 3D models from the sequential cross-sections. This data could be valuable for developing computational models, and as a basis for comparison of normal and diseased tissues.

Acknowledgements: This study was supported by NIH grant #HL57236.

References: (1) Kastelic, et al., The multicomposite structure of tendon. *Connect Tissue Res*, 6(1), 1978.

(2) Doehring, et al., A new mesostructural testing system..., *ASME Proceedings of IMECE*, Anaheim, CA 2004.

BIOMECHANICS ASSOCIATED WITH INJURY: ATHLETE INTERVIEWS AND REVIEW OF INJURY TAPES

Tron Krosshaug, Roald Bahr, Lars Engebretsen
Oslo Sports Trauma Research Center, Department of Sports Medicine,
Norwegian University of Sport & Physical Education, Oslo, Norway

A precise description of the biomechanics associated with injury – the injury mechanism – is a key component to understand the causes of any particular injury type in sports. In this overview, we highlight that any attempt to describe the injury mechanisms raises a number of issues. Meeuwisse (1994) developed a model to account for all of the factors involved. While the injury may appear to have been caused by a single inciting event, it could result from a complex interaction between different internal and external risk factors. Olsen et al. (2004) recently showed that there is an increased risk for ACL injuries on certain artificial floors, but for female players only. This indicates that there is an interaction between gender and floor friction on injury risk, which could lead us to hypothesize that there may be a difference in the characteristics of the inciting event between genders, as well.

The term “injury mechanism” is widely used in medical literature, but its meaning is not well defined. The term is being extensively used for injury descriptions on completely different levels. Some studies only provide simple characteristics such as “contact/non-contact injuries” (Arendt and Dick, 1995), or “jumping/non-jumping injuries” (Paul *et al.*, 2003). Others use terms like “side-step cutting manoeuvres”, “tackle” or “long shot” (Strand *et al.*, 1990), and “spiking” or “blocking” (Ferretti *et al.*, 1992) – variables that are related to a specific sport (European team handball and volleyball, respectively). Others again, use various biomechanical variables to describe the mechanism of injury. The level of detail here also varies, e.g. “deceleration injury” (Boden *et al.*, 2000) versus “pivot shift injury of the posterolateral tibial rim and meniscus” (Speer *et al.*, 1992). We would argue that – to provide a complete understanding of the causes of injuries – a description of the inciting event needs to address the characteristics of the injury situation in each of these categories.

A number of different methodological approaches have been used to describe the inciting event. Here we will limit the description to two possible methods, athlete interviews and video analysis. There were very different descriptions of the injury mechanisms in these studies, probably due to the fact that they were categorized according to the researcher/surgeon’s predefined criteria. Interestingly, in one study (Nakajima *et al.*, 1979), where the injury mechanism description was written down as stated by the patients, seventeen different descriptions were found. This indicates that the injury mechanism descriptions in many cases are probably filtered by the researcher who interprets the patient statements.

Although video analysis may seem a more reliable way of analyzing injury mechanism compared to interviews, current methods for estimating kinematics from uncalibrated video sequences are inadequate (Krosshaug and Bahr, 2005). None of the studies listed in Table 4 used other methods than simple visual inspection to extract kinematic information from the videos. It is inherently difficult to interpret segment attitudes and further to calculate joint angles in three planes simply through visual inspection. In two of the studies, a consensus-approach was used, but this method was not validated. Finally, these methods cannot produce continuous estimates of joint angles and positions, which are necessary for detailed biomechanical analyses of the injury mechanisms, e.g. joint angle time histories, velocities and accelerations.

The studies seem to agree that the knee was relatively straight, at least no flexion more than 30° is reported, the same as was reported from the interview studies. On the other hand, while Boden et al. (2000) reported an inconsistency between the questionnaires and videos in terms of the description of the kinematics, Olsen et al. (2004) reported good agreement. Also, there does not seem to be a complete consensus between the studies regarding the injury mechanisms. Boden et al. (2000) reported the amount of internal and external rotation in the videos at the time of injury was minimal, whereas Olsen et al. (2004) and Ebstrup and Bojsen-Moller (2000) emphasized the role of internal/external, as well as valgus rotation. Teitz (2001) did not report varus/valgus or internal/external angles. Two of the studies stated that most of the injuries occurred in high-speed situations. This implies that the forces involved were relatively high. This is also further emphasized by the estimated weight distribution in the study of Olsen et al. (2004), where all except of one injured athlete had at least 80% of the weight distribution on the injured leg.

Although several of the interview studies report hyperextension to be an injury mechanism in ball/team sports, no such incident was reported among the 60 ACL injury videos analyzed in these four studies. One of the studies (Teitz, 2001) reported the center of gravity being posterior to the knee as an important factor. None of the other studies reported similar findings. It is, however, difficult to understand the rationale behind this theory as it is normally expected that, in the braking phase, the leg is indeed placed in front of the body in order to generate a

ground reaction force vector that will prevent the body from gaining too much forward angular momentum, thereby falling. Since it is not possible to determine the ground reaction force vector and its angle from viewing a video it is also questionable whether the hip joint moment is flexor dominated as suggested.

CONCLUSIONS

- Studies based on athlete interviews are fraught with significant methodological limitations: it is difficult to interpret the injury situation in the first place, recall and reporting bias may be important additional factors, and non-standardized variables and criteria are used
- There are only a few studies using video analysis, the cases are few, and these have been analysed using visual inspection alone
- The proportion of non-contact injuries seems to be greater among females
- Only “crude” descriptions are given, but the following biomechanics are suggested to be associated with non-contact ACL injuries in ball/team sports:
 - Injuries seem to occur most often in landing, cutting and other similar deceleration movements on a relatively straight leg
 - Although some hyperextension injuries are reported in interviews, but were not seen in any of the non-contact injuries from video analysis
 - Internal rotation seem is a likely mechanism of injury, but the studies suggesting this mechanism are limited in their methodological approach, thus more evidence is necessary to fully support the hypothesis.
 - Valgus/external rotation also seems to be a likely mechanism of injury, but also here, the obvious lack of good studies prevents us from decisive conclusions.

INFERIOR RESULTS OBSERVED IN FEMALES FOLLOWING SURGICAL REPAIR MAY NOT BE DUE TO THE MECHANICAL PROPERTIES OF THE SHOULDER CAPSULE

*S.M Moore, **P.J. McMahon, +*R.E. Debski

+*Musculoskeletal Research Center, Department of Bioengineering, University of Pittsburgh, Pittsburgh, PA

**Department of Orthopaedics, University of Pittsburgh, Pittsburgh, PA

INTRODUCTION

Gender has been associated with soft tissue injury while hormones, bony geometry, joint kinematics, and differences in soft tissue properties among men and women may be the cause. [1-3] Gender has also been a factor in poor surgical outcomes for the glenohumeral capsule. [4] This may be due to differences in the mechanical properties of the normal glenohumeral capsule in males and females. Most injuries to the glenohumeral capsule involve the axillary pouch (AP) or posterior capsule (PC). The objective of this study was to determine the bi-directional mechanical properties of the AP and PC in male and female specimens. Tissue samples were in the directions parallel (longitudinal) and perpendicular (transverse) to the longitudinal axis of the anterior (AB) or posterior (PB) band of the inferior glenohumeral ligament (IGHL), respectively.

METHODS

Dog-bone shaped tissue samples were obtained from the AP of 10 (60.6±9.9 yrs.) cadaveric shoulder specimens (4 male, 6 female) while 11 (60.5±9.7 yrs.; 5 male, 6 female) were used to obtain tissue samples from the PC. Tissue samples were excised longitudinal and transverse to the longitudinal axis of the AB-IGHL or the PB-IGHL for the AP and PC, respectively. The tissue sample ends were wrapped in gauze and fixed in customized clamps. The cross-sectional area was taken using a laser micrometer system (avg. of three midsubstance measurements). Two reflective markers (1.6 mm diameter, 318 µm thick) were fixed to the tissue sample midsubstance using cyanoacrylate for non-contact video strain analysis. The tissue samples were then mounted in a saline bath (37°C) on a uniaxial material testing machine (Instron Model 4502). The load cell had a range of 0-44.8 N with an accuracy of ±0.07 N. A 0.1 N preload was applied to the tissue sample which was then preconditioned via cyclic elongation from 0-0.3 mm for 10 cycles. A load-to-failure test was performed at a crosshead displacement rate of 10 mm/min. From the stress vs. strain curve, the tangent modulus and the ultimate stress were obtained. Each parameter was normally distributed (Kolmogorov-Smirnov test); thus, an unpaired t-test (male vs. female) was performed for the AP and PC tissue samples in the longitudinal and transverse directions, respectively. (p<0.05)

RESULTS

No significant differences (longitudinal: p=0.113; transverse: p=0.76) were detected for the tangent modulus of the longitudinal or transverse tissue samples of the AP or PC (longitudinal: p=0.26; transverse: p=0.63). (Table 1) Moreover, no differences were detected between the ultimate stress of the male and female specimens for the AP (longitudinal: p=0.14; transverse: p=0.74) and PC (longitudinal: p=0.42; transverse: p=0.26) tissue samples. With 80% power, 108 specimens would be needed to detect a difference of 5 MPa (smallest mean value) in tangent modulus between males and females.

DISCUSSION

The bi-directional mechanical properties of the AP and PC in the directions parallel (longitudinal) and perpendicular (transverse) to the longitudinal axis of the AB-IGHL or PB-IGHL, respectively, were determined and the results in male and female specimens compared. The values reported in this study agree well with a previous study of the AP that determined the ultimate stress to be 5.5±2.0 MPa in the longitudinal direction. [5] In the current study, no significant differences were detected between the male and female specimens. This suggests that the inferior results observed in females following surgical repair may not be due to the mechanical properties of the tissue. In the future, these surgical repair procedures can be mimicked via finite element analyses and the affect of varying bony geometry, joint kinematics, and mechanical properties on the stress distribution in the capsule can be evaluated.

REFERENCES

[1] Ireland, ML. Orthop Clin North Am. 2002. [2] Sallis RE, et al. Int J Sports Med. 2001. [3] Hsu, W-H, et al. Ortho Res Soc 2004. [4] Izquierdo, et al. Amer Soc Shoulder & Elbow Surg. 2004. [5] Bigliani, LU, et al. J Orthop Res. 1992.

ACKNOWLEDGMENTS

The support of the Whitaker Foundation (RG-99-0.76) and NIH (AR050218) are gratefully acknowledged.

Table 1. Effect of gender on AP and PC mechanical properties (transverse and longitudinal) (p>0.05)

		Axillary Pouch		Posterior Capsule	
		Tangent Modulus	Ultimate Stress	Tangent Modulus	Ultimate Stress
Long	Male	23.5±17.6	2.6±1.1	25.2±10.0	5.7±3.9
	Female	8.6±5.3	1.6±0.6	33.1±10.7	4.2±1.2
Trans	Male	5.0±2.5	0.9±0.4	9.2±5.2	0.9±0.6
	Female	5.6±3.4	0.8±0.4	11.3±8.0	1.9±1.8

THE CARPAL TUNNEL IS LESS COMPLIANT IN FEMALE THAN IN MALE

Zong-Ming Li

Hand Research Laboratory, Department of Orthopaedic Surgery
University of Pittsburgh, Pittsburgh, PA 15213, USA (zmli@pitt.edu)

INTRODUCTION: Carpal tunnel syndrome results from compression of the median nerve within the carpal tunnel. The tunnel is formed by the carpal bones and the transverse carpal ligament, and is unaccommodating for the expansion of its contents. The detrimental limitation by the transverse carpal ligament is exemplified by carpal tunnel release, a universally used surgical treatment of carpal tunnel syndrome by cutting the ligament. Surprisingly little attention has been paid to the understanding of the mechanical properties of this ligament [1]. The purposes of this study were (i) to characterize indentation force-displacement relationship of the carpal tunnel related to the transverse carpal ligament, and (ii) to compare the effective compliance between male and female groups.

METHODS: A hand-held Myotonometer (Neurogenic Technologies, Inc) was used to measure force and displacement during indentation testing (Figure 1B). The indentation probe has a flat end with a diameter of 10 mm. To standardize indentation location on the skin overlying the transverse carpal ligament, a line was drawn to connect the palpable pisiform and scaphoid. A point 10 mm distal from the connection line on the bisector was marked as the center of indentation (Figure 1A). During the testing, the hand was placed in an arm holder with the palmar side facing upward. The probe was manually pressed down perpendicular to the skin surface. The device took measurements from 0.25 to 2.00 kg at an increment of 0.25 kg. Twelve males (age 29.3 ± 6.6 years) and twelve females (age 26.2 ± 4.3 years) who had no neuromusculoskeletal disorders to the upper extremity participated in the study. Effective compliance was defined as the slope of the linear regression line of a set of force-displacement data. Repeated measures 2-way ANOVAs were used to compare the displacement differences. A t-test was used to compare the effective compliances between males and females.

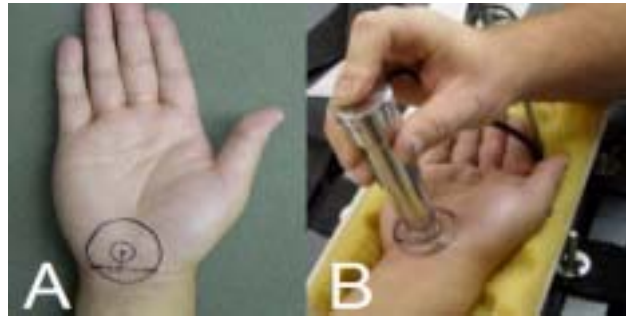


Figure 1. Center of indentation above the carpal tunnel (A) and manual indentation testing (B).

RESULTS: In the tested force range, the displacement increased linearly with applied force for either male or female group (Figure 2, R^2 ranged from 0.936 to 0.981). Females showed significantly smaller displacements than males ($F = 30.4$, $p < 0.001$). Force increases from 0.25 to 2.00 kg caused average indentation displacements of 1.82 ± 0.30 mm and 1.38 ± 0.25 mm for males and females, respectively. The effective compliance of females, 0.077 ± 0.014 mm/N, was 24.5% lower than that of males, 0.101 ± 0.018 mm/N ($p < 0.005$, Figure 3).

DISCUSSION: The results show that the soft tissues forming the carpal tunnel are distensible. A change in the mechanical properties of these soft tissues (e.g. hypertrophy of transverse carpal ligament due to repetitive use of the hand [2]) may critically elevate the carpal tunnel pressure that is inductive to carpal tunnel syndrome. The fact that females have less compliant soft tissues than males may partially explain the higher prevalence of carpal tunnel syndrome in women [3]. Future studies are needed to investigate the material and structural properties of the transverse carpal ligament, the relationship of the ligament to the carpal tunnel pressure, and the biological and biomechanical adaptations of the ligament to repetitive hand use.

REFERENCES: [1] Sucher, B.M. and R.N. Hinrichs, J Am Osteopath Assoc, 1998. 98(12): p. 679-86. [2] Moore, J.S., Am J Ind Med, 2002. 41(5): p. 353-69. [3] Phalen, G.S., J Bone Joint Surg Am, 1966. 48(2): p. 211-28.

ACKNOWLEDGEMENT: The author thanks Dr. Leland Albright for providing the Myotonometer device.

Figure 2. Force and displacement data from indentation testing.

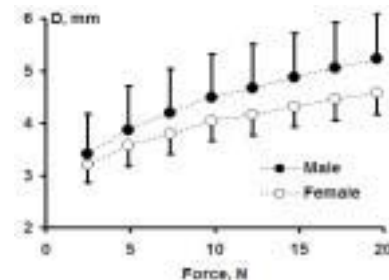
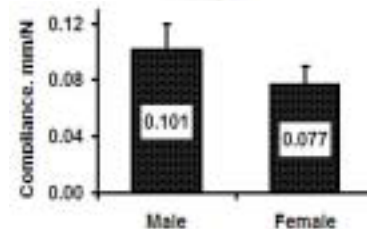


Figure 3. Effective compliance (mm/N).



GENDER DIFFERENCES ASSOCIATED WITH THE RISK OF NON-CONTACT ACL INJURY: KINEMATICS DURING A SINGLE LIMB DROP LANDING

*Y. Nagano, **H. Ida, **M. Akai and *T. Fukubayashi

*Graduate School of Human Sciences, University of Waseda, Tokorozawa, JAPAN,

**Research Institute National Rehabilitation Center for the Disabled, Tokorozawa, JAPAN,

INTRODUCTION

Rupture of the anterior cruciate ligament (ACL) occurs frequently during sports activities. ACL injuries often occur in non-contact situations, i.e., cutting or landing on a single limb. The mechanism of these high risk movements is thought to be a forceful valgus collapse with the knee close to full extension combined with external or internal rotation of the tibia [1]. Additionally, female athletes are at an increased risk for ACL injuries with an injury rate 3 to 5 times higher than male athletes [2]. Although a number of hypotheses have been suggested to explain the motions that actually occur in-vivo as well as the reason for the difference among genders, the mechanism of the ACL injuries is still unknown.

The purpose of this study was to analyze knee kinematics during a single limb drop landing and to compare the kinematics between females and males. The hypothesis was that internal rotation and valgus rotation of the tibia occur during a single limb drop landing, and that females show a larger degree of internal tibial rotation than males.

METHODS

Ten healthy subjects (5 males Age:25±3 yrs, 5 females Age:20±2 yrs) with no history of musculoskeletal injury participated in this study. All subjects performed a drop landing from a platform 30 cm in height. Subjects were asked to stop and balance on a single limb after landing. Each trial was recorded using an optical motion capture system (VICON system, Oxford Metrics, Inc). Data were processed using the point cluster technique [3] with 24 markers on the stance limb. Internal/external rotation and varus/valgus rotation of the tibia with respect to the femur were analyzed during the first 150 ms after toe contact.

Statistical analysis was performed using an unpaired t-test for gender comparison. The level of significance was set at $p < 0.05$.

RESULTS

Figure 1 shows a gender-based comparison of the average (or 'of a typical') tibial rotation during the single limb drop landing. All subjects experienced internal tibial rotation after toe contact. Maximum internal tibial rotation occurred approximately 50 ms after toe contact. The maximum internal tibial rotation was significantly larger for females (6.1 ± 1.2 degrees) than for males (3.3 ± 0.8 degrees) ($p = 0.002$).

Almost all subjects experienced valgus rotation of the tibia after toe contact; however there were no significant differences in valgus rotation of the tibia between females and males (4.1 ± 2.7 degrees for females, 4.9 ± 3.5 degrees for males).

DISCUSSION

These results showed that internal rotation and valgus rotation of the tibia occur during single limb drop landing. Maximum internal rotation of the tibia occurred 50 ms after toe contact which is approximately when heel strike occurs. It is thought that non-contact ACL injuries occur just after heel strike [1]. Therefore, internal and valgus rotation of the tibia is associated with non-contact ACL injuries occurring during single limb drop landing.

These results showed that females experience a larger internal tibial rotation than males. Increased internal tibial torque in combination with valgus torque leads to increased in-situ force in the ACL [4]. Therefore an increase of internal tibial rotation at the time of a heel strike can be one of the reasons for female athletes to have a higher incidence of non-contact ACL injuries.

This study has shown that the likely mechanism of non-contact ACL injuries that occur during single limb drop landing is internal tibial rotation combined with valgus rotation occurring at heel strike. Furthermore, one reason that females have a higher incidence of ACL injuries is that they land from a single limb drop with increased internal tibial rotation.

REFERENCES

1. Olsen, O.-E. and et al., Injury Mechanisms for Anterior Cruciate Ligament Injuries in Team Handball. *Am J Sports Med.*, 2004. 32: p. 1002-1012.
2. Huston, L.J., Anterior cruciate ligament injuries in the female athlete. Potential risk factors. *Clin Orthop.*, 2000. 372: p. 50-63.
3. Andriacchi, T.P. and et al., A Point Cluster Method for In-Vivo Motion Analysis Applied to a Study of Knee Kinematics. *J Biomech Eng.*, 1998. 120: p. 743-749.
4. Kanamori, A. and et al., The effect of axial tibial torque on the function of the anterior cruciate ligament. *Arthroscopy*, 2002. 18: p. 394-398.

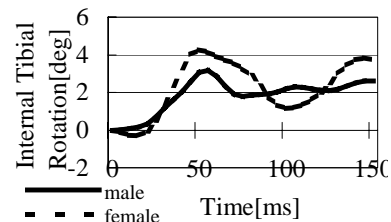


Figure 1. Gender-based comparisons of tibial rotation.

THE ROLE OF HAMSTRINGS MUSCLES TO PROTECT THE ACL

Giuliano Cerulli^{1*}, Mario Lamontagne^{2,3}, Auro Caraffa¹, Antonella Liti¹,
Fabio Vercillo¹, and Mélanie Beaulieu²

Let People Move¹, and University of Perugia*, Perugia, Italy.

Laboratory for Research on Biomechanics² and Department of Mechanical Engineering³, University of Ottawa,
Ottawa, Ontario, Canada

INTRODUCTION

Direct relationship between the ACL elongation and the neuromuscular control of the flexor and extensor muscles has not been frequently investigated. Few investigations have been carried out in order to study the in vivo ACL mechanical behaviour during dynamics motions such as the jump, quick stop, and cut (Beynon and Fleming 1998, Fleming et al 1999, Benoit et al. 2000, and Cerulli et al. 2003).

The purpose of this study is to investigate the preventive role of the hamstrings in relation with knee flexion angle and ACL in vivo elongation during jumping, stopping and cutting motions.

METHODS

Three healthy participants (mean age: 23.2 yrs; mean mass: 72 kg), having no previous history or current incidence of musculoskeletal disease or injury were recruited from the medical student population at the University of Perugia. After informed consent, the calibrated strain gauge device (DVRT) was surgically implanted by arthroscopy in the antero-medial band of the intact ACL while the participant was under local anaesthesia. The participant was then transported from the surgery room of the hospital to the biomechanics laboratory for data collection. The zero strain position of the ACL was determined using the slack-taut technique (Beynon and Fleming 1998). The subject was asked to perform three types of motion: jumping, stopping, and cutting. All of these motions consisted of jumping from about a distance of 1.5m to the centre of a force plate, landing with the instrumented left leg. The entire collection window was 8 seconds at 1000Hz for the electromyography, force plate, and DVRT signals and at 50 Hz for the kinematics data. A total of three to five trials were collected and averaged over a jump, stop or cut cycle of less than one second. After the experimental testing, the participant returned to the hospital in order to remove the DVRT.

The rectified EMG signals recorded during the three motions were synchronised to match the time of DVRT, ground reaction force, and kinematics data. The rectified EMG signals were normalised by peak amplitude for the dynamic contractions of the three manoeuvres using the stopping motion EMG data as normalisation basis.

RESULTS AND DISCUSSION

For the purpose of this abstract, only the stopping motion is discussed. During the stopping experimental conditions, the maximum peak elongation of the ACL coincided with the maximum knee angle the maximum vertical ground reaction force occurred later in the cycle (Fig. 1). The maximum normalised EMG of the Semitendinosus and both Gastrocnemius took place before the maximum ACL elongation. On the other hand, the quadriceps muscle reached their maximum after the peak GRF. In the analysed conditions with less extent for the cutting, the subject's neuromuscular strategy does anticipate the impact by contracting the Hamstrings and Gastrocnemius muscles with high intensity whereas the quadriceps muscles contracted right after the impact with the ground. It shows that the Hamstring and Gastrocnemius muscles are used as protective mechanism to the ACL elongation as in jumping and cutting conditions. The quadriceps muscles played their anti-gravitational role in order to avoid collapsing to ground.

CONCLUSION

This investigation has confirmed that the stopping, jumping and cutting manoeuvres generate a relatively high level of ACL elongation that initiates at or just before foot contact, when the leg is most extended. The muscle contraction anticipatory of the hamstring and Gastrocnemius play an important role of protecting excessive ACL elongation whereas the quadriceps muscle prevent the collapsing of the knee joint after the foot impact with the ground.

REFERENCES

- Benoit, D., Cerulli, G., Caraffa, A., Lamontagne, M., Liti, A., & Brue, S. (2000). Arch of Physiology and Biochemistry, 18(1/2), p.100.
Beynon BD, Fleming BC (1998) J. of Biomechanics. 31: 519-525
Cerulli, G., Benoit, D., Lamontagne, M., Caraffa, A., Liti, A., & Brué, S. (2003). KSSTA. 11(5), 307-311

POSTERIOR CRUCIATE LIGAMENT FUNCTION: EFFECT OF DEFICIENCY AND RECONSTRUCTION ON JOINT KINEMATICS

JT Shearn¹, FR Noyes²

¹Department of Biomedical Engineering, University of Cincinnati, Cincinnati, OH; ²Cincinnati Sports Medicine and Orthopaedic Center, Cincinnati, OH

INTRODUCTION. In addition to posterior translation increase, external tibial rotation, which is produced as a coupled motion in response to a posterior load, is lost after PCL injury as the “pivot point” created by the PCL is no longer present.[1,2] After PCL sectioning, external tibial rotation and posterior translation will be significantly different than normal. PCL reconstruction will restore normal coupled external tibial rotation under posterior loading.

METHODS. Joint kinematics for 31 cadaveric lower limbs from 22 donors were determined as the knee was cycled from 5 to 120° flexion while a 100 N posterior force was applied. For the intact, PCL sectioned, and reconstructed knees, knee motions were measured with an instrumented spatial linkage, and for the reconstructed knees, graft tension was recorded with strain gage load cells. The reconstructions[3] were performed with either a one or two-strand graft and tensioned to restore posterior translation to within ± 1 mm of the intact knee at 90° flexion.

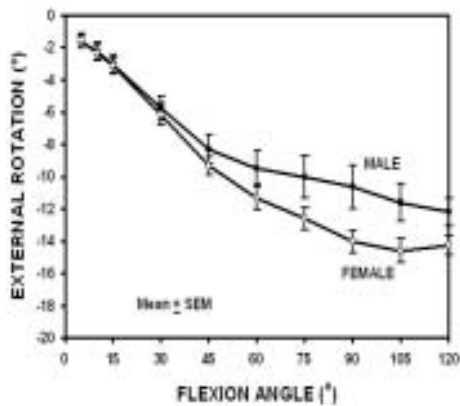


Fig. 2 After PCL sectioning, the change in external rotation from the intact knee based on the sex of the specimen

following PCL sectioning. A majority of the specimen have increases in posterior translation of 10 mm or more without associated injury to other ligament structures. These large increases can be attributed to limited restraint of posterior translation by secondary structures. Excessive posterior translation for an isolated PCL rupture does not indicate the need for higher initial graft tension to restore the normal posterior translation limit. In addition, the abnormal joint kinematics were restored to normal after PCL reconstruction.

ACKNOWLEDGMENTS. Support from Cincinnati Sportmedicine and Orthopaedics Center.

REFERENCES. 1 Fukubayashi et al, JBJS, 1982. 2 Gollehon et al, JBJS, 1987. 3. Shearn et al, JBJS, 2004.

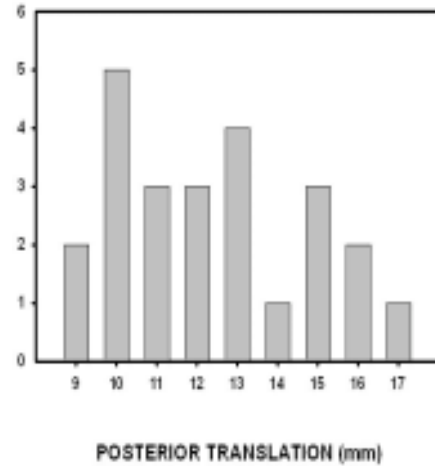


Fig. 1 The distribution of posterior translation at 90° flexion after PCL sectioning

RESULTS. After sectioning the PCL, the posterior translation increase at 90° flexion was 12.1 ± 0.46 mm. The posterior translation increase was greater than 10 mm for 64% (14/22) of the specimens, Fig 1. The mean decrease in external rotation was $5.9 \pm 0.49^\circ$ and $12.3 \pm 0.83^\circ$ at 30 and 90° flexion, respectively, Fig 2. PCL reconstruction restored the normal coupled external tibial rotation under posterior loading. The graft tension for two-strand PCL reconstructions to restore the normal posterior translation limit was independent of the magnitude of abnormal posterior translation, Fig 3.

DISCUSSION.

Significant changes are produced in posterior translation and coupled external tibial rotation

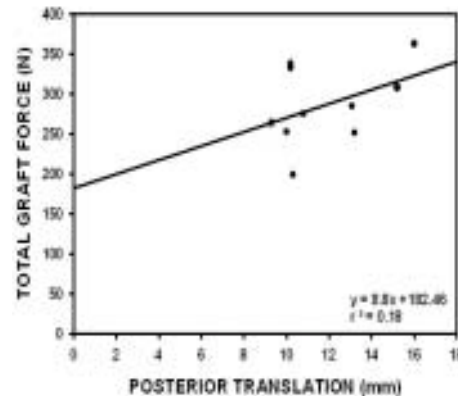


Fig. 3 For the AD2-MM reconstruction, graft force to restore normal posterior translation as a function of the posterior translation after the PCL was resected (90° flexion)

DETERMINATION OF ANGLES OF KNEE FLEXION FOR GRAFT FIXATION IN DOUBLE BUNDLE ANTERIOR CRUCIATE LIGAMENT RECONSTRUCTION

*K. Miura, *M. Thomas, *R. Brinkley, *S. Noorani, *Y-C. Fu, and *S.L-Y. Woo

*Musculoskeletal Research Center, Department of Bioengineering, University of Pittsburgh, Pittsburgh, PA
Email: ddecenzo@pitt.edu

OBJECTIVE

In recent years, double bundle ACL reconstruction (DB-ACLR) has gained popularity. In this procedure, overloading either one of the two grafts should be avoided since it may cause higher risk of graft failure. Thus, the objective of this study was to determine a safer range of knee flexion angles for graft fixation in DB-ACLR to restore the force distribution between each bundle of the intact ACL.

METHODS

Seven human cadaveric knees (44.6 ± 7.0 yrs) were tested. The DB-ACLR was performed with two different protocols for graft fixation. 1) For the first protocol, Fixation 60/0, the anteromedial (AM) graft was fixed at 60° and the posterolateral (PL) graft was fixed at full extension (FE).¹ 2) For the second protocol, Fixation 30/30, both grafts were fixed at 30° simultaneously.² Using a robotic/universal force-moment sensor testing system, the kinematics and the in-situ force of the AM and PL grafts were obtained in response to two external loading conditions: 1) Anterior tibial load of 134 N applied from FE to 90° and 2) a combined rotatory load of 10 N-m valgus and 5 N-m internal tibial torques at 15° and 30° (simulated pivot shift test). These data were compared with those for the AM and PL bundles of the intact ACL. Statistical analysis was done using a repeated measures ANOVA with significance set at $p < 0.05$.

RESULTS

In response to anterior tibial load, knee kinematics of the DB-ACLR and overall in-situ forces in the grafts were similar to those for the intact knee for both fixation protocols (Fig.1). However, the forces in the AM and PL grafts were significantly different from those in the two bundles of the intact ACL. For Fixation 60/0, the AM graft carried 1.5 times higher load than the AM bundle of the intact ACL ($p < 0.05$). In contrast, for Fixation 30/30, the forces in the AM graft became lower while the forces for the PL graft increased 1.9 times that of the PL bundle of the intact ACL ($p < 0.05$). Similar findings were also observed in the case of combined rotatory loads.

CONCLUSIONS

Following DB-ACLR, both fixation protocols could restore the knee stability and graft function to the level of the intact ACL. Nevertheless, the distribution of the forces between the AM and PL grafts was too high when fixed at 60° and 30° , respectively. These data suggest that safer knee flexion angles for fixation of the grafts would be slightly less than 60° for the AM and 30° for the PL in DB-ACLR.

REFERENCES

- 1) Yagi M: Am J Sport Med, 30(5): 660-666, 2002
- 2) Muneta T: Arthroscopy 15(6): 618-624, 1999.

ACKNOWLEDGEMENT

This research was supported by NIH Grant AR39683.

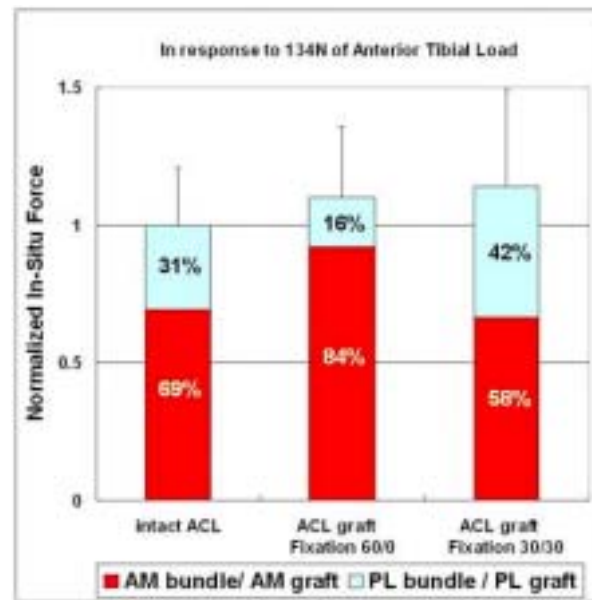


Figure1) Force distribution between AM and PL bundle or AM and PL graft.

Kubo, T	38	Rajan, L	12, 41
Kuo, CK	25	Renström, P	37
		Riley, GP	39
Lamontagne, M	55		
Laudier, DM	41	Sakamoto, H	38
Lee, EH	29	Sawaguchi, N	42
Lee, H	41	Schaffler, MB	12, 41
Lee, TQ	17	Shearn, JT	28, 48, 56
Les, CM	16	Shimode, K	42
Li, G	13	Simmons-Byrd, A	32
Li, S	47	Soslowsky, LJ	11
Li, Z-M	53	Spalazzi, JP	21, 27
Liang, R	46	Spindler, KP	36
Liti, A	55	Stehle, JH	14
Lu, HH	21, 27, 33, 44	Stewart, SS	13
		Stewart-Akers, AM	32
Majima, T	42		
Manmoto, T	47	Takakura, Y	46
McGarry, MH	17	Tashman, S	16
McMahon, PJ	14, 52	Thomas, M	57
Mihata, T	17	Toh, SL	29
Minami, A	42	Tsai, J	33
Miura, K	57	Tuan, RS	25
Moffat, KL	27, 44		
Moon, DK	45, 46		
Moore, SM	52	Vercillo, F	55
Murray, MM	36		
		Wang, IE	33
Nagano, Y	54	Wang, JH-C	19
Nanney, LB	36	Wang, VM	12, 20, 41
Nation, A	22	Warner, JP	13
Nishino, A	47	Watanabe, N	38
Noorani, S	57	Weinhold, P	43
Noyes, FR	56	Wen, P	40
		Wenstrup, RJ	35
		West, JR	24
Onodera, T	42	Wong, WMN	40
Oshima, Y	38	Wong, YP	40
Ouyang, HW	29	Woo, SL-Y	23, 45, 46, 57
Papannagar, R	13	Yang, X	22
Pennington, CJ	39		
		Zantop, T	26
Qi, J	34	Zheng, N	18

NOTES

ANNOUNCEMENT



THE INTERNATIONAL CENTRE OF ORTHOPAEDIC RESEARCH, EDUCATION, AND TREATMENT (I.C.O.R.E.T.)

The I.C.O.R.E.T. is pleased to announce a special award for young researchers of orthopaedics, biomechanics/biology, operative techniques, and sports - the Y-ROBOTS Award. Manuscripts in the areas of orthopaedic biomechanics, orthopaedic biology, operative techniques in orthopaedics or sports medicine are being accepted for consideration of this outstanding research award. The first author must be less than 40 years or within no more than 8 years after his/her last academic degree (Ph.D. or M.D.) at the time of submission.

All applications will be reviewed and up to 10 finalists will be selected and invited for presentation at the 9th International Conference on Orthopaedics, Biomechanics, Sports Rehabilitation in Assisi/Perugia, Italy, between 11-13 November 2005. The winner of the Y-ROBOTS Award will be selected following the presentations by the finalists. The Members of the Award Committee are:

Chair: Savio L-Y. Woo, Ph.D.
Members: Giuliano Cerulli, M.D.
Ejnar Eriksson, M.D., Ph.D.
Mario LaMontagne, Ph.D.
Ronny Lorentzon, M.D.



The award consists of:

- * \$5,000 Euros
- * Award Certificate or Plaque
- * Consideration for Publication in Knee Surgery, Sports Traumatology, Arthroscopy after the peer review process

The deadline for receipt of manuscripts will be October 1, 2005. Six (6) copies of the completed application and manuscript should be submitted to:

Savio L-Y. Woo, Ph.D.
c/o Let People Move
Via G.G. Pontani, 9
06128 Perugia - Italy

Note:

- Submissions, including papers, photographs, illustrations, etc. submitted will not be returned unless a self-address stamped envelope is included.
- Members of the research groups of the Award Committee are not eligible.

International Symposium on Ligaments & Tendons - V

February 19, 2005
Wyndham Washington, DC

7:30 am - 8:00 am	Registration & Check-In
8:00 am - 8:15 am	Opening Ceremony, Welcome & Announcements Savio L-Y. Woo, PhD, DSc, Steven Abramowitch, PhD
8:15 am - 9:45 am	Symposium: Rotator Cuff Tendinopathy Moderators: Giuliano Cerulli, MD & Kai-Nan An, PhD
9:45 am - 10:15 am	Break and Poster Session 1
10:15 am - 12:00 pm	Symposium: Functional Tissue Engineering - Part 1 Moderators: Joanne Archambault, PhD & Toru Fukubayashi, MD
12:00 pm - 1:00 pm	Lunch and Poster Viewing
1:00 pm - 1:55 pm	Symposium: Functional Tissue Engineering - Part 2 Moderators: Steven Arnoczky, DVM & Christos Papageorgiou, MD
1:55 pm - 3:20 pm	Symposium: Tendon Healing & ACL Moderators: Chih-Hwa Chen, MD & Scott Rodeo, MD
3:20 pm - 3:50 pm	Break and Poster Session 2
3:50 pm - 5:00 pm	Symposium: Gender-Related Differences and Knee Kinematics Moderators: Angela Smith, MD & Thay Lee, PhD
5:00 pm - 5:10 pm	Closing Remarks: Savio L-Y. Woo, PhD, DSc
6:00 pm -	Cocktails, Dinner & Award Ceremony: Tony Cheng Seafood Restaurant